Crystal Structures and Spectral Investigation of Aroylhydrazones and their Mixed Ligand Metal Chelates

Thesis submitted to

Cochin University of Science and Technology

in partial fulfillment of the requirements

for the award of the degree of

DOCTOR OF PHILOSOPHY

in

CHEMISTRY

T 582

By

JESSY EMMANUEL

Department of Applied Chemistry
Cochin University of Science and Technology
Kochi 682 022

July 2012

Crystal Structures and Spectral Investigation of Aroylhydrazones and their Mixed Ligand Metal Chelates

Ph. D. Thesis under the Faculty of Science

Author:

Jessy Emmanuel
Research Fellow, Department of Applied Chemistry
Cochin University of Science and Technology
Kochi, India 682 022
E mail: jessycusat@yahoo.com

Research Advisor:

Dr. M. R. Prathapachandra Kurup
Professor
Department of Applied Chemistry
Cochin University of Science and Technology
Kochi, India 682 022
Email: mrp@cusat.ac.in

Department of Applied Chemistry
Cochin University of Science and Technology
Kochi, India 682 022

July 2012

Front cover : Molecular packing of [Cu(BB)(bipy)] CH₃OH (**29**) viewed down b axis

Back cover : Molecular packing in [VO₂(HBN)] H₂O (7) to form Channels by metal ring and π-π interaction

.........to my beloved

Ammachi, Chachan and Amma

in the heavenly abode.

DEPARTMENT OF APPLIED CHEMISTRY
COCHIN UNIVERSITY OF SCIENCE AND TECHNOLOGY
KOCHI - 682 022, INDIA

Dr. M.R. Prathapachandra Kurup
Professor

Phone Off : 0484-2862423
Phone Res : 0484-2576904
Telex   : 885-5019 CUIN
Fax   : 0484-2577595
Email   : mrp@cusat.ac.in
            mrp_k@yahoo.com

Date: 26.07.2012

Certificate

This is to certify that the thesis entitled "Crystal Structures and Spectral Investigation of Aroylhydrazones and their Mixed Ligand Metal Chelates" submitted by Ms. Jessy Emmanuel, in partial fulfillment of the requirements for the degree of Doctor of Philosophy, to the Cochin University of Science and Technology, Kochi-22, is an authentic record of the original research work carried out by her under my guidance and supervision. The results embodied in this thesis, in full or in part, have not been submitted for the award of any other degree.
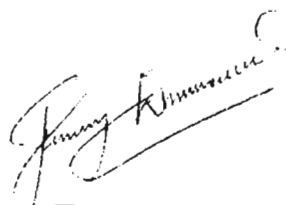
M. R. Prathapachandra Kurup
(Supervisor)

———"Your word is a lamp to my feet and a light for my path"———
(Psalms 119:105)

DECLARATION

I hereby declare that the work presented in this thesis entitled **"Crystal Structures and Spectral Investigation of Aroylhydrazones and their Mixed Ligand Metal Chelates"** is entirely original and was carried out independently under the supervision of Prof. M. R. Prathapachandra Kurup, Department of Applied Chemistry, Cochin University of Science and Technology and has not been included in any other thesis submitted previously for the award of any other degree.

Date: 25/07/2012

Kochi-22

Jessy Emmanuel

Acknowledgement

completely plunged into it. My dear Jocha and my beloved Minna and Tom...this achievement is theirs too.

This is dedicated to my loving Chachan and Amma, showering their blessings upon me from heaven.

I am sure that my achievement would have given great joy and pride to my Ammachi, my beloved mother-in-law who parted us just a few days before the submission of my thesis. She had always inspired me and definitely that was a driving force indeed.

This would be incomplete unless I thank a big community who had always been my strength and support....eight loving families of my own elder sisters and brothers and nine families of my sisters and brothers-in-law.

Above all, thanks to the Almighty, the source of my power and wisdom.

Jessy Emmanuel

PREFACE

Hydrazones are a versatile class of compounds with a broad spectrum of applications. Hydrazone derivatives possess antiHIV, antimicrobial, antitubercular, anticonvulsant and anti inflammatory activities. The transition metal complexes of aroylhydrazones have been investigated extensively because of their biological, especially as potent inhibitors for many enzymes, NLO and magnetic activities. They are also proved to have potential applications as catalysts, analytical agents, luminescent probes and molecular sensors.

Supra molecular architectures of coordination complexes of hydrazones through non covalent interactions have been explored. Molecular self-assembly driven by weak interactions such as hydrogen- bonding, $\pi \cdots \pi$, C–H$\cdots\pi$, van der Waals interactions, and so forth are currently of tremendous research interest in the fields of molecule based materials. The directional properties of the hydrogen-bonding interaction associate discrete molecules into aggregate structures that are sufficiently stable to be considered as independent chemical species. Chemistry can borrow nature's strategy to utilize hydrogen-bonding as well as other noncovalent interactions as found in secondary and tertiary structures of proteins such as the double helix folding of DNA, hydrophobic self-organization of phospholipids in cell membrane etc. In supramolecular chemistry hydrogen bonding plays an important role in forming a variety of architectures. Thus, the wise modulation and tuning of the complementary sites responsible for hydrogen-bond formation have led to its application in

supramolecular electronics, host-guest chemistry, self-assembly of molecular capsules, nanotubes etc.

The work presented in this thesis describes the synthesis and characterization of metal complexes derived from some substituted aroylhydrazones. The thesis is divided into seven chapters. Chapter 1 gives a brief outline of aroylhydrazones, diversity in their chelating behavior and their applications. This chapter also describes different physicochemical techniques employed for the characterization of aroylhydrazones and their metal complexes.

Chapter 2 includes the synthesis and characterization of five different aroylhydrazones and their characterization by elemental analyses, FTIR, ^{1}H NMR, UV–Vis spectral studies and single crystal X-ray diffraction studies. Chapters 3-7 discuss the synthesis and characterization of some transition metal complexes derived from the aroylhydrazones under study.

Contents

Chapter **1**

AROYLHYDRAZONES: A BRIEF OUTLINE

1.1 Introduction

The research interest in inorganic chemistry has steadily evolved over hundreds of years and has been flourished by the versatile development in the area of coordination chemistry. Widespread interest in the chemistry of coordination compounds is associated with their broad spectrum of applications in different areas such as catalysis, molecular sensors nonlinear optics, bioinorganic, biomimetic, magnetic and medicinal chemistry. The design and synthesis of multifunctional molecules combining in their structure several active moieties, sensitive towards different external influences have attracted significant interest recently. Coordination chemistry has greatly contributed to the rational design of new classes of host molecules. For instance, crystal structure of a copper complex which resembles a 'wheel and axle' may belong to a new category of host molecules [1]. Molecules with this shape is not suitable for close packing but tend to accommodate other molecules thus serving as adsorbents, sensors and catalysts. The architectural beauty of coordination compounds is due to the interesting ligand systems containing different donor sites say ONO, NNO, NO and NNS. It provides many new directions in research such as, in molecular magnetism, supramolecular chemistry, non-silicon-

based devices, precursors for vapor phase deposition and single molecule-based photonic devices and sensors [2]. Schiff bases play an important role in inorganic chemistry as they easily form stable complexes with most transition metal ions in the periodic table. The development of the field of bioinorganic chemistry has increased the interest in Schiff base complexes, since it has been recognized that many of these complexes may serve as models for biologically important species.

Transition metal complexes derived from hydrazone Schiff bases can form diverse supramolecular networks as reported by various research groups [3-5]. Blending supramolecular chemistry with materials science defines a field of supramolecular materials that rests on the explicit implementation of intermolecular interactions in the design and synthesis of novel materials presenting novel properties. Slight steric and electronic modifications in the ligand backbone provoke differences in the supramolecular architectures of the complexes, leading to a variety of one, two and three-dimensional hydrogen bonded networks in complexes.

It is well established that aroylhydrazones form stable chelate complex with transition metal cations by utilizing both their oxygen and imine nitrogen as donor atoms [6]. Among nitrogen-oxygen donor ligands, hydrazones occupy an important position due to their widespread applications and versatile coordination capability with transition metal ions [7].

1.2 Aroylhydrazones

Hydrazones which belong to a class of azomethines having the group –C=N–N– are interesting ligands in coordination chemistry. Introduction of a –C=O group in the hydrazide part increases the electron delocalization and denticity of the hydrazone and the resulting compound is known as an aroylhydrazone. N-aroylhydrazones are usually obtained by condensation of

aldehydes or ketones with aroylhydrazines, in the presence of an acid catalyst, in reaction times varying from 30 minutes to several hours [8,9]. Their purification can be accomplished by simple recrystallization and they are stable at ambient temperature. Recently a variety of N-aroylhydrazones were synthesized by another method i.e., under microwave irradiation within 2.5-10 minutes, starting from benzo, salicyloyl and isonicotinic hydrazides. The protocol developed employs microwave irradiation in the absence of solvents and catalysts, leading to high yields [10]. Fig. 1.1 represents the general formulae of a hydrazone and an aroylhydrazone.

Hydrazone   Aroylhydrazone

Fig. 1.1. Hydrazones, a class of azomethines with triatomic >C=N–N< linkage

Aroyl hydrazones allow additional donor sites to be introduced (*via* R, R^1 and R^2, Fig.1.1) inorder to increase the denticity of the resulting ligands. In an aroylhydrazone the basic coordination sites are carbonyl oxygen and the azomethine nitrogen. It is interesting to note that aroylhydrazones can potentially form amido/iminol tautomers and *syn/anti* forms as indicated in Figs.1.2 and 1.3.

amido form   iminol form
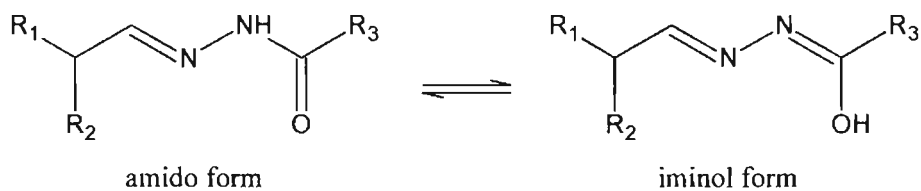
Fig. 1.2. Tautomerism in aroylhydrazone.

Recent studies have shown that *syn/anti* isomerisation and tautomerisation processes affect the metal chelating properties of these ligands [11]. In solid state amido form predominates while in solution state iminol form (Fig. 1.2). This property offers the formation of a variety of complexes, *i.e.*, the hydrazones can coordinate to the metal either in neutral amido form or in deprotonated iminolate form. The π conjugation over the hydrazone moiety is increased by the enolization of the ligand which improves the electron delocalization.

Syn form   *Anti form*
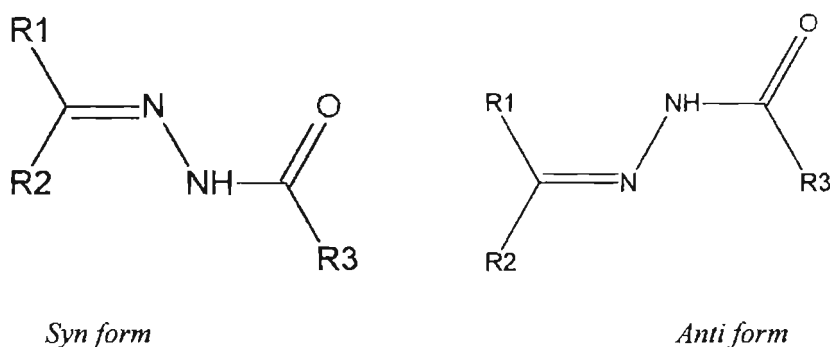
Fig. 1.3. Geometrical isomers of aroylhydrazone.

1.3 Coordination modes of hydrazones

The high efficacy, selectivity and specificity of the coordination of aroylhydrazones towards transition metal ions has rendered these Schiff bases prime candidates in the formation of coordination compounds. Hydrazones can act as potential multifunctional ligands with interesting coordination modes. The coordination mode adopted by a hydrazone depends on different factors like tautomerism, reaction conditions, stability of the complex formed, number and nature of the substituent on hydrazone skeleton. Number of coordination sites can be increased by introducing suitable substituents on the hydrazide part as

well as on the carbonyl part. For example if a hetero atom is present on the carbonyl part of a hydrazone, it can coordinate to the central metal by adopting an *NNO* coordination mode, either through the deprotonated iminolate form (Structure I) or through neutral amido form (Structure II) [12,13].
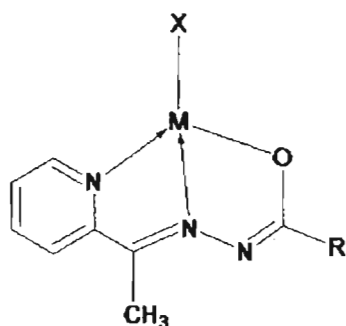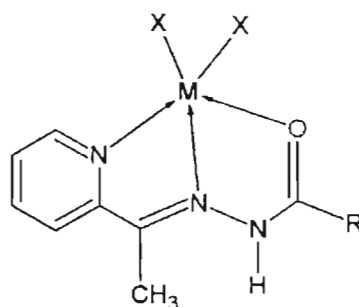
Structure I   Structure II

Another mode is the formation of a six coordinated metal complex with two deprotonated ligands. Stable metal chelates of distorted octahedral geometry are expected in this case (Structure III) [14].
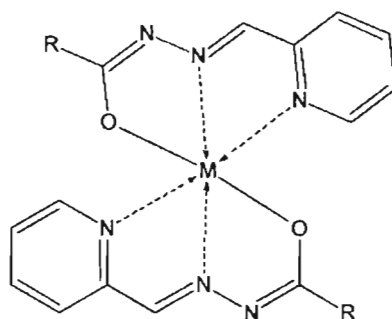
Structure III

Bridged complexes are formed by another mode of coordination. In this case anions (like halogens, azide or thiocyanate) present in the metal salt, an

atom or group of atoms can act as a bridging ligand which results in the formation of a dimeric structure (Structure IV) [15,16].
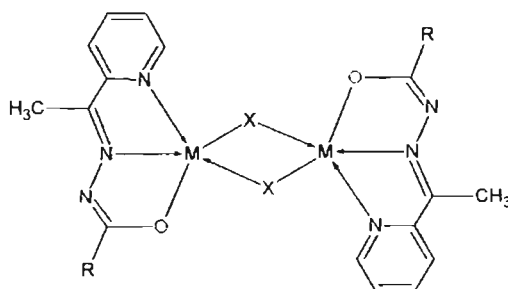
Structure IV

If the hydrazone possesses a phenolic group in the aldehyde/ketone part which is in suitable position for coordination, it leads to an *ONO* coordination mode, resulting in the formation of dimeric complexes with phenolate oxygen bridges (Structure V) [17].
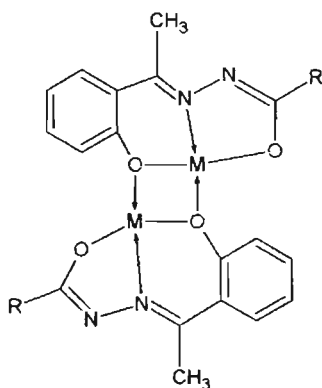
Structure V

In the case of complexes with ONO donor hydrazones we can incorporate heterocyclic bases to the central metal (Structure VI) resulting in a distorted square pyramidal structure [18].
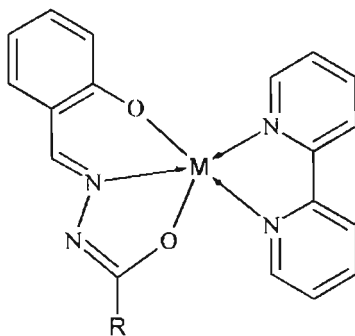
Structure VI

If the hydrazone possesses an electron donating group like methoxy group in the carbonyl part it may also take part in coordination to the central metal (Structure VII) [19]. Here the methoxy group can act as a chelating group and as a bridging group resulting in a multinuclear complex.
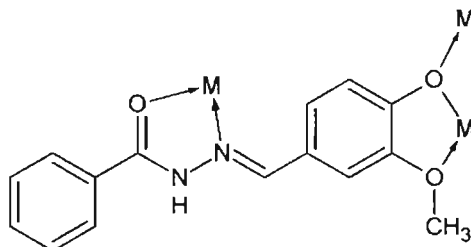
Structure VII

1.4 Applications of hydrazones

The interest in the design, syntheses and characterization of aroylhydrazones and their metal complexes has come from their applications in various fields. Their ease of syntheses, easily tunable steric and electronic properties and good solubility in common solvents has enhanced research interest in this area. They have wide applications in biology, medicine, optics, catalysis and analytical chemistry.

1.4.1 Hydrazones in magnetochemistry

Variable temperature magnetic susceptibility measurements reveal that moderate antiferromagnetic interactions operate between phenoxo bridged Ni(II) dimers whereas very weak antiferromagnetic exchange occurs through hydrogen bonding and $\pi \cdots \pi$ stacking interactions. All complexes are proved to be efficient catalysts for the epoxidation of alkenes by NaOCl under phase transfer condition [20].

Several coordination complexes derived from aroylhydrazones were reported for their pharmacological activity and magnetic properties [21] but such complexes were devoid of any hydrogen-bonding interactions that could generate supramolecular architectures with intriguing structures. The interactions of hydrogen bonds play vital roles for molecular recognition in a wide variety of biological systems and have also been applied in the synthesis of molecular magnetic materials [22]. Supramolecular architectures of singly phenoxo-bridged copper(II) and doubly phenoxo-bridged manganese(II) complexes derived from an unusual ONOO donor hydrazone ligand were reported and cryomagnetic, DFT and EPR studies were done [23]. The chemistry of multinuclear coordination metal complexes, especially of couple systems is of special interest because the phenomenon of interaction between metal centers lies at the crossover point of the two areas, namely the physics of the magnetic materials and the role of polymer-clear reaction sites in biological processes [24]. Manoj *et al.* investigated temperature dependence of magnetic susceptibility and EPR characteristics which appeared relevant to the coordination chemistry of potential class of carbohydrazone ligands [25].

1.4.2 Hydrazones in nonlinear optics

Aromatic hydrazones are known to exhibit good NLO activity. Hydrazones and their metal complexes have been studied with regard to their physical properties, reactivity patterns and application in a variety of processes, including non linear optics and molecular sensing [26].

Electronic materials, which have been at the heart of the telecommunication industry, are fast approaching their limitations, and soon, photonics will be the key in revolutionizing the telecommunication industry. The area of nonlinear optics (NLO) is a rapidly progressing field of science and technology that has the potential to offer unparalleled switching speed and bandwidth for optical signal processing. One of the major hurdles to the realization of second-order NLO polymer devices, has been overcoming the loss of noncentrosymmetric order at elevated manufacturing and operating temperatures.

Hydrazone derivatives are an attractive class of non-linear optical (NLO) crystalline materials because of their large molecular nonlinearities and their remarkable propensity to form non-centrosymmetric crystal systems [27]. The current approach to the development of practical NLO materials has focused on the use of a dihydroxy –functionalised hydrazone chromophore that can be easily synthesized and subsequently incorporated into a commercial epoxy polymer system

The synthesis and properties of six hydrazone-functionalized crosslinked polymers possessing stable nonlinear optics (NLO) properties were presented [28]. The NLO activity of hydrazone derivatives has been investigated in detail as crystals and as Langmuir–Blodgett films, as characterized by Kurtz and Perry

[29]. Second-order nonlinear optical properties of copper and palladium complexes of *N*-salicylidene-*N'*-aroylhydrazones were studied and the results showed that the complexes have considerable nonlinearity [30].

1.4.3 Hydrazones in supramolecular chemistry

Supramolecular chemistry is by nature a dynamic chemistry in view of the lability of the noncovalent interactions connecting the molecular components of a supramolecular entity [31]. Supramolecular architectures of the coordination complexes through hydrazone ligand-based hydrogen-bonding interactions are explored [32]. Chattopadhyay and his group have shown how the supramolecular architecture of manganese(II) aroylhydrazone complexes can be controlled by slight modification of the substituents attached to the ligand framework [33]. The self-assembly of multimetallic assemblies held together by intermolecular forces (hydrogen bonds, van der Waals forces etc.) is greatly dependent on the metal ions [34]. Metal ions can read the information coded in the organic ligands according to their coordination algorithm [35] and thereby give rise to metal–organic ligand complex species that are simultaneously assembled *via* complementary interligand hydrogen bonding forming supramolecular multimetallic assemblies. Quinolyl hydrazones are known to function as chelating agents and have versatile modes of bonding [36].

1.4.4 Metal complexes of hydrazones as catalysts

Hydrazones are able to change their coordination behaviour depending on the starting reagents, pH of the medium and reaction conditions. Metal–organic frameworks containing channels or pores with various sizes and shapes have attracted much attention because of their potential applications in catalysis, separation and gas sorption and storage [37,38]. According to Mahmudov *et al.*,

a copper(II) dimer with 3-(2-hydroxy-4-nitrophenylhydrazo)pentane-2,4-dione exhibits a good catalytic activity in the peroxidative oxidation of cyclohexane by aqueous H_2O_2, under mild conditions, to afford cyclohexanol, cyclohexanone and cyclohexyl hydroperoxide [39]. Transition metal complexes derived from hydrazones are proved to be efficient catalysts for the epoxidation of alkenes by NaOCl under phase transfer condition. Hydrazone complexes show remarkable catalytic activity in various organic reactions. Monfared *et al.* studied the catalytic abilities of some oxo- and dioxovanadium(V) complexes of tridentate hydrazones towards the oxidation of various hydrocarbons and found that the complexes are effective catalysts [40].

1.4.5 Hydrazones: Biological and Medicinal studies

Aroylhydrazones of various aldehydes and ketones occupy a special place among the biologically important organic ligands containing a variety of donor groups. N-aroylhydrazones which include the fragment (–CO–NH–N–CH–), have attracted much attention in the last 20 years because of their biological properties as well as their chelating properties toward metal ions. Many of them have been reported to possess a broad spectrum of biological activities, such as antifungal [41], antimalarial [42], antitubercular [43], antiplatelet [44] activities and have been studied extensively as potential therapeutic agents in a number of pharmaceutical contexts. Some hydrazone analogues such as pyridoxal isonicotinoyl hydrazone derivatives have been investigated as potential iron chelating drugs *in vivo* and *in vitro* and could be used in the treatment of iron overload [45].

The search for new HIV-1 CA assembly inhibitors has led to the synthesis and antiviral evaluation of new N-acylhydrazones containing glycine residue which show potent antiviral activities. They can bind HIV-1 capsid

1.4.6 Other applications

Aromatic hydrazones dispersed in a binder polymer possess hole-transporting properties and are used in electro photographic photoreceptors of laser printers [51]. Some of the arylhydrazones can act as herbicides, insecticides, nematocides, rodenticides and plant-growth regulators. Hydramethylnon is an amidinohydrazone insecticide which is used against cockroaches [52]. Metal complexes of hydrazones proved to have potential applications as luminescent probes [53] and molecular sensors [54]. Hydrazones of 2-methylphthalazone are effective sterilants for houseflies [55]. Many hydrazones are found to be effective corrosion inhibitors of metals. The effect of 2-hydroxyacetophenone aroylhydrazone derivatives on the inhibition of copper was studied and found that the corrosion is significantly decreased in presence of the investigated compounds [56].

1.5 Scope and objectives of the work

The ability of aroylhydrazones to engage in coordination to transition metals is a developing area of research interest and a great variety of complexes can be attained by attaching different donor groups to the hydrazone. Aroylhydrazones have continued to attract extensive attention from chemists because of their widespread uses in biology, pharmacology, catalysis, analytical chemistry and optics. Hydrazones, a member of the Schiff base family with triatomic >C=N–N< linkage, takes the forefront position among other organic ligands. Also these compounds contain the basic unit of peptide linkage [–C(=O)–NH] group closely related to the primary structure of proteins.

The coordination chemistry of transition metal complexes that contain polydentate ligand moieties including heterocyclic bases and anions is of current

research interest. Syntheses, spectral and structural studies of mixed-ligand metal complexes based on heterocyclic bases like 1,10-phenanthroline, 2,2'-bipyridine (the classical N,N donor ligands) and 4-picoline (the N donor ligand) can reveal different bonding modes, spectral properties and geometries in coordination compounds. Incorporation of anions like azide, thiocyanate and perchlorate in the complexes may demonstrate coordination modes of various combinations of the coligands.

The coordination properties of hydrazones can be tuned by the appropriate choice of parent aldehyde or ketone and hydrazide and the substituents attached to them. So in the present investigation we selected five different ONO/NO donor hydrazones as principal ligands. We selected 2-hydroxy-3-methoxybenzophenone and 5-bromo-3-methoxy-salycilaldehyde as the carbonyl part as it can provide an additional binding site for metal cation and thus increase the denticity.

The importance of aroylhydrazones and their transiton metal complexes in the application level and their interesting coordination abilities kindle our interest in the investigation of transition metal complexes with *ONO/NO* donor hydrazones with the following objectives.

> To synthesize some *ONO/NO* donor aroylhydrazones by the condenzation of 2-hydroxy-4-methoxybenzophenone, furan-2-carboxaldehyde and 5-bromo-3-methoxysalicylaldehyde with nicotinic acid hydrazide, N'-4-nitrobenzhydrazide and benzhydrazide.

> To characterize the synthesized hydrazones by different physicochemical techniques like partial elemental analysis and spectroscopic techniques like UV, IR and NMR.

➢ To analyse the crystal structures of aroylhydrazones. A systematic crystal structure analysis of the compounds may provide further information concerning the structural characteristics required for different applications.

➢ To synthesize different transition metal complexes using the synthesized hydrazones as principal ligands and some heterocyclic bases and anions as coligands. Oxido/dioxidovanadium(IV/V), manganese(II/IV), cobalt(II/III), copper(II), zinc(II) and cadmium(II) complexes are to be synthesized.

➢ To analyse the crystal structures of metal complexes by single crystal XRD studies.

➢ To study the coordination modes of different hydrazones in metal complexes by using physicochemical methods like molar conductance measurements, magnetic susceptibility measurements, cyclic voltammetry, thermogravimetry and by different spectroscopic techniques like UV, IR and EPR.

1.6 Physical measurements

Details of physicochemical techniques employed for the present study is discussed below.

1.6.1 Elemental analyses

Microanalysis for carbon, hydrogen and nitrogen in the synthesized aroylhydrazones and in their metal complexes were carried out on an Elementar model Vario EL III CHNS analyzer at the Sophisticated Analytical Instrument Facility (SAIF), Sophisticated Test and Instrumentation Centre (STIC), Kochi.

1.6.2 Conductivity measurements

Molar conductivities of the complexes in dimethylformamide (DMF) solutions (10^{-3} M) were measured at room temperature using a Systronic model 303 direct-reading conductivity bridge at the Department of Applied Chemistry, CUSAT, Kochi, India.

1.6.3 Magnetic susceptibility measurements

The magnetic susceptibility measurements of the powdered samples were done at room temperature using a Sherwood Scientific Magnetic Susceptibility Balance (M.S.B.) at the Department of Applied Chemistry, CUSAT, Kochi, India. The compound used as calibrant was $HgCo(SCN)_4$.

1.6.4 Thermogravimetric analysis

TG-DTG analyses of the complexes were carried out in a Perkin Elmer Pyris Diamond TG / DTA analyzer at a heating rate of 10 °C per minute in an atmosphere of nitrogen, at the Department of Applied Chemistry, CUSAT, Kochi, India.

1.6.5 Cyclic voltammetric analysis

Cyclic voltammograms were recorded on a CHI 608D electrochemical analyzer at Bharathiar University, Coimbatore, India. Electrochemical properties of complexes were studied in DMF/ DMSO medium with tetrabutylammonium phosphate as supporting electrolyte at a scan rate of 100 mV s^{-1} with platinum wires as working and counter electrodes and Ag/Ag^+ as a reference electrode.

1.6.6 Infrared spectroscopy

Infrared spectra of the compounds were recorded on a JASCO FT IR-4100 Fourier Transform Infrared Spectrometer using KBr pellets in the range of 4000-400 cm^{-1} at the Department of Applied Chemistry, CUSAT, Kochi, India

and also on a Thermo Nicolet AVATAR 370 DTGS model FT IR Spectrometer using KBr pellets in the range of 4000-400 cm^{-1} and ATR technique at Sophisticated Analytical Instrument Facility (SAIF), Sophisticated Test and Instrumentation Centre (STIC), Kochi.

1.6.7 Electronic spectroscopy

Electronic spectra of all the compounds were taken on a Spectro UV-vis Double Beam UVD-3500 spectrometer in the 200-900 nm range at the Department of Applied Chemistry, CUSAT, Kochi, India. The solvents used were dimethylformamide and acetonitrile.

1.6.8 NMR spectroscopy

^{1}H NMR spectra of the hydrazones and some complexes were recorded using Bruker AMX 400 FT-NMR Spectrometer with DMSO-d_6 as the solvent and TMS as internal standard at the Sophisticated Analytical Instrument Facility (SAIF), Indian Institute of Science, Bangalore, India and also on a Bruker Avance DPX-300 MHz NMR Spectrometer at NIIST Trivandrum.

1.6.9 EPR spectroscopy

The EPR spectra of the complexes in the solid state at 298 K, in DMF at 298 K and at 77 K were recorded on a Varian E-112 spectrometer using TCNE as the standard, with 100 kHz modulation frequency, modulation amplitude 2 G and 9.1 GHz microwave frequency at the SAIF, IIT Bombay, India.

1.6.10 Mass spectroscopy

Mass spectra were recorded by direct injection on Waters 3100 mass detector using electron spray ionization technique at the Department of Applied Chemistry, CUSAT, Kochi, India. Mass spectroscopy is used to measure relative

molecular masses. A mass spectrum is a plot of relative abundance against the ratio mass/charge.

1.6.11 Single crystal XRD

The Single crystal X-ray diffraction data of six of the compounds, say two aroylhydrazones, two vanadium complexes, copper and cobalt complexes one each were collected on an Oxford Xcalibur Eos (Mova) Diffractometer at 100 K using Mo Kα radiation (λ=0.7107 Å)with X-ray generator operating at 50 kV and 1 mA [57]. The structures were solved and refined using SHELX97 [58] module in the program suite WinGX [59]. The molecular diagrams were generated using ORTEP-3 [60] and the packing diagrams were generated using Mercury 2.3. The geometric calculations were carried out by PARST95 and PLATON [61] and all the hydrogen atoms were fixed in calculated positions.

Single crystal X-ray diffraction data of one of the aroylhydrazones, Furan-2-carboxaldehyde nicotinoylhydrazone was collected on a CrysAlis CCD, Oxford Diffraction Ltd. diffractometer, equipped with a graphite crystal, incident-beam monochromator, and a fine focus sealed tube, Mo Kα (λ = 0.71073 Å) X-ray source at the National Single Crystal X-ray diffraction Facility, IIT, Bombay, India. The trial structure was solved using SHELXS-97 and refinement was carried out by full-matrix least squares on F^2 using SHELXL-97 [58], and all the hydrogen atoms were fixed in calculated position

Single crystal X-ray diffraction analyses of two copper complexes were performed with a Bruker SMART APEX CCD X−ray diffractometer at the University of Hyderabad, using graphite monochromated Mo Kα radiation (λ=0.71073 Å, φ and ω scans). The data was reduced using SAINTPLUS [62]. The structure was solved using SHELXS−97 and full matrix least squares

refinement against F^2 was carried out using SHELXL–97 in anisotropic approximation for non-hydrogen atoms [63]. All hydrogen atoms were assigned on the basis of geometrical considerations and were allowed to ride upon the respective carbon atoms.

The single crystal X-ray diffraction data of two aroylhydrazones and two copper complexes, were collected were collected using Bruker SMART APEX diffractometer, equipped with graphite –crystal, incident-beam monochromator, and a fine focus sealed tube with Mo Kα ($\lambda = 0.71073$ Å) as the X-ray source at SAIF, Kochi, India. Single crystal X-ray diffraction data were collected at 296(2) K. The Bruker SAINT software was used for data reduction and Bruker SMART software for data acquisition [64]. The structure was solved using SHELXL-97 by direct methods and refined by full-matrix least- squares calculations with the SHELXL-97 software package. All non-hydrogen atoms were refined anisotropically, and all hydrogen atoms on carbon were placed in calculated positions, guided by difference maps and refined isotropically. The molecular diagrams were generated using ORTEP-3 [60] and the packing diagrams were generated using Mercury 2.3. and DIAMOND version 4.2g [65].

References

[1]   E.B. Coropceanu, L. Coroitor, M.M. Botoshansky, A.V. Siminel, M.S. Fonari, Polyhedron 30 (2011) 2592.

[2]   A.B.P. Lever, Comprehensive Coordination Chemistry II (1987).

[3]   N. Chitrapriya, V. Mahalingam, M. Zeller, K. Natarajan, Inorg. Chim. Acta 363 (2010) 3685.

[4]   A.-M. Stadler, Puntoriero, F. Nastasi, S. Campagna, J.-M. Lehn. Chem. Eur. J. 16 (2010) 5645.

[5]   M. V. Angelusiu, S.-F. Barbuceanu, C. Draghici, G.L. Almajan, Eur. J. Med. Chem. 45 (2010) 2055.

[6]   B. Bottari, R. Maccari, F. Monforte, R. Ottana, E. Rotondo, M.G. Vigorita, Bioorg. Med. Chem. Lett. 10 (2000) 657.

[7]   A. Jamadar, A.K.D. Klair, K. Vemuri, M. Sritharan, P. Dandawate, S. Padhye, Dalton Trans. 41 (2012) 9192.

[8]   Q. Li, Z. Zhao, Chinese J. Org. Chem. 29 (2009).

[9]   M. I. Marzouk, Bulgarian Chem. Commun. 41 (2009) 84.

[10]   M.M. Andrade, M.T. Barros, J. Comb. Chem. 12 (2010) 245.

[11]   E.A. Enyedy, M.F. Primik, C.R. Kowol, V.B Arion, T. Kiss, B.K. Keppler, Dalton Trans. 40 (2011) 5895.

[12]   P. Barbazán, R. Carballo, E.M. Vázquez-López, Cryst. Eng. Comm. 9 (2007) 668.

[13]   M.F. Iskander, T.E. Khalil, R. Werner, W. Haase, I. Svoboda, H. Fuess, Polyhedron 19 (2000) 949.

[14]   N.A. Mangalam, S.R. Sheeja, M.R.P. Kurup, Polyhedron 29 (2010) 3318.

[15]   S. Sen, S. Mitra, D.L. Hughes, G. Rosair, C. Desplanches, Polyhedron 26 (2007) 1740.

[16]   A. Datta, K. Das, Y.-M. Jhou, J.-H. Huang, H.M. Lee, Acta Cryst. E66 (2010) 1271.

[17]   N.A. Mangalam, S. Sivakumar, S.R. Sheeja, M.R.P. Kurup, E.R.T. Tiekink, Inorg. Chim. Acta 362 (2009) 4191.

[18]   N. Mathew, M. Sithambaresan, M.R.P. Kurup, Spectrochim. Acta Part A 79 (2011) 1154.

[19]   Li, S. Gao, S. Liu, Y. Guo, Cryst. Growth Des. 10 (2010) 495.

[20]   D. Sadhukhan, A. Ray, G. Pilet, C. Rizzoli, G.M. Rosair, C.J. Gomez-García, S. Signorella, X.S. Bellu, S. Mitra, Inorg. Chem. 50 (2011) 8326.

[21]   R. Pedrido, M.J. Romero, M.R. Bermejo, A.M. González-Noya, M. Maneiro, M. Jesús Rodríguez, G. Zaragoza, Dalton Trans. (2006) 5304.

[22]   D.B. Leznoff, B.-Y. Xue, C.L. Stevens, A. Storr, R.C. Thompson, B.O. Patrick, Polyhedron 20 (2001) 1247.

[23]   A. Ray, C. Rizzoli, G. Pilet, C. Desplanches, E. Garribba, E. Rentschler, S. Mitra, Eur. J. Inorg. Chem. (2009) 2915.

[24]   O. Khan, Angew. Chem, Int. Ed. Engl. 24 (1985) 834.

[25]   E. Manoj, M.R.P. Kurup, A. Punnoose, Spectrochim. Acta Part A 72 (2009) 474.

[26]   M. Bakir, K.A. Rashid, W.H. Mulder, Talanta 51 (2000) 735.

[27]   C. Serbutoviez, C. Bosshard, G. Knopfle, P. Wyss, P. Pretre, P. Gunter, K. Schenk, E. Solan, G. Chapuis, Chem Mater 7 (1995) 1198.

[28]   R.K. Singh, J.O. Stoffer, T.D. Flaim, D.B. Hall, J.M. Torkelson, J. Appl. Polym. Sci. 92 (2004) 770.

[29]   S.K. Kurtz, T.T. Perry, J. Appl. Phys. 39 (1968) 3798.

[30]   F. Cariati, U. Caruso, R. Centore, W. Marcolli, A. De Maria, B. Panunzi, A. Roviello, A. Tuzi, Inorg. Chem. 41 (2002) 6597.

[31]   J.-M. Lehn, Chem. Eur. J. 5 (1999) 2455.

[32]   N.M.H. Salem, L. El-Sayed, M.F. Iskander, Polyhedron 27 (2008) 3215.

[33]   S. Naskar, M. Corbella, A.J. Blake, S.K. Chattopadhyay, Dalton Trans. (2007) 1150.

[34]   D. Braga, F. Grepioni, G.R. Desiraju, Chem. Rev. 98 (1998)1375.

[35]   A.M. Beatty, Coord. Chem. Rev. 246 (2003) 131.

[36]   H.S. Seleem, G.A. El-Inany, B.A. El-Shetary, M. Mousa, F.I. Hanafy, Chemistry Central Journal 5 (2011) 20.

[37]   M. Eddaoudi, J. Kim, N. Rosi, D. Vodak, J. Wachter, M.O'Keeffe, O.M. Yaghi, Science 295 (2002) 469.

[38]   L. Pan, K.M. Adams, H.E. Hernandez, X. Wang, C. Zheng, Y. Hattori, K. Kaneko, J. Am. Chem. Soc. 125 (2003) 3062.

[39]   K.T. Mahmudov, M.N. Kopylovich, M.F.C. Guedes da Silva, P.J. Figiel, Y.Yu. Karabach, A.J.L. Pombeiro, J. Mol. Cat. A Chem. 318 (2010) 44.

[40]   H.H. Monfared, R. Bikas, P. Mayer, Inorg. Chim. Acta 363 (2010) 2574.

[41]   C. Loncle, J.M. Brunel, N. Vidal, M. Dherbomez, Y. Letourneux, Eur. J. Med. Chem. 39 (2004) 1067.

[42]   P. Melnyk, V. Leroux, C. Sergheraert, P. Grellier, Bioorg Med Chem Lett. 16 (2006) 31.

[43]   J. Patole, U. Sandbhor, S. Padhye, D.N. Deobagkar, C.E. Anson, A. Powell, Bioorg. Med. Chem. Lett. 13 (2003) 51.

[44]   A.C. Cunha, J.M. Figueiredo, J.L.M. Tributino, A.L.P. Miranda, H.C. Castro, R.B. Zingali, C.A.M. Fraga, M.C.V. de Souza, V.F. Ferreira, E.J. Barreiro, Bioorg Med Chem. 11 (2003) 2051.

[45]   J.L. Buss, J. Neuzil, P. Ponka, Biochem. Soc. Trans. 30 (2002) 755.

[46]   C. Tang, E. Loeliger, I. Kinde, S. Kyere, K. Mayo, E. Barklis, Y. Sun, M. Huang, M.F. Summers J. Mol. Biol. 327 (2003) 1013.

[47]   B. Tian, M. He, Z. Tan, S. Tang, I. Hewlett, S. Chen, Y. Jin, M. Yang, Chem. Biol. Drug Des. 77 (2011) 189.

[48]   W.B. Júnior, M.S. Alexandre-Moreira, M.A. Alves, A.Perez-Rebolledo, G.L. Parrilha, E.E. Castellano, O.E. Piro, J. Eliezer, L.M. Lima, H. Beraldo, Molecules 16 (2011) 6902.

[49]   B. Szewczyk, M. Kubera, G. Nowak, Prog. Neuro-Psycopharmacol. Biol. Psychiatry 35 (2011) 693.

[50]   P.D. Zalewski, A.Q. Truong-Tran, D. Grosser, L. Jayaram, C. Murgia, R.E. Ruffin, A review. Pharmacol. Ther. 105 (2005) 127.

[51]   V. Getuatis, M. Daskeviciene, T. Malinauskas, V. Jankauskas, J. Sideravicius, Thin Solid Films 516 (2008) 8979.

[52] J.G. Hollingshaus, Pest. Biochem. Physiol. 27 (1987) 61.

[53] C. Basu, S. Chowdhury, R. Banergee, H.S. Evans, S. Mukherjee, Polyhedron 26 (2007) 3617.

[54] M. Bakir, O. Green, W.H. Mulder, J. Mol. Struct. 873 (2008) 17.

[55] R.B. Singh, P. Jain, R.P. Singh, Talanta 29 (1982) 77.

[56] A.S. Fouda, M.M. Gouda, S.I. Abd El-Rahman, Bull. Korean Chem. Soc. 21 (2000) 1085.

[57] Oxford Diffraction CrysAlis PRO CCD and CrysAlis PRO RED. Oxford Diffraction Ltd, Yarnton, England (2009).

[58] G.M. Sheldrick, Acta Crystallogr. Sect. A: 64 (2008) 112.

[59] L.J. Farrugia, J. Appl. Crystallogr. 32 (1999) 837.

[60] L.J. Farrugia, J. Appl. Crystallogr. 30 (1997) 565.

[61] A.L. Spek, J. Appl. Crystallogr. 36 (2003) 7.

[62] SAINTPLUS, Bruker AXS Inc., Madison, USA (2003).

[63] G.M. Sheldrick, SHELXTL-PLUS, Crystal Structure Analysis Package; Bruker Analytical X-ray, Madison, USA (1997).

[64] SMART and SAINT, Area Detector Software Package and SAX Area Detector Integration Program, Bruker Analytical X-ray; Madison, USA (1997).

[65] K. Brandenburg, Diamond version 3.2g, Crystal Impact GbR Bonn, Germany, (2011).

Chapter 2

SYNTHESIS, CRYSTAL STRUCTURES AND SPECTRAL CHARACTERIZATION OF SOME AROYLHYDRAZONES

2.1. Introduction

Aroylhydrazones are known to be a class of versatile ligands, capable of generating varied molecular architectures and coordination polyhedra. Aroylhydrazones with ONO donor atoms are most noteworthy for their excellent fungicidal [1], bactericidal [2,3], anticonvulsant [4], analgesic and anti-inflammatory activities [5,6]. A series of aroylhydrazones have displayed modest antitumor activity both *in vitro* and *in vivo* [7-9]. Hydrazones, RR'C=N–NR"R"', are used as intermediates in syntheses [10], as functional groups in metal carbonyls [11], in organic compounds [12,13] and are employed as catalysts [14]. Furthermore, hydrazones exhibit physiological activities in the treatment of several diseases such as tuberculosis [15,16], which is attributed to the formation of stable chelate complexes with transition metals which then catalyze physiological processes [17,18]. Aroylhydrazones exhibit interesting electric and magnetic properties [19-21]. They can act as effective catalysts in alkene epoxidation reaction [22].

Hydrazides condense with aromatic aldehydes or ketones to form hydrazones which belong to the general family of Schiff bases. Condenzation results in an extended electron delocalization along the azomethine bond. Also these compounds contain the basic unit of peptide linkage [–C(=O) –NH–] group closely related to the primary structure of proteins. So research interest in the biological properties of their metal complexes has been growing in recent years [23] and were widely investigated with regards to their function as model compounds for biological enzymes [24-25].

Many of their properties are a function of the parent aldehyde or ketone and hydrazide and these properties can therefore be elegantly tuned by the appropriate choice of parent. The flexible design and synthesis of aroylhydrazine or aroylhydrazone type ligands with an appropriate nature is crucial for the synthesis of N-arylazoles by copper-catalyzed Ullmann reaction [26].

From a structural perspective, aroylhydrazones attract attention as interesting ligands due to their tendency to undergo tautomerism and form planar, highly rigid hydrazine systems capable of imposing a variety of mixed donor coordination environments about metal cations [27].

We are particularly interested in the ability of the aroylhydrazone of 2-hydroxy-4-methoxybenzophenone to form complexes of high coordination number, mono and dinuclear structures. We have synthesised five aroylhydrazones for investigating their structural chemistry and for assessing their performance as chelating ligands in metal complexes. Fortunately crystals suitable for single crystal XRD studies were obtained for all the five compounds. A systematic crystal structure analysis and other spectrochemical characterisation of the compounds may provide further information concerning

the structural characteristics required for their antitumor, cytotoxic, catalytic, magnetic, nonlinear optical activities and chelating behavior.

Aroylhydrazones from 2-hydroxy-3-methoxybenzophenone are not reported and that from furan-2-carboxaldehyde and 5-bromo-3-methoxy-salicylaldehyde are not studied much. Benzophenone based hydrazone systems have a special structure constituted with a larger π-bond conjugated system [28]. In this chapter the crystal structure and spectral perspectives of the aroylhydrazones are discussed. The newly synthesised dynamic ligand systems consist of ONO and NO donor acylhydrazones. The ligand systems of our interest and their abbreviations are as follows

1. 2-Hydroxy-4-methoxybenzophenone benzoylhydrazone (H$_2$BB)

2. 2-Hydroxy-4-methoxybenzophenone nicotinoylhydrazone (H$_2$BN)

3. *N*-2-hydroxy-4-methoxybenzophenone-*N'*-4-nitrobenzoylhydrazone (H$_2$BF)

4. Furan-2-carboxaldehyde nicotinoylhydrazone (HFN)

5. 5-Bromo-3-methoxysalicylaldehyde benzoylhydrazone [H$_2$SB]

2.2. 2-Hydroxy-4-methoxybenzophenone benzoylhydrazone (H$_2$BB)

The compound 2-hydroxy-4-methoxybenzophenone benzoyl hydrazone was prepared from 2-hydroxy-4-methoxybenzophenone and benzhydrazide.
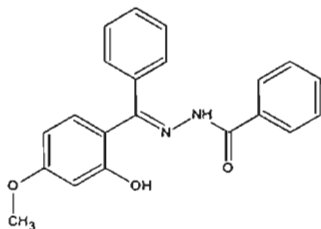
2-Hydroxy-4-methoxybenzophenone benzoylhydrazone

2.2.1. Experimental

2.2.1.1. Materials

2-Hydroxy-4-methoxybenzophenone (Aldrich), benzhydrazide (Aldrich) and DMF (S.D.Fine) were used as received. Solvents were purified by standard procedures before use.

2.2.1.2. Synthesis

The compound was synthesized by the reported procedure [29]. 2-Hydroxy-4-methoxybenzophenone (0.228 g, 1 mmol) and benzhydrazide (0.136 g, 1 mmol) were dissolved in 50 mL of absolute EtOH. Three drops of conc. HCl were added and the resulting solution was refluxed for 3 h. The compound precipitated upon cooling to room temperature, was collected by filtration and recrystallized from EtOH. Colorless block shaped crystals suitable for single crystal X-ray diffraction studies were obtained by slow evaporation of its solution in ethanol and carefully separated. The scheme for the reaction is shown below (Scheme 1). Yield: 45%, M. P.: 205° C. Elemental Anal. Found (Calcd.) (%): C: 72.42 (72.82) H: 5.56 (5.24) N: 8.07 (8.09).

2-hydroxy-4-methoxy benzophenone   benzhydrazide   2-hydroxy-4-methoxybenzophenone benzoylhydrazone
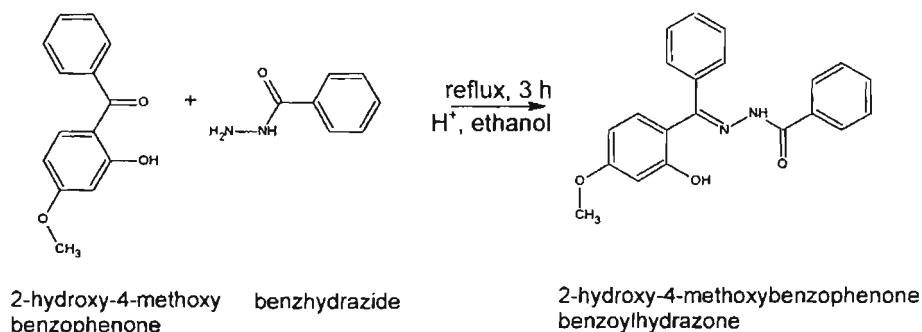
Scheme 1. Synthesis of 2-hydroxy-4-methoxybenzophenone benzoylhydrazone

2.2.2. Single crystal XRD studies

The Single crystal X-ray diffraction data of H_2BB were collected on an Oxford Xcalibur Eos (Mova) Diffractometer at 100 K using Mo Kα radiation (λ=0.7107 Å) with X-ray generator operating at 50 kV and 1 mA. The structures were solved and refined using SHELX97 module in the program suite WinGX. The molecular diagrams were generated using ORTEP-3 and the packing diagrams were generated using Mercury 2.3. The geometric calculations were carried out by PARST95 and PLATON and all the hydrogen atoms were fixed in calculated positions.

2.2.2.1. Crystal structure of H_2BB

H_2BB crystallizes in space group *P*-1 with Z=2. Colorless block shaped crystals suitable for diffraction analyses were grown by slow evaporation of a saturated solution of H_2BB in ethanol. A view of the molecule showing the atom labeling scheme is shown in Fig. 2.1 and selected structural refinement parameters are given in Table 2.1.

The C15–O3 bond (1.2196(19) Å) has a double bond character [30] which shows that the molecule exists in amido form in the solid state. The torsion angle of -8.8(2)° perceived by N1–C8–C5–C6 moiety supports the *cis* configuration with respect to C8-C5 bond in the ligand. So the potential donors O2 and N1 are found in *syn* disposition. This arrangement enables the O(2)–H to involve in H-bonding (Fig. 2.2) with azomethine N1 atom of the aroylhydrazone resulting in a six membered pseudo-aromatic ring (N1–C8–C5–C6-O2-H) which is enhanced by electron delocalization as it is seen easily from the bond lengths within the ring (Table 2.2). Such resonance assisted hydrogen bonds seem to be the general feature of the crystal structures of Schiff bases derived from salicylaldehyde [31].

Table 2.1. Crystal data and structure refinement for H_2BB

Empirical formula	$C_{21} H_{18} N_2 O_3$
Formula weight	346.37
Temperature/K	293(2)
Crystal system	triclinic
Space group	$P\bar{1}$
a/Å, b/Å, c/Å	7.5957(3), 10.6146(4), 11.2385(4)
$\alpha/°$, $\beta/°$, $\gamma/°$	97.967(3), 90.056(3), 99.093(3)
Volume/Å^3	885.84(6)
Z	2
ρ_{calc}/mg mm^{-3}	1.299
μ/mm^{-1}	0.088
F(000)	364
Crystal size/mm^3	0.20 × 0.20 × 0.20
Θ range for data collection	2.49 to 25.99°
Index ranges	$-9 \leq h \leq 9$, $-13 \leq k \leq 13$, $-13 \leq l \leq 13$
Reflections collected	19806
Independent reflections	3479[R(int) = 0.0323]
Data/restraints/parameters	3479/0/245
Goodness-of-fit on F^2	1.036
Final R indexes [I > 2σ (I)]	R$_1$ = 0.0445, wR$_2$ = 0.1168
Final R indexes [all data]	R$_1$ = 0.0616, wR$_2$ = 0.1276
Largest diff. peak/hole/e Å^{-3}	0.166/-0.140

$R_1 = \Sigma||F_o| - |F_c|| / \Sigma|F_o|$ $wR_2 = [\Sigma w(F_o^2 - F_c^2)^2 / \Sigma w(F_o^2)^2]^{1/2}$

The strong intramolecular O–H⋯N hydrogen bond (1.78 Å, and 148.2°) locks the molecular conformation. However, any strong classical intermolecular hydrogen bond is absent in the crystal structure. Instead, a variety of C–H⋯O interactions that is present in the structure supports building up the supramolecular assemblage (Fig. 2.3).

Mass spectrum is used for determining masses of particles, for determining the elemental composition of a sample or molecule, and for elucidating the chemical structures of molecules. MS works by ionizing chemical compounds to generate charged molecules or molecule fragments and measuring their mass-to-charge ratios [38]. MS [ESI(M+1)] exact mass calculated for $[M]^+$ ($C_{21} H_{18} N_2 O_3$) requires m/z 346.37, found m/z 347 (Fig. 2.9).

2.3. 2-Hydroxy-4-methoxybenzophenone nicotinoylhydrazone (H₂BN)

The compound 2-hydroxy-4-methoxybenzophenone nicotinoylhydrazone was prepared from 2-hydroxy-4-methoxybenzophenone and nicotinic hydrazide.
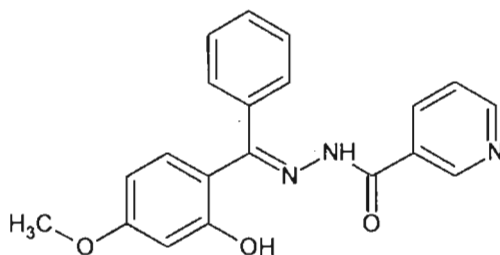
2-Hydroxy-4-methoxybenzophenone nicotinoylhydrazone

2.3.1. Experimental

2.3.1.1. Materials

2-Hydroxy-4-methoxybenzophenone (Aldrich), nicotinic hydrazide (Aldrich) and DMF (S.D.Fine) were used as received. Solvents were purified by standard procedures before use.

2.3.1.2. Synthesis

The compound was synthesized by the reported procedure [29]. 2-Hydroxy-4-methoxybenzophenone (0.228 g, 1 mmol) and nicotinic hydrazide

(0.137 g, 1 mmol) were dissolved in 50 mL of absolute EtOH. Three drops of conc. HCl were added and the resulting solution was refluxed for 3 h. The compound precipitated upon cooling to room temperature, was collected by filtration and recrystallized from EtOH. Colorless block shaped crystals suitable for single crystal analyses were obtained by slow evaporation of its solution in ethanol and were carefully separated. The scheme for the reaction is shown below (Scheme 2). Yield: 45%, M. P.: 210 °C. Elemental Anal. Found (Calcd.) (%): C: 68.76(69.15) H: 4.99(4.93) N: 12.08(12.1).

2-hydroxy-4-methoxy benzophenone   nicotinic hydrazide

2-hydroxy-4-methoxybenzophenone nicotinoylhydrazone
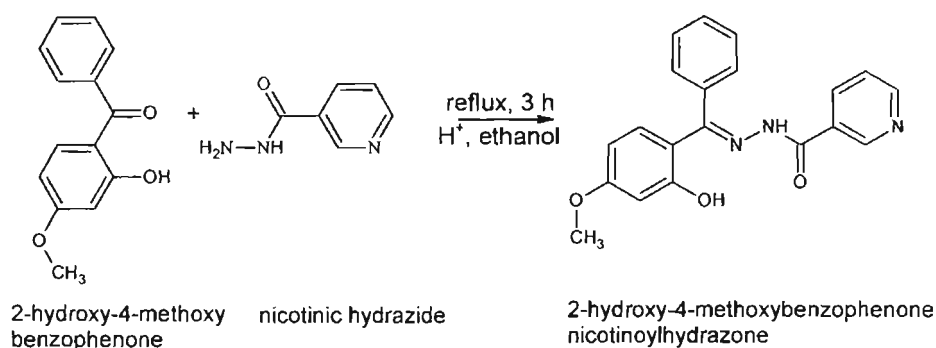
Scheme 2. Synthesis of 2-hydroxy-4-methoxybenzophenone nicotinoylhydrazone

2.3.2. Single crystal XRD studies

The Single crystal X-ray diffraction data of H$_2$BN were collected on an Oxford Xcalibur Eos (Mova) Diffractometer at 100 K using Mo Kα radiation (λ=0.7107 Å) with X-ray generator operating at 50 kV and 1 mA. The structures were solved and refined using SHELX97 module in the program suite WinGX. The molecular diagrams were generated using ORTEP-3 and the packing diagrams were generated using Mercury 2.3. The geometric calculations were carried out by PARST95 and PLATON and all the hydrogen atoms were fixed in calculated positions.

The molecular structure of H_2BN with atom labeling scheme is shown in Fig. 2.10 and selected structural refinement parameters are given in Table 2.4. The C15–O3 bond distance (1.215(2) Å) agrees well with similar bonds in related compounds [32] which shows the existence of the ligand in amido form in the solid state.

Table 2.4. Crystal data and structure refinement for H_2BN

Empirical formula	$C_{20} H_{17} N_3 O_3$
Formula weight	347.37
Temperature/K	293(2)
Crystal system	triclinic
Space group	$P1$
a/Å, b/Å, c/Å	7.1565(10), 10.5650(14), 11.5235(6)
$\alpha/°$, $\beta/°$, $\gamma/°$	95.761(8), 95.368(8), 97.430(11)
Volume/$Å^3$	854.57(17)
Z	2
ρ_{calc}/mg mm^{-3}	1.350
μ/mm^{-1}	0.093
F(000)	364
Crystal size/mm^3	$0.20 \times 0.20 \times 0.10$
2Θ range for data collection	4.9802 to 61.6792°
Index ranges	$-9 \leq h \leq 10$, $-14 \leq k \leq 15$, $-15 \leq l \leq 16$
Reflections collected	22495
Independent reflections	3353[R(int) = 0.0355]
Data/restraints/parameters	3353/21/239
Goodness-of-fit on F^2	1.108
Final R indexes [I > 2σ (I)]	$R_1 = 0.0565$, $wR_2 = 0.1613$
Final R indexes [all data]	$R_1 = 0.0704$, $wR_2 = 0.1716$
Largest diff. peak/hole/e $Å^{-3}$	0.359/-0.289

$R_1 = \Sigma||F_o| - |F_c|| / \Sigma|F_o|$, $wR_2 = [\Sigma w(F_o^2 - F_c^2)^2 / \Sigma w(F_o^2)^2]^{1/2}$

The N1–N2 and N2–C15 bond lengths (Table 2.5) are indicative of some double bond character suggesting delocalization of π electron density over the hydrazone portion of the molecule. Atoms N2–N1–C8–C5–C9 are coplanar with a maximum deviation of 0.010(2) Å for C8 from the plane which also enhances the delocalisation.

Table 2.5. Selected bond lengths (Å) and bond angles (°) for H₂BN

Bond lengths		Bond angles	
C15–O3	1.215(2)	N1–N2–C15	120.17(16)
C15–N2	1.354(2)	N2–N1–C8	117.59(16)
N2–N1	1.380(2)	C6–C5–C8	122.68(16)
N1–C8	1.295(2)	N1–C8–C5	116.88(16)
C8–C5	1.465(2)	N1–C8–C9	121.68(16)
C15–C16	1.492(3)	O3–C15–N2	122.77(18)
C2–O1	1.362(2)	O3–C15–	122.69(17)
C6–O2	1.359(2)	C16	116.68(16)
C5–C6	1.414(2)	C6–C5–C4	

The configuration about C8–C5 bond is *cis* with respect to N1 and C6 as shown by the torsion angle of 8.3(3)° perceived by N1–C8–C5–C6 moiety and the configurations about N1–C8 and N2–C15 are also *Z* which are supported by the torsion angles N2–N1–C8–C9, 0.5(3)° and N1–N2–C15–O3, -1.5(3)° respectively. This arrangement enables the O(2)–H to involve in H-bonding with azomethine N2-atom of the ligand resulting in a six membered pseudo-aromatic ring (N1–C8–C5–C6–O2–H) which is enhanced by electron delocalization as can be seen easily from the bond lengths within the ring (Table 2.6). Such resonance assisted hydrogen bonds seem to be the general feature of the crystal structures of Schiff bases derived from salicylaldehyde [39]. The strong intramolecular O–H⋯N hydrogen bond (1.76 Å, and 146.2°) locks the molecular conformation (Fig. 2.11) and minimizes the rotational freedom about the C5–C8 bond.

The salicyl-hydrazone part of the molecule is essentially planar due to the presence of this hydrogen bond. The maximum deviations from the least-squares planes calculated for the hydrazone moiety i.e. N2–N1–C8–C5–C9, is 0.010(2) Å for C8 and N1–N2–C15–C16–O3, is 0.019(2) Å for N2.

The above said planarity and bond distances indicate significant delocalization of π-electron density over the hydrazone portion of the molecule.

The ligand molecule as a whole has no planarity. The methoxysalicyl ring and pyridyl ring make dihedral angles of 9.43(10)° and 17.07(13)° with the hydrazone bridge. The phenyl substituent is attached nearly orthogonal to the central hydrazone moiety as proved by the dihedral angle between the two, 71.23(11)°. The dihedral angle between the phenyl ring and the pyridyl ring is 80.91(2)° and that with methoxysalicyl ring is 76.49(10)°. These dispositions are to cope up with steric factors mainly around C8. The steric repulsion between the phenyl ring and the methoxysalicyl group contracts the N1–C8–C5 and C6–C5–C4 angles to 116.88(16)° and 116.68(16)° respectively [40].

The above observations indicate nonplanarity of the aroylhydrazone although the hydrazone part itself is planar. The molecule exists in an anti configuration with respect to the C8–N1 and C15–N2 bonds. This is confirmed by the torsion angles of 179.88(12)° and -177.57(12)° respectively for N2–N1–C8–C5 and N1–N2–C15–C16 moieties.

As in case of H_2BB, the strong intramolecular O–H⋯N hydrogen bond (1.76 Å, and 146.9°) locks the molecular conformation. The main structural feature that facilitate the crystal packing is the stacking of molecules along crystallographic a direction by means of π⋯π interaction (3.72 Å) and intermolecular C–H⋯O interaction (2.35 Å, and 172.6°) which act in a

The assignments are confirmed by the deuteriated proton spectrum in which the intensity of these signals are considerably reduced. Multiplets observed in the 6.2–8.7 ppm range are assigned to the aromatic protons. A singlet at 3.8 ppm corresponds to the methoxy proton. Fig. 2.18 shows the ^{1}H NMR spectrum of H_2BN.

2.3.3.4. Mass spectrum

Mass spectrometry (MS) is an analytical technique that measures the mass-to-charge ratio of charged particles. MS works by ionizing chemical compounds to generate charged molecules or molecule fragments and measuring their mass-to-charge ratios [38]. MS [ESI(M+1)] exact mass calculated for [M]$^+$ (C_{20} H_{17} N_3 O_3) requires m/z 347.37, found m/z 348.2 (Fig. 2.19).
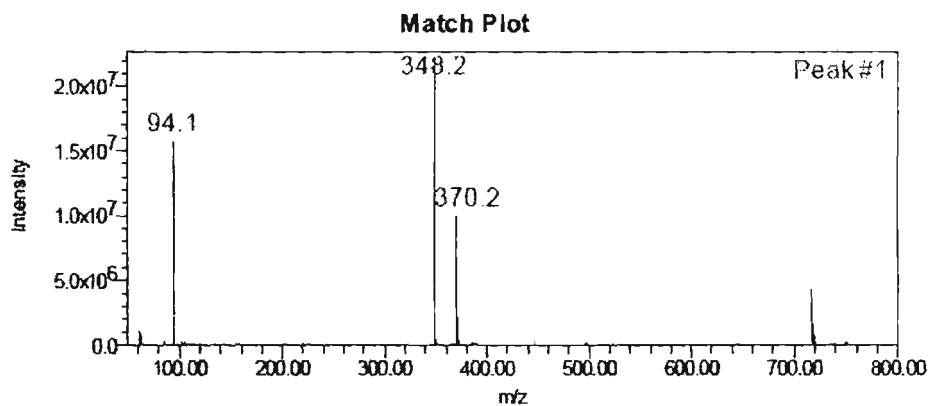
Fig. 2.19. Mass spectrum of H_2BN (M+1).

2.4. N-2-Hydroxy-4-methoxybenzophenone-N'-4-nitrobenzoylhydrazone (H_2BF)

The compound N-2-hydroxy-4-methoxybenzophenone-N'-4-nitrobenzoylhydrazone was prepared from 2-hydroxy-4-methoxybenzophenone and N'-4-nitrobenzoyl hydrazide.
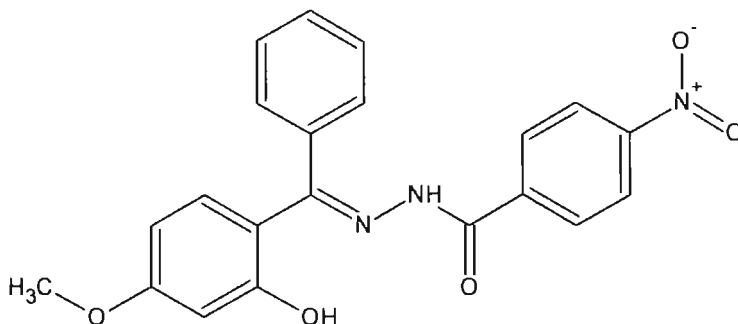
N-2-Hydroxy-4-methoxybenzophenone-*N'*-4-nitrobenzoylhydrazone

2.4.1. Experimental

2.4.1.1. Materials

2-Hydroxy-4-methoxybenzophenone (Aldrich), and *N'*-4-nitrobenzoylhydrazide (Aldrich) and DMF (S.D.Fine) were used as received. Solvents were purified by standard procedures before use.

2.4.1.2. Synthesis

The compound was synthesized by adapting the reported procedure [29]. 2-Hydroxy-4-methoxybenzophenone (0.228 g, 1 mmol) and *N'*-4-nitrobenzoylhydrazide (0.181 g, 1 mmol) were dissolved in 50 mL of absolute EtOH. Three drops of conc. HCl were added and the resulting solution was refluxed for 3 h. The compound precipitated upon cooling to room temperature, was collected by filtration and recrystallized from EtOH. Colorless block shaped crystals suitable for single crystal analyses were grown from a solution of the compound in a mixture of DMF and ethanol (1:1 v/v). The scheme for the reaction is shown below (Scheme 3). Yield: 45%, M. P.: 207 °C. Elemental Anal. Found (Calcd.) (%): C: 64.27 (64.45) H: 4.52 (4.38) N: 10.57 (10.74).

2-Hydroxy-4-methoxy- N'-4-nitrobenzhydrazide   N-2-Hydroxy-4-methoxy-benzophenone
benzophenone   N'-4-nitrobenzhydrazone
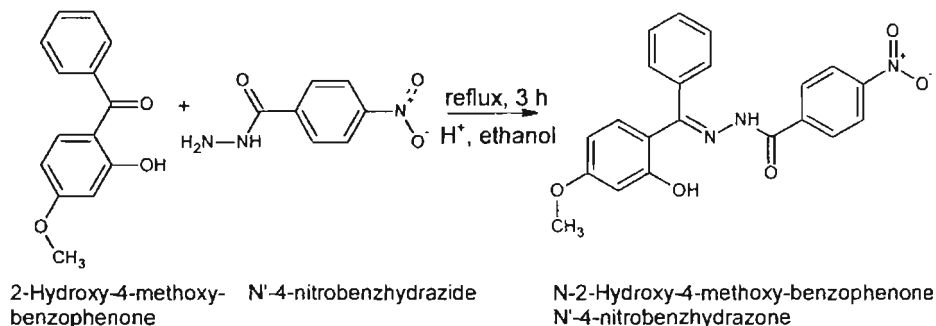
Scheme 3. Synthesis of N-2-hydroxy-4-methoxybenzophenone-
N'-4-nitrobenzoylhydrazone

2.4.2. Single crystal XRD studies

The single crystal X-ray diffraction data of H_2BF, were collected using Bruker SMART APEX diffractometer, equipped with graphite –crystal, incident-beam monochromator, and a fine focus sealed tube with Mo Kα (λ = 0.71073 Å) as the X-ray source. The structure was solved by direct methods and refined by full-matrix least- squares calculations with the SHELXL-97 software package and all hydrogen atoms on carbon were placed in calculated positions, guided by difference maps and refined isotropically. The molecular diagrams were generated using ORTEP-3 and the packing diagrams were generated using Mercury 2.3. and DIAMOND version 4.2g.

Table 2.7 Crystal data and structure refinement for H_2BF

Empirical formula	$C_{21} H_{17} N_3 O_6$
Formula weight	391.38
Temperature	296(2) K
Wavelength	0.71073 Å
Crystal system, space group	Monoclinic $P2_1/n$
Unit cell	a = 11.2512(10) Å
	b = 24.105(2)) Å
	c = 13.9105(11) Å
	$\alpha = 90°$
	$\beta = 93.204(3)°$
	$\gamma = 90°$
Volume	3766.8(5) Å^3
Z	8
Calculated density	1.380 Mg/ m^3
Absorption coefficient	0.101 mm^{-1}
F(000)	1632.0
Crystal size	0.35x0.30 x 0.25 mm^3
Theta range for data collection	2.24 to 25.00°.
Limiting indices	-13≤h≤13
	-28≤k≤28
	-16≤l≤14
Reflections collected	56673
Independent reflections	6644
Absorption correction	Semi-empirical from equivalents
Max. and min. transmission	0.9792 and 0.9711
Refinement method	Full-matrix least-squares on F^2
Data / restraints / parameters	6627 / 4 / 542
Goodness-of-fit on F^2	1.045
Final R indices [I > 2sigma(I)]	$R_1 = 0.0505$, $wR_2 = 0.1205$
R indices (all data)	$R_1 = 0.1099$, $wR_2 = 0.1648$
Largest diff. peak and hole	0.529 and -0.265 e. A^{-3}

$R_1 = \Sigma||F_o| - |F_c|| / \Sigma|F_o| \, wR_2 = [\Sigma w(F_o^2-F_c^2)^2 / \Sigma w(F_o^2)^2]^{1/2}$

The C7–N1 bond length of 1.298(3) Å confirms its significant double-bond character which indicates the formation of azomethine bond by condenzation. The values of 1.372(3) and 1.343(3) Å for the bond distances of

N1–N2 and N2–C14 respectively, are greater than the value for a double bond and less than the value for a single bond, which indicate significant delocalization of π-electron density over the hydrazone portion of the molecule [45].

Table 2.8 Selected bond lengths (Å) and bond angles (°) for H_2BF

Bond lengths		Bond angles	
O(1)–C(3)	1.363(4)	C(7)–N(1)–N(2)	117.5(2)
C(5)–C(6)	1.405(3)	C(14)–N(2)–N(1)	120.4(2)
O(2)–C(5)	1.349(3)	C(5)–C(6)–C(1)	116.6(2)
C(6)–C(7)	1.459(4)	N(1)–C(7)–C(6)	116.8(2)
C(7) – N(1)	1.298(3)	N(2)–C(14)–O(3)	122.7(3)
N(1)–N(2)	1.372(3)		
N(2)–C(14)	1.343(3)		
C(14)–O(3)	1.220(3)		

The formation of strong intramolecular $O(2)–H(2)\cdots N(1)$ hydrogen bond (1.80(3) Å and 146(3)°) locks the molecular conformation resulting in a six membered pseudo-aromatic ring (N1–C8–C5··C6 O1·-H) which is enhanced by electron delocalization as can be seen easily from the bond lengths within the ring (Table 2.9). This is also supported by the *cis* configuration of C6–C7 bond with respect to N1 and C5 as shown by the torsion angle of -5.2(4)° perceived by N1–C7–C6–C5 moiety. N2–C14 and C14 C15 are also in *cis* configuration with respect to N1 and O3, N2 and C20 respectively as shown by the torsion angles N1–N2–C14 O3, 4.0(4)° and N2 C14 C15–C20, 23.5(4)°. The maximum deviation from the least-squares plane calculated for atoms O3, N1, N2, C14 and C15 is 0.036(2) Å for the N2 atom. The 4-methoxysalicyl ring is syn-periplanar to 4-nitro phenyl ring as seen from the dihedral angle of 7.65° between the rings. These facts support the planarity and delocalization of π-electron density over the central hydrazone moiety.

2.5. Furan-2-carboxaldehyde nicotinoylhydrazone (HFN)

The compound furan-2-carboxaldehyde nicotinoylhydrazone was prepared from furan-2-carboxaldehyde and nicotinichydrazide.
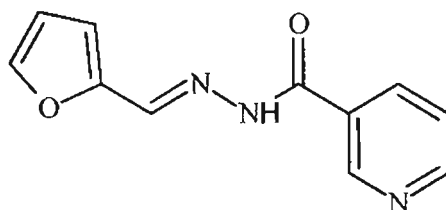
Furan-2-carboxaldehyde nicotinoylhydrazone

2.5.1. Experimental

2.5.1.1. Materials

Furan-2-carboxaldehyde (Aldrich), nicotinichydrazide (Aldrich) and DMF (S.D.Fine) were used as received. Solvents were purified by standard procedures before use.

2.5.1.2. Synthesis

The compound was synthesized by adapting the reported procedure [29]. Furan-2-carboxaldehyde (0.08 mL, 1 mmol) and nicotinic hydrazide (0.137 g, 1 mmol) were dissolved in 50 mL of absolute EtOH and the resulting solution was refluxed for 3 h. The compound precipitated upon cooling to room temperature, was collected by filtration and recrystallized from EtOH. Colorless block shaped crystals suitable for single crystal analysis were grown by slow evaporation of a saturated solution of HFN in ethanol. The scheme for the reaction is shown below (Scheme 4). Yield: 45%, M. P.: 210° C. Elemental Anal. Found (Calcd.) (%): C: 61.21(61.39) H: 4.12 (4.22) N: 19.38 (19.53).

| furan-2-carboxaldehyde | nicotinichydrazide | | furan-2-carboxaldehyde nicotinoylhydrazone |
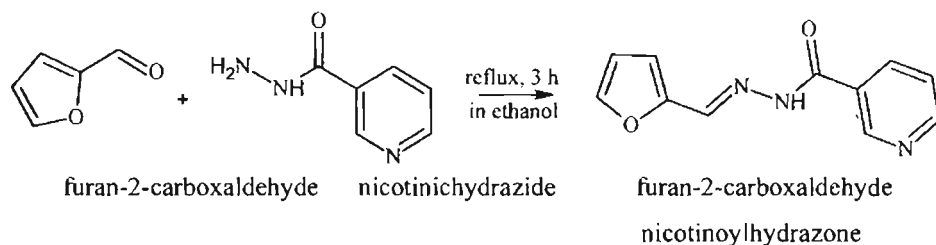
Scheme 4. Synthesis of furan-2-carboxaldehyde nicotinoylhydrazone.

2.5.2. Single crystal XRD studies

Single crystal X-ray diffraction data of aroylhydrazone (HFN) is collected on a CrysAlis CCD, Oxford Diffraction Ltd. diffractometer, equipped with a graphite crystal, incident-beam monochromator, and a fine focus sealed tube, Mo Kα $(\lambda = 0.71073$ Å) X-ray source at the National Single Crystal X-ray diffraction Facility, IIT, Bombay, India. The trial structure was solved using SHELXS-97 and refinement was carried out by full-matrix least squares on F^2 using SHELXL-97, and all the hydrogen atoms were fixed in calculated positions.

2.5.2.1. Crystal structure of HFN

Pale pink block shaped crystals suitable for diffraction analyses were grown by slow evaporation of a saturated solution of HFN in ethanol. The aroylhydrazone crystallizes in triclinic space group P-1. There are two independent molecules (Fig. 2.27) in the asymmetric unit with almost the same bond length and bond angle, and therefore the detailed description can be limited to one of these molecules. Fig. 2.28 shows the centrosymmetric dimers linked through H bonding.

The molecule adopts an E configuration with respect to C7=N3 bond and it exists in the keto form with C6=O1 bond length of 1.226 (2) Å which is

Table 2.10. Crystal data and structure refinement for HFN

Empirical formula	$C_{22} H_{18} N_6 O_4$
Formula weight	430.42
Temperature	150(2) K
Wavelength	0.71073 Å
Crystal system, space group	Triclinic, P-1
Unit cell dimensions	a = 9.441(2) Å
	α = 75.10(2)°.
	b = 10.237(3) Å
	β = 85.413(19)°
	c = 11.023(2) Å
	γ = 84.11
Volume	1022.5(4) Å^3
Z, Calculated density	2, 1.398 Mg/m^3
Absorption coefficient	0.100 mm^{-1}
F(000)	448
Crystal size	0.26 x 0.21 x 0.18 mm
Theta range for data collection	2.98 to 25.00 deg.
Limiting indices	-11 < =h< =11, -12< =k< =11, -12< =l< = 13
Reflections collected / unique	9430 / 3589 [R(int) = 0.0230]
Completeness to theta	= 25.00 99.7 %
Absorption correction	Semi-empirical from equivalents
Max. and min. transmission	0.9822 and 0.9744
Refinement method	Full-matrix least-squares on F^2
Data / restraints / parameters	3589 / 0 / 297
Goodness-of-fit on F^2	0.893
Final R indices [I > 2sigma(I)]	R_1 = 0.0408, wR_2 = 0.1150
R indices (all data)	R_1 = 0.0570, wR_2 = 0.1255
Largest diff. peak and hole	0.213 and -0.329 e. A^{-3}

$R_1 = \Sigma||F_o| - |F_c|| / \Sigma|F_o| wR_2 = [\Sigma w(F_o^2 - F_c^2)^2 / \Sigma w(F_o^2)^2]^{1/2}$

The molecules shown participate in C–H···π interactions formed between the H atoms attached at the C10 and C12 atoms and the furan rings (Table 2.12). The presence of π–π interactions, with centroid centroid distances of 3.7864(15), 3.7864(15), 3.7274(15) and 3.7273(15) Å between the rings, is also noted [48].

their mass-to-charge ratios [38]. MS [ESI(M+1)] exact mass calculated for [M]'
(C$_{11}$ H$_9$ N$_3$ O$_2$) requires *m/z* 215, found *m/z* 216.2 (fig. 2.34).

Match Plot
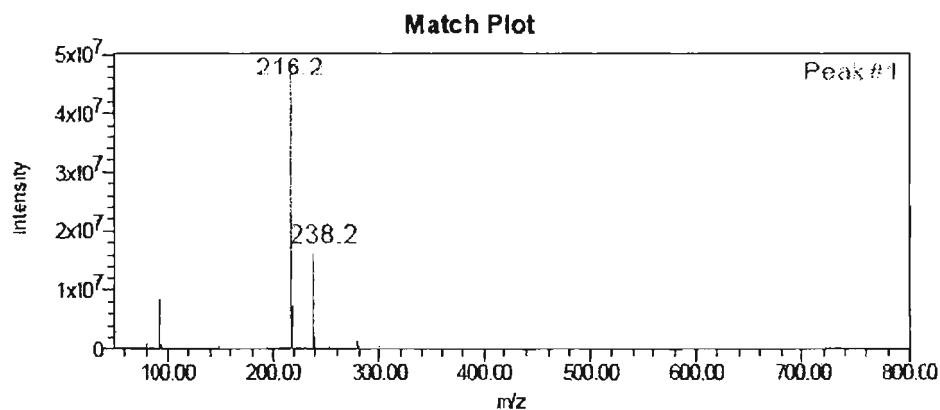
Fig. 2.34. Mass spectrum of HFN (M+1).

2.6 . 5-Bromo-3-methoxysalicylaldehyde benzoylhydrazone (H$_2$SB)

The compound 5-bromo-3-methoxysalicylaldehyde benzoylhydrazone (H$_2$SB)
was prepared from 5-bromo-3-methoxysalicylaldehyde and benzhydrazide.
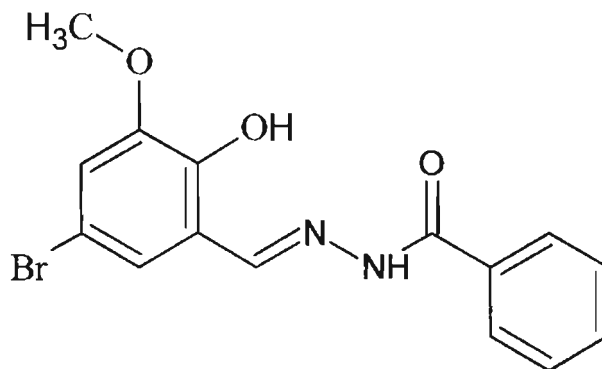
5-Bromo-3-methoxysalicylaldehyde benzoylhydrazone

2.6.1. Experimental

2.6.1.1. Materials

5-Bromo-3-methoxysalicylaldehyde (Aldrich), benzhydrazide (Aldrich) and DMF (S.D.Fine) were used as received. Solvents were purified by standard procedures before use.

2.6.1.2. Synthesis

The compound was synthesized by adapting the reported procedure [29]. 5-Bromo-3-methoxysalicylaldehyde (0.231 g, 1 mmol) and benzhydrazide (0.136 g, 1 mmol) were dissolved in 50 mL of absolute EtOH. The resulting solution was refluxed for 3 h. The compound precipitated upon cooling to room temperature, was collected by filtration and recrystallized from EtOH. Colorless block shaped crystals suitable for single crystal analyses were grown from a solution of the compound in a mixture of DMF and ethanol (1:1 v/v). The scheme for the reaction is shown below (Scheme 5). Yield: 45%, M. P.: 202 °C. Elemental Anal. Found (Calcd.) (%): C: 51.22 (51.60) H: 3.42 (3.75) N: 7.88 (8.02).

5-bromo-3-methoxysalicyl aldehyde   benzhydrazide   5-bromo-3-methoxysalicylaldehyde benzoylhydrazone
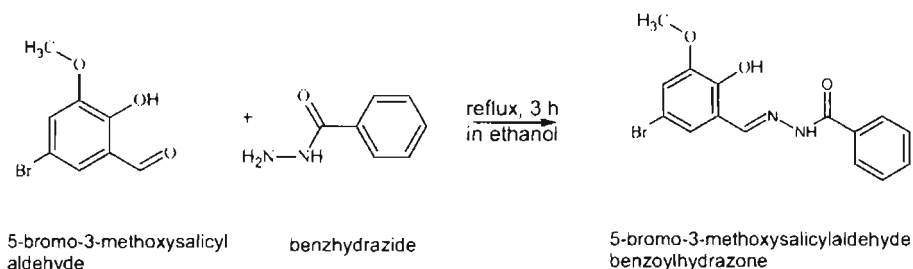
Scheme 5. Synthesis of 5-bromo-3-methoxysalicylaldehyde benzoylhydrazone

2.6.2. Single crystal XRD studies

The single crystal X-ray diffraction data of H_2BF, were collected using Bruker SMART APEX diffractometer, equipped with graphite –crystal,

The bond angles and bond lengths are summarised in Table 2.14. They are similar to those reported for substituted aroyl hydrazones [44]. The C8–O3 bond has a significant double bond character, 1.214(7) Å shows the existence of the ligand in amido form in the solid state. The C7–N1 bond length of 1.273(9) Å confirms its significant double-bond character.

Table 2.13. Crystal data and structure refinement for H_2SB

Empirical formula	$C_{15} H_{15} Br N_2 O_4$
Formula weight	367.19
Temperature	293(2) K
Wavelength	0.71073 Å
Crystal system, space group	Orthorhombic, $P2_1 2_1 2_1$
Unit cell dimensions	a = 4.7223(5) Å α = 90°
	b = 13.9357(17) Å β = 90°.
	c = 23.028(3) Å γ = 90°.
Volume	1515.4(3) Å³
Z, Calculated density	4, 1.609 Mg/m³
Absorption coefficient	2.732 mm⁻¹
F(000)	744.0
Crystal size	0.32 x 0.25 x 0.22 mm
Theta range for data collection	1.71 to 26.00°
Limiting indices	-5 < =h< =5, -17 < =k < =17, -22 < =l < = 28
Reflections collected / unique	12769 / 2969 [R(int) = 0.0899]
Completeness to theta	= 26.00 99.9 %
Absorption correction	Semi-empirical from equivalents
Max. and min. transmission	0.549 and 0.446
Refinement method	Full-matrix least-squares on F^2
Data / restraints / parameters	2968 / 3 / 208
Goodness-of-fit on F^2	1.070
Final R indices [I > 2sigma(I)]	R_1 = 0.0541, wR_2 = 0.1390
R indices (all data)	R_1 = 0.0798, wR_2 = 0.1680
Absolute structure parameter	0.00(2)
Largest diff. peak and hole	1.210 and -0.372 e.A⁻³

$R_1 = \Sigma||F_o| - |F_c|| / \Sigma|F_o| wR_2 = [\Sigma w(F_o^2 - F_c^2)^2 / \Sigma w(F_o^2)^2]^{1/2}$

The values of 1.378(7) and 1.353(7) Å for the bond distances of N1–N2 and N2–C8 respectively, are greater than the value for a double bond and less than the value for a single bond, which indicate significant delocalization of π-electron density over the hydrazone portion of the molecule.

The configuration of C6–C7 bond is *cis* with respect to N1 and C1 as shown by the torsion angle of -1.0(9)° perceived by N1–C6–C7–C1 moiety. This arrangement enables the O(1)–H to form strong intramolecular H-bond with azomethine N1 atom (1.93 Å and 145°) resulting in a six membered pseudo-aromatic ring (N1–C8–C5–C6–O1–H) which is enhanced by electron delocalization as can be seen easily from the bond lengths within the ring (Table 2.15) configuration about N2–C8 and C8–C9 are also *cis* with respect to N1 and O3, N2 and C10 respectively which is supported by the torsion angles N1–N2–C8–O3, - 0.6(8)° and N2–C8–C9–C10, 4.9(8)°. This supports the disposition of O3, N2 and C10 to involve in H-bonding with water molecules on either side of the hydrazone moiety (Table 2.15).

The molecule as a whole is roughly planar with a maximum dihedral angle of 5.2(3)° between the rings formed by the atoms C1, C2, C3, C4, C5, C6 and C9, C10, C11, C12, C13, C14 respectively. The maximum deviation from the least-squares plane calculated for all non hydrogen atoms is 0.095(7) Å for the C13 atom. The torsion angle values, 179.7(5)° and 179.4(5)° attained by C8–N1–N2–C7 and N1–N2–C8–C9 suggest the existence of the ligand in *trans* configuration along the N1–N2 which supports the possibility of intermolecular C7–H7···O1W weak hydrogen bonding (2.50 Å, 146°) and trans along N2– C8 which supports the possibility of intermolecular C10–H10···O1W weak hydrogen bonding (2.42 Å, 166°). The structure of the compound is given in Fig. 2.35.

Table 2.14. Bond lengths [Å] and angles [°] for H$_2$SB

Bond lengths (g)		Bond angles (°)	
C(1)–O(1)	1.337(7)	C(7)–N(1)–N(2)	116.2(6)
C(2)–O(2)	1.363(7)	C(8)–N(2)–N(1)	119.1(5)
C(1)–C(6)	1.398(8)	C(5)–C(6)–C(1)	119.7(5)
C(6) –C(7)	1.441(9)	N(1)–C(7)–C(6)	122.3(6)
C(7) – N(1)	1.273(9)	N(2)–C(8)–C(9)	115.3(5)
N(1)–N(2)	1.378(7)		
N(2)–C(8)	1.353(7)		
C(8)–O(3)	1.214(7)		

The principal feature of the crystal packing is the formation of a supramolecular chain mediated by a network of hydrogen bonds (Fig. 2.36 and Table 2.15). The water molecules present in the lattice are involved in a double donor-single acceptor hydrogen bond (Fig. 2.38). The novelty about this crystal lies in the packing; three molecules are involved in intermolecular hydrogen bonding interactions with one water molecule. H(1A) from water is connected to O3 of one hydrazone molecule, H(1B) of the same water molecule is bonded to O1 of a second molecule and O1W of the water molecule is attached to N2–H(2N) of a third hydrazone moiety through intermolecular hydrogen bonding interactions. Finally these chains are linked in to highly ribbed 3D array by extensive hydrogen bonding interactions including C–H···O contacts (Fig. 2.37).

Molecules are stacked one dimensionally along 'a' axis (Fig.2.36). C–H···O, C–H···π and very weak Cg···Cg interactions support this (Table 2.15). The molecules form separate slanding layers in a zig-zag fashion progressing along crystallographic 'b' axis (Fig.2.39). Neighboring molecules in each layer are linked through a water molecule by H-bonding interactions. This linking continues infinitely in the direction of the crystallographic 'b' axis as shown in Fig. 2.39.

[6]   M.A.A. Radhwan, E. A. Ragah, N.M. Sabry, S.M. El- Shenawy, Bioorg. Med. Chem. 15 (2007) 3832.

[7]   N. Terzioglu, A. Gursoy, Eur. J. Med. Chem. 38 (2003) 781.

[8]   P. Vicini, M. Incerti, I.A. Doytchinova, P.L. Colla, B. Busonera, R. Loddo, Eur. J. Med. Chem. 41 (2006) 624.

[9]   K. Sztanke, K. Pasterhak, J. Rzymowska, M. Sztanke, M. Kandefer-Szerszen, Eur. J. Med. Chem. 43 (2007) 404.

[10]   F. Armbruster, U. Klingebiel, M. Noltemeyer, Z.   Naturforsch. 61b (2006) 225.

[11]   O.S. Senturk, S. Sert, U. Ozdemir, Z. Naturforsch. 58b   (2003) 1124.

[12]   A.E.G.E. Amr, A.M. Mohamed, A.A. Ibrahim, Z. Naturforsch. 58b (2003) 861.

[13]   H. Mohrle, G. Keller, Z. Naturforsch. 58b (2003) 885.

[14]   C. Janiak, P.-G. Lassahn, V. Lozan, Macromol. Symp. 236 (2006) 88.

[15]   K. Bedia, O. Elcin, U. Seda, K. Fatma, S. Nathalay, R. Sevim, A. Dimoglo, Eur. J. Med. Chem. 41 (2006) 1253.

[16]   D. Sriram, P. Yogeeswari, R.V. Devakaram, Bioorg. Med. Chem. 14 (2006) 3113.

[17]   M. Mohan, M.P. Gupta, N.K. Jha, Inorg. Chim. Acta. 151 (1988) 61.

[18]   E.M. Sah, D.J. Drain, M. Seiler, J. Pharm. Pharmacol. 4 (1952) 844.

[19] R. Sumita, D.D. Mishra, R.V. Maurya, N. Nageswara, Polyhedron 16 (1997) 1825.

[20] M.F. Iskander, T.E. Khalil, R. Werner, W. Haase, I. Svoboda, H. Fuess, Polyhedron 19 (2000) 1181.

[21] S.C. Chan, L.L. Koh, P.-H. Leung, J.D. Ranford, K. Y. Sim, Inorg. Chim. Acta. 236 (1995) 83.

[22] O. Pouralimardan, A.C. Chamayou, C. Janiak, H.H. Monfared, Inorg. Chim. Acta. 360 (2007) 1599.

[23] D.S. Kalinowski, P.C. Sharpe, P.V. Bernhardt, Des R. Richardson, J. Med. Chem. 51 (2008) 331.

[24] A.S.N. Murthy, A.R. Reddy, Proc. Indian Acad. Sci. Chem. Sci. 90 (1981) 519.

[25] D.K. Johnson, M.J. Pippard, T.B. Murphy, N.J. Rose, J. Pharmacol. Exp. Ther. 221(1982) 399.

[26] V.I. Sorokin, Mini-Reviews in Organic Chemistry, 2008, 5, 323.

[27] P.B. Sreeja, M.R.P. Kurup, Spectrochim Acta Part A 61 (2005) 331.

[28] P.V. Bernhardt, G.J. Wilson, P.C. Sharpe, D.S. Kalinowski, D.R. Richardson, J. Biol. Inorg. Chem.(2008) 107.

[29] M. Kuriakose, M.R.P. Kurup, E. Suresh, Spectrochim Acta Part A 66 (2007) 353.

[30] X.-F. Shi, C.-Y. Liu, B. Liu and C.-C. Yuan Acta Cryst. E63 (2007) o1295.

[31] R.G. Baughman, K.L. Martin, R.K. Singh and J.O. Stoffer, Acta Cryst. C60 (2004) o103.

[32]   Allen. F. H. Acta Cryst. B58 (2002) 380.

[33]   H.-Y. Bana and C.-M. Lib, Acta Cryst. (2009). E65, o3272.

[34]   P.B. Sreeja, A. Sreekanth, C R. Nayar, M.R.P. Kurup, A. Usman, I.A. Razak, S. Chantrapromma, H.-K. Fun, J. Mol. Struct. 645 (2003) 221.

[35]   A. Manimekalai, N. Saradhadevi, A. Thiruvalluvar,   Spectrochim. Acta Part A 77 (2010) 687.

[36]   S.Patai, The chemistry of Carbon-Nitrogen Double Bond, Interscience publishers, John Wiley & Sons, London (1970).

[37]   R.M. Silverstein, G.C. Bassler, T.C. Morrill, Spectrometric Identification of Organic Compounds, fourth ed., Wiley, New York, 1981.

[38]   Price, Phil, J. A. Soc. for Mass Spectrometry 2, 4 (1991) 336.

[39]   E.B. Seena, M.R.P. Kurup, E. Suresh, J. Chem. Cryst. (2008) 38:93.

[40]   G.-B. Cao, Acta Cryst. E65 (2009) o2645.

[41]   S. Hashemian, V. Ghaeinee and B. Notash, Acta Cryst. E67 (2011) o171.

[42]   M. Shalash, A. Salhin, R. Adnan, C.S. Yeap, H.-K. Fun, Acta Cryst. E66 (2010) o3126.

[43]   Y. Lei, Acta Cryst. E67 (2011) o162.

[44]   W.Y. Liu, Y.Z. Li, Acta Cryst. E60 (2004) o694.

[45]   C.-B. Tang, Acta Cryst. E68 (2010) o602.

[46]   S.R. Sheeja, N.A. Mangalam, M.R.P. Kurup, Y.S. Mary, K. Raju, H.T. Varghese, C.Y. Panicker, J. Mol. Struct. 973 (2010) 36.

[47]   F.H. Allen, O. Kennard, D.G. Watson, L. Brammer, A.G. Orpen, R. Taylor, J. Chem. Soc. Perkin Trans. 2. (1987) S1–19.

[48]   M.-Z. Song, C.-G. Fan, Acta Cryst. E65 (2009) o2800.

SYNTHESES, CRYSTAL STRUCTURES AND SPECTRAL STUDIES OF OXIDO/DIOXIDOVANADIUM(IV/V) COMPLEXES DERIVED FROM TRIDENTATE AROYLHYDRAZONES

3.1 Introduction

Nowadays, one of the major research goals of a chemist is to find new and efficient catalysts for the industrially important reactions. Oxido vanadium(IV) Schiff base complexes have obtained much attention due to their catalytic properties [1]. The metal ions and their biomolecular complexes are essential for life on earth and are important not only in metalloproteins and metalloenzymes but also in gene expression [2]. Vanadium is normally present in very low concentrations ($<10^{-8}$ M) in all plant and animal cells. Vanadium complexes containing diazo and hydrazido group attracts attention as they are useful in understanding the mechanism of metalloenzymatic reduction of nitrogen. Vanadium has an electronic configuration of $[Ar]3d^3 4s^2$, and the common oxidation states of vanadium include +2, +3, +4, and +5. The +1 oxidation state is rarely seen. Under physiological conditions, both the +4 and +5 oxidation states of vanadium are accessible kinetically and thermodynamically.

Vanadium exists in a plethora of oxidation states 3, 4 and 5. It readily forms V–O bonds and comfortably binds N and S, forming chemically robust coordination compounds. Vanadium(V) in particular, exhibits stereochemically flexible coordination geometries ranging from tetrahedral and octahedral to trigonal pyramidal and pentagonal bipyramidal [3]. The potential for redox interplay, whether $V^{(V)}/V^{(IV)}$ or $V^{(IV)}/V^{(III)}$, increases the versatility of this element in the biological milieu [4]. Coordination chemistry of vanadium is interesting because of its involvement in the inhibition of phosphate metabolizing enzymes, stimulation of phosphomutases, anticancer activity, insulin mimetic activity etc. One of the most widespread lifestyle-related diseases in the 21st century is thought to be diabetes mellitus (DM). To treat DM, several types of insulin preparations are in clinical use, but have several side effects. Thus, the disease demands extraordinary effects to define pathobiochemical pathways and strategies for prevention. For this purpose, oxido vanadium(IV) (vanadyl, VO^{2+}) containing complexes have been explored for the treatment of different types of DM [5].

Vanadium coordination chemistry is further enthused as it can originate structural and/or functional models for vanadate-dependent haloperoxidases, for vanadium nitrogenases and other biologically active vanadium compounds [6,7]. The active site structures of the vanadate-dependent haloperoxidases have been revealed by X-ray diffraction studies. *N*-Salicylidenehydrazides are versatile tridentate ligands and several types of $V^{IV}O$-, $V^{V}O$- and $V^{V}O_2$-complexes have been obtained [8]. Some of these complexes have been reported as, structural as well as functional mimics of vanadiumbromoperoxidases [9]. Maurya *et al.* reported the synthesis and characterization of the binucleating hydrazones of oxidovanadium(IV) and dioxidovanadium(V) complexes as well as their catalytic and reactivity patterns [10].

The coordination chemistry of vanadium compounds with polydentate ligands acquired a special status in the last decade because of its catalytic [11,12] and medicinal [13–16] input. Complexes of vanadium exhibit significant role in nitrogen activation and fixation and are also important in normal mammalian metabolism [17]. At pharmacological concentrations, vanadium acts as a potential therapeutic agent [18,19]. Maurya *et al.* reported VO_2^+ complexes of aroylhydrazones, in search of vanadium compounds with neutral charge [20] (one of the desirable qualities of vanadium compounds to be useful as biomimetic drugs include neutral charge). Thus vanadium complexes are important in catalytically conducted redox reactions [21], potential pharmaceutical applications [22-24] and in the studies on the metabolism and detoxification of vanadium compounds under physiological conditions [25] which initiates much interest in the structural elucidation of its coordination compounds. It is interesting to note that Kuriakose *et al.* have synthesized the oxidovanadium compound $VOL(OCH_3)$, crystallized as a dioxidoovanadium species due to aerial oxidation into a monoclinic lattice with $P2_1/c$ symmetry [26].

The heterocyclic adducts of VO^{2+} complexes of ONO donor α-amino acid Schiff bases with NN donor phenanthroline bases display efficient DNA binding tendancy [24]. A series of oxidovanadium(IV) complexes incorporating heterocyclic bases have been synthesized in the presence of a heterocyclic base 2,2'-bipyridine [27]. Oxidovanadium(IV) and dioxidovanadium(V) complexes are commonly synthesized (i) by the reaction of vanadates with ONO-functional ligands in aqueous solution [28] (ii) by the reaction of $[VO(OEt)_3]$ with appropriate ligands [29] and (iii) by the reaction of $[VO(acac)_2]$ (acacH = acetylacetone) or $VOSO_4$ with the ligands in non-aqueous or mixed solvent media followed by oxidation with O_2 [30,31].

Herein we report the synthesis and characterization of some new vanadium(IV/V) complexes including mixed ligand compounds. Fortunately we could isolate X-ray quality single crystals of two compounds, one each of oxidovanadium(V) and dioxidovanadium(V). It is interesting to note that the dioxido vanadium compound crystallizes into channels which may tend to accommodate other molecules, atoms or ions and can possess good catalytic properties.

3.2 Experimental

3.2.1 Materials

All chemicals and reagents are of reagent grade quality. 2-Hydroxy-4-methoxybenzophenone (Aldrich), furan-2-carboxaldehyde (Aldrich), nicotinic acid hydrazide (Aldrich), benzhydrazide (Aldrich), vanadyl sulphate monohydrate (Aldrich), 4-picoline (Qualigens), 2,2'-bipyridine (Qualigens), 1,10-phenanthroline (Ranchem) and DMF (S.D. Fine) were used without further purification. Methanol and ethanol were used as solvents.

3.2.2 Syntheses of aroylhydrazones

The aroylhydrazones, 2-hydroxy-4-methoxybenzophenone benzoylhydrazone (H_2BB), 2-hydroxy-4-methoxybenzophenone nicotinoylhydrazone (H_2BN) and furan-2-carboxaldehyde nicotinoylhydrazone (HFN) were synthesized as described in Chapter 2.

3.2.3 Syntheses of vanadium complexes

[VO(BB)]$_2$ (1): To a hot methanolic solution of H_2BB (0.346 g, 1 mmol), vanadyl sulfate (0.163 g, 1 mmol) dissolved in hot methanol was added. The resulting solution was refluxed for 5 h. and then kept at room temperature.

The reddish brown crystalline precipitate of **1** that separated out was filtered, washed with ether and dried over P_3O_{10} *in vacuo*. Elemental Anal. Found (Calcd.) (%): C: 60.96 (61.32), H: 3.90 (3.92), N: 6.45 (6.81).

[VO(BB)(bipy)]·H₂O (2): Methanolic solutions of 2,2'-bipyridine (0.156 g, 1 mmol) and H₂BB (0.346 g, 1 mmol), were added to methanolic solution of $VOSO_4·H_2O$ (0.163 g, 1 mmol). The resulting dark brown solution was refluxed for 4 h. On cooling brown crystalline precipitate was separated, filtered, washed with methanol, followed by ether and dried over P_4O_{10} *in vacuo*. Elemental Anal. Found (Calcd.) (%):C: 63.82 (63.59), H: 4.19 (4.48), N: 9.48 (9.57).

[VO(BB)(phen)]·H₂O (3): To a methanolic solution of $VOSO_4·H_2O$ (0.163 g, 1 mmol), were added methanolic solutions of 1,10-phenanthroline (0.198 g, 1 mmol) and H₂BB (0.346 g, 1 mmol). The resulting dark brown solution was refluxed for 4 h. Kept at room temperature for cooling, brown crystalline precipitate was separated, filtered, washed with methanol, followed by ether and dried over P_4O_{10} *in vacuo*. Elemental Anal. Found (Calcd.) (%):C: 64.61 (65.03), H: 4.44 (4.30), N: 8.78 (9.19).

[VO(BB)(OCH₃)] (4): Methanolic solution of H₂BB (0.346 g, 1 mmol) was added to $VOSO_4·H_2O$ (0.163 g, 1 mmol) dissolved in a mixture of methanol (20 mL) and dimethylformamide (2 mL). The resulting dark brown solution was refluxed for 4 h. On cooling brown crystalline precipitate was separated, filtered, washed with methanol, followed by ether and dried over P_4O_{10} *in vacuo*. Dark brown blocks suitable for single crystal X-ray diffraction studies were obtained by slow evaporation of its solution in methanol and DMF (10:1 ratio v/v). Elemental Anal. Found (Calcd.) (%):C: 59.66 (59.87), H: 4.02 (4.11), N: 6.21 (6.35).

[VO(BN)]₂ (5): To H₂BN (0.347 g, 1 mmol) dissolved in methanol, were added methanolic solutions of 2,2'-bipyridine (0.156 g, 1 mmol) and

$VOSO_4·H_2O$ (0.163 g, 1 mmol). The resulting dark brown solution was refluxed for 4 h. On cooling brown crystalline precipitate was separated, filtered, washed with methanol, followed by ether and dried over P_4O_{10} *in vacuo*. Elemental Anal. Found (Calcd.) (%):C: 57.85 (58.26), H: 3.23 (3.67), N: 9.91 (10.19).

[VO(BN)(phen)] (6): To a methanolic solution of $VOSO_4·H_2O$ (0.163 g, 1 mmol), were added methanolic solutions of 1,10-phenanthroline (0.198 g, 1 mmol) and H_2BN (0.347 g, 1 mmol). The resulting dark brown solution was refluxed for 4 h. Kept at room temperature for cooling, brown crystalline precipitate was separated, filtered, washed with methanol, followed by ether and dried over P_4O_{10} *in vacuo*. Elemental Anal. Found (Calcd.) (%):C: 64.73 (65.13), H: 3.89 (4.47), N: 11.7 (11.5).

[VO$_2$(HBN)]·H$_2$O (7): To H_2BN (0.346 g, 1 mmol) dissolved in methanol, methanolic solution of 4-picoline (2-3 mL) and $VOSO_4·H_2O$ (0.163 g, 1 mmol) dissolved in a mixture of methanol and DMF (10:1 v/v) were added. The resulting dark brown solution was refluxed for 4 h. On slow evaporation by keeping at room temperature yellow needle shaped single crystals suitable for single crystal X-ray diffraction studies were obtained, 2-5 crystals separated and the remaining filtered, washed with methanol, followed by ether and dried over P_4O_{10} *in vacuo*. Elemental Anal. Found (Calcd.) (%):C: 55.64 (55.95), H: 3.55 (3.76), N: 9.54 (9.79).

[VO$_2$(FN) (H$_2$O)] (8): To HFN (0.215 g, 1 mmol) dissolved in methanol, was added methanolic solution of $VOSO_4·H_2O$ (0.163 g, 1 mmol). The resulting dark brown solution was refluxed for 4 h. On cooling brown crystalline precipitate was separated, filtered, washed with methanol, followed by ether and dried over P_4O_{10} *in vacuo*. Elemental Anal. Found (Calcd.) (%):C: 41.56 (41.92), H: 3.49(3.20), N: 14.72 (13.33).

3.3 Results and discussion

We synthesized and characterized eight vanadium complexes which are found to be stable. The complexes are soluble in organic solvents like acetonitrile and DMF. The hydrazones coordinate to the central metal ion in the amido form in compound **7** and in iminolate form in all other complexes. The elemental analyses values showed that the found and calculated values are in close agreement with the general formula of the complexes. All the complexes are characterized by various physicochemical techniques such as elemental analyses, FT-IR, EPR, electronic spectral studies, single crystal XRD studies, thermogravimetric analyses, conductance and magnetic susceptibility measurements. Compounds [VO(BB)(OCH$_3$)] (**4**), [VO$_2$(HBN)]·H$_2$O (**7**) and [VO$_2$(FN)(H$_2$O)] (**8**) are vanadium(V) with d^0 configuration and are diamagnetic in nature and the remaining five compounds are paramagnetic with central vanadium ion in +4 oxidation state. Complexes **1** and **5** exhibit subnormal magnetic moments (μ_{eff} = 1.34 and 1.42 B.M. at room temperature) due to the strong antiferromagnetic coupling, which proposes a dimeric nature to these complexes. Magnetic susceptibility values for complexes [VO(BB)(bipy)]·H$_2$O (**2**), [VO(BB)(phen)]·H$_2$O (**3**) and [VO(BN)(phen)] (**6**) are near to the spin only value for a d^1 system. The molar conductivity values for all the complexes in 10^{-3} M DMF solution are found to be in the range 4-12 ohm^{-1} cm^2 mol^{-1} which is less than the value of 65-90 ohm^{-1} cm^2 mol^{-1} reported for a 1:1 electrolyte in the same solvent. This confirmed the non-electrolytic nature of the complexes. The magnetic susceptibility and molar conductivity values of the complexes are listed in Table 3.1.

X-ray quality single crystals of compounds [VO(BB)(OCH$_3$)] (**4**) and [VO$_2$(HBN)]·H$_2$O (**7**) were grown and analysed by single crystal XRD studies.

The coordination geometry of the complexes are found to be distorted square pyramidal. Crystal packing shows that compound **7** polymerises to form one dimensional channel like molecular architecture. EPR spectra of the compounds in DMF at 77 K display axial features with eight hyperfine splitting and in all complexes the $g_\parallel < g_\perp$ and $A_\parallel > A_\perp$ relationship, show an axially compressed d_{xy}^1 configuration. For dimeric species, EPR spectrum in polycrystalline state exhibits half field signal due to spin-spin interaction.

Table 3.1 Molar conductivities and magnetic susceptibilities of vanadium complexes

Compound	λ_m#	μ_{eff} (B.M.)
[VO(BB)]₂ **(1)**	5	1.34
[VO(BB)(bipy)]·H₂O **(2)**	10	1.81
[VO(BB)(phen)]·H₂O **(3)**	8	1.76
[VO(BB)(OCH₃)] **(4)**	7	Diamagnetic
[VO(BN)]₂ **(5)**	4	1.42
[VO(BN)(phen)] **(6)**	5	1.79
[VO₂(HBN)]·H₂O **(7)**	6	Diamagnetic
[VO₂(FN)(H₂O)] **(8)**	7	Diamagnetic

#molar conductivity (in ohm⁻¹ cm² mol⁻¹) taken in 10⁻³ M DMF solution.

3.3.1. X-ray crystallography

The Single crystal X-ray diffraction data of two vanadium complexes, [VO(BB)(OCH₃)] **(4)** and [VO₂(HBN)]·H₂O **(7)** were collected on an Oxford Xcalibur Eos (Mova) Diffractometer at 100 K using Mo Kα radiation ($\lambda=0.7107$ Å)with X-ray generator operating at 50 kV and 1 mA. The structures were solved and refined using SHELX97 module in the program suite WinGX. The molecular diagrams were generated using ORTEP-3 and the packing diagrams were generated using Mercury 2.3.The geometric calculations were carried out by PARST95 and PLATON and all the hydrogen atoms were fixed in calculated positions.

Table 3.2. Crystal data and structure refinement parameters for
$[VO(BB)(OCH_3)]$ (4)

Empirical formula	$C_{22}H_{19}N_5O_5V$
Formula weight	442.34
Temperature (T) K	298(2)
Crystal system	monoclinic
Space group	$P2_1/c$
a (Å), b (Å), c (Å)	11.1413(5), 8.7739(4), 21.3208(9)
α (°), β (°), γ (°)	90.00, 102.573(4), 90.00
Volume (Å^3)	2034.19(16)
Z	4
ρ_{calc} (mg mm^{-3})	1.444
μ (mm^{-1})	0.524
F(000)	912
Crystal size (mm^3)	$0.30 \times 0.20 \times 0.20$
2Θ range for data collection	4.8 to 52°
Index ranges	$-13 \leq h \leq 13, -10 \leq k \leq 10, -26 \leq l \leq 26$
Reflections collected	23362
Independent reflections	4000[R(int) = 0.0433]
Data/restraints/parameters	4000/0/273
Goodness-of-fit on F^2	1.041
Final R indexes [I > 2σ (I)]	$R_1 = 0.0425$, $wR_2 = 0.1051$
Final R indexes [all data]	$R_1 = 0.0543$, $wR_2 = 0.1111$
Largest diff. peak/hole e (Å^{-3})	0.307/-0.256

$R_1 = \Sigma ||F_o| - |F_c|| / \Sigma F_o| wR_2 = [\Sigma w(F_o^2 - F_c^2)^2 / \Sigma w(F_o^2)^2]^{1/2}$

The fourth and fifth coordination positions are occupied by one methoxy oxygen (O5) and one terminal oxo group (O4). Comparing the bond angles and bond lengths, it is evident that the square pyramidal geometry is considerably distorted, with the axial site taken up by the terminal oxo atom (O4). The V–O$_{apical}$ distance 1.5823(18) is comparable to that in similar compounds [32]. The

V–O2, O3, and O5 bond lengths are less than 2 Å and that of V–N1 is 2.093(18) Å indicating a strong coordination of the methoxy group and the ligand to the metal centre. The relatively short C8 N1 and C15–N2 bond distances of 1.311(3) Å and 1.292(3) Å coupled with the N1 N2 distance of 1.396(3) Å, indicate that there is conjugation along the backbone of the tridentate ligand and it is coordinated to the vanadium ion in the iminolate form [33]. The bond distances are in the range of those similar reported compounds [34].

Table 3.3 Selected bond lengths (Å) and bond angles (°) of [VO(BB)(OCH$_3$)] (4)

Bond lengths		Bond angles	
V(1)–N(1)	2.0903(18)	O(4)–V(1)–O(5)	104.33(6)
V(1)–O(2)	1.8299(16)	O(2)–V(1)–O(3)	135.35(7)
V(1)–O(3)	1.9081(16)	O(4) –V(1)–O(5)	106.03(9)
V(1)–O(4)	1.5823(18)	O(2)–V(1)–O(4)	108.33(9)
V(1)–O(5)	1.7607(1)	O(4)–V(1)–O(3)	111.83(9)
C(4)–O(2)	1.340 (3)	O(3)–V(1)–O(5)	88.78(8)
C(15)–O(3)	1.317(3)	O(5)–V(1)–O(2)	98.33(8)
C(22)–O(5)	1.415(4)	O(5)–V(1)–N(1)	157.33(8)
C(2)–O(1)	1.355(3)	O(3)–V(1)–N(1)	75.02(7)
C(4)–C(5)	1.408(3)	O(4)–V(1)–N(1)	94.83(9)
C(5)–C(8)	1.448(3)	O(2)–V(1)–N(1)	83.06(7)
N(1)–C(8)	1.311(3)	O(5)–V(1)–O(5a)	74.99(5)
N(1)–N(2)	1.396(3)	V(1)–O(3)–C(15)	118.39(14)
N(2)–C(15)	1.292(3)	C(15)–N(2)–N(1)	108.45(17)

The vanadium(V) ion in the five coordinate complex adopts a distorted square pyramidal structure with O2, O5, O3 and N1 atoms defining the equatorial plane and terminal oxo atom (O4) at the apical position. The trans angles O2- V1–O3, 135.35(7)° and O5 V1–N1, 157.33(8)° are practically compressed. The apical V-O4 bond is not exactly perpendicular to the basal square plane as seen from the bond angles of O4–V1–O3, 111.83(9)° and O4–V1-O2, 108.33(9)°. The equatorial bond angles deviate much from the expected value of 90.0°. When these bond angles are summed it comes below 360.0°

The V(V) centre is surrounded by two fused five and six membered chelate rings Cg(1){V, N1, N2, C15, O3} and Cg(2) {V, N1, C8, C5, C4,O2} with a dihedral angle of 21.00(8)° between them which indicates deviation of the basal portion from planarity. The five membered chelate rings Cg(1) and Cg(2) make dihedral angles of 62.08(12)° and 43.84(11)° with the ring Cg(4) {C9-C14} indicating that the ring Cg(4) twists significantly out of planarity. The mean plane deviation calculation shows that from the plane containing atoms V, O2, N1, C4, C5, and C8, atoms O3 and O5 show deviations of 0.467(2) Å and ⁻0.038.(2) Å respectively. From ring puckering analysis [36] it is clear that the five membered rings Cg(1) and Cg(2) are puckered with Q values 0.1012(16) Å and 0.5207(15) Å and ϕ values 1.3(12)° and 194.1(2)° respectively. The five membered ring Cg(1) exhibits a T (twist boat) conformation and forms an envelope on V, the central metal atom [37]. Thus the five coordinate complex exhibits a distorted square pyramidal geometry, and the significant deviation from regular square pyramidal geometry is evident from the values of bond angles and bond lengths as summarized in Table 3.3.

Centrosymmetric molecular dimers are formed via C-H⋯N interactions (2.66 Å, and 145.4°) and C-H⋯O interactions (2.65 Å, and 153.2°) (Fig. 3.2). In addition, a different kind of C-H⋯O interaction also occurs between methyl C-H donor and terminal oxo- oxygen atom acceptor (2.63 Å, and 130.7°).This along with a C_{methyl} -H⋯π (2.82 Å) interaction enhances the stability of crystal packing. It is to be noted that in this case the C_{methyl} -H hydrogen bond donor is pointed towards the centre of the C11-C12 bond. Interestingly, weak homonuclear C-H⋯H-C dihydrogen interaction (2.30 Å) are formed in a centrosymmetric fashion (Fig. 3.3) between the dimers formed by C-H⋯N and C-H⋯O interactions. In this crystal structure, the weak C-H⋯H-C dihydrogen interaction can add to the packing stability owing to the absence of any classical hydrogen

than 2 Å and that of V1 N1 is 2.175(4) Å indicating a strong coordination of the dioxido group and the ligand to the metal centre.

Table 3.5. Crystal data and structure refinement parameters for $[VO_2(HBN)]\cdot H_2O$ (7)

Formula	$C_{20}H_{18}N_3O_6V$
Formula weight	447.32
Temperature (K)	293(1)
Crystal system	Triclinic
Space group	$P.1$
a (Å)	5.900(5)
b (Å)	8.067(5)
c (Å)	20.153(5)
α (°)	85.164(5)
β (°)	81.887(5)
γ (°)	82.614(5)
Volume (Å^3)	939.6(10)
Z	2
Density (gcm^{-3})	1.5810
μ (mm^{-1})	0.574
F (000)	460.9
$h_{min, max}$	-8, 8
$k_{min, max}$	-11, 11
$l_{min, max}$	-30, 29
No. of unique reflections	3290
No.of parameters	284
R_{all}, R_{obs}	0.0794, 0.0676
wR_{2all}, wR_{2obs}	0.1834, 0.1716
$\Delta\rho_{min.max}$ (e Å^{-3})	1.095
GOOF	0.936, 1.039

$R_1 = \Sigma |F_o| - |F_c|| / \Sigma|F_o|; wR_2 = [\Sigma w(F_o^2-F_c^2)^2 / \Sigma w(F_o^2)^2]^{1/2}$

The relatively short C7–N1 and C14–N2 bond distances of 1.302(5) Å and 1.296(5) Å coupled with the N1–N2 distance of 1.410(5) Å, indicate that there is conjugation along the backbone of the tridentate ligand and it is coordinated to the vanadium ion in the enolate form [33]. The bond distances are in the range of those reported in the Cambridge Structural Database for similar compounds [34].

Table 3.6. Selected bond lengths (Å) and bond angles (°) of $[VO_2(HBN)] \cdot H_2O$ (7)

Bond lengths		Bond angles	
V(1)–O(1)	1.890(3)	O(1)–V(1)–O(2)	145.91(14)
V(1)–O(2)	1.974(4)	O(1)–V(1)–O(3)	94.88(14)
V(1)–O(3)	1.654(3)	O(1)–V(1)–O(4)	105.63(15)
V(1)–O(4)	1.612(4)	O(1)–V(1)–N(1)	82.17(13)
V(1)–N(1)	2.175(4)	O(2)–V(1)–O(3)	91.39(13)
C(1)–O(1)	1.330(5)	O(2)–V(1)–O(4)	103.79(15)
C(14)–O(2)	1.309(5)	O(2)–V(1)–N(1)	73.37(12)
C(8)–C(7)	1.504(6)	O(3)–V(1)–O(4)	109.18(16)
N(1)-N(2)	1.410(5)	O(3)–V(1)–N(1)	143.91(15)
N(1)-C(7)	1.302(5)	O(4)–V(1)–N(1)	106.21(14)
C(14)-N(2)	1.296(5)	V(1)-O(1)-C(1)	130.0(3)
C(14)-C(15)	1.487(6)	V(1)-O(2)-C(14)	118.3(2)
C(1)-C(6)	1.404(6)	V(1)–O(3)–C(37)	142.0(4)
C(6)-C(7)	1.467(6)	N(1)-N(2)-C(14)	107.7(3)

The vanadium(V) ion in the five coordinate complex adopts a square pyramidal structure with O1, O2, one of the oxygen atoms of the dioxido group O3 and N1 atoms defining the equatorial plane and the other terminal oxo atom (O4) at the apical position. Comparing the bond angles and bond lengths, it is evident that the square pyramidal geometry is considerably distorted. The trans angles O1–V1–O2, 145.91(14)° and O3 V1 N1, 143.91(15)° are practically compressed. The apical V1–O4 bond is not exactly perpendicular to the basal square plane as seen from the bond angles of O4–V1–O3, 109.18(16)° and O4–

value 0.435(3) Å and φ value 28.7(5)° respectively. The six membered ring Cg(1) exhibits a S-form conformation with the central metal atom [37]. Thus the five coordinate complex exhibits a distorted square pyramidal geometry, and the significant deviation from regular square pyramidal geometry is evident from the values of bond angles and bond lengths as summarized in Table 3.6.

Pyridinium moiety in the ligand involves in N—H···O hydrogen bond (1.718 Å, 174.12 Å) with the oxo-oxygen atom forming centrosymmetric molecular dimers (Fig. 3.6). These dimers are further interlinked via water mediated O—H···O hydrogen bonds assisted by a variety of C—H···O and C—H···π interactions. Water oxygen atom acts as the hydrogen bond acceptor in one of the C—H···O interactions, and oxo-oxygen atom in another (Fig. 3.7). Similarly, hydrogen atoms in the methoxy group are involved in two different kinds of C—H···π interactions, adding to the stability of the crystal. Molecular packing in $[VO_2(HBN)]\cdot H_2O$ (7) results in channel like assembly as shown in Figs. 3.8 a,b. Some additional interaction parameters are given in Table 3.7.

Table 3.7. Interaction parameters of the $[VO_2(HBN)]\cdot H_2O$ (7)

H-bonding interactions

D-H···A	D·H/Å	D···A/Å	H···A/Å	∠D-H-A/°	Symmetry codes
O1W—H1WB···O3	0.84(7)	2.961(5)	2.18(7)	152.3(6)	x,y,z
O1W—H1WA···O4	0.84(7)	3.155(5)	2.36(7)	154.5(5)	x+1,+y,+z
C2—H2···O4	0.93(4)	3.391(5)	2.532(3)	153.7(2)	x+1,+y,+z
C18—H18···O1W	0.930(5)	3.367(6)	2.643(4)	135.1(2)	-x,-y,-z+1
N3-H3N···O3	0.89(2)	2.607(5)	1.71(2)	174.1(2)	-x,-y,-z+1
π-π interaction					
Cg(I)···Cg(J)	Cg···Cg (Å)	α (°)	β (°)		
Cg(1)···Cg(5)	3.711(8)	9.5(6)	11.39		1+x,y,z
Cg(5)···Cg(1)ᶜ	3.711(8)	9.5(6)	20.56		-1+x,y,z
Cg (1) = V(1), O(3), C(15), N(2), N(1)					
Cg (1) = C(8)-C(13)					

D, Donor; A, acceptor; Cg, centroid; α (°), dihedral angle between planes I and J; β (°), angle between Cg(I)-Cg(J) vector and normal to plane I.

cation, superhyperfine coupling due to nitrogen atom of the ligand is not resolved in a typical X-band EPR spectrum as the single electron is residing in a sigma non-bonding orbital pointing away from the ligands in the equatorial (xy) plane. The unpaired electron staying in the b_{2g} (d_{xy} $^2B_2$ ground state) orbital is localized on metal for most of the time, excludes the possibility of its direct interaction with the ligand [39,40]. The V(IV) complexes **1, 2, 3, 5 and 6** are EPR active and their spectra were recorded in polycrystalline state at 298 K and in DMF solution at 77 K. The spectral parameters are collected in Table 3.8. V(V) complexes 4, 7 and 8 are EPR silent as vanadium is in +5 oxidation state with d^0 configuration and are diamagnetic.

Table 3.8 EPR spectral assignments of oxidovanadium(IV) complexes in polycrystalline state at 298 K and DMF solution at 77 K

Compound	Polycryst alline state (298 K)	DMF solution (77 K)						α^2	β^2
		$g_{\parallel}$	$g_\perp$	g_{iso}/g_{av}	$A_{\parallel}$	$A_\perp$	A_{iso}/A_{av}		
[VO(BB)]₂ (1)	1.991/ 1.997 $g_\parallel \mid g_\perp$	1.964	1.993	1.979	157	70	113	-0.6908	-0.8325
[VO(BB)(bipy)].H₂O (2)	1.990	1.965	1.987	1.980	168	55	93	-0.5600	-1.0661
[VO(BB)(phen)].H₂O 3)	1.989	1.959	1.990	1.979	159	55	90	-0.6532	-0.9922
[VO(BN)]₂ (5)	1.964 1.979 $g \mid g$	_	_		_	_			
[VO(BN)(phen)] (6)	1.984	1.957	1.988	1.977	157	54	88	-0.7290	-0.9848

The molecular orbital coefficients α^2 and β^2 were also calculated for the complexes using the EPR parameters $g_\parallel$, $g_\perp$, $A_\parallel$ and $A_\perp$ and energies of d-d transitions, by means of the following equations:

$$\alpha^2 = \frac{(2.00277 - g_\parallel)E_{d-d}}{8\lambda\beta^2}$$

$$\beta^2 = \frac{7}{6}\left[\left(\frac{-A_{\parallel}}{P}\right) + \left(\frac{A_{\perp}}{P}\right) + \left(g_{\parallel} - \frac{5}{14}g_{\perp}\right) - \frac{9}{14}g_e\right]$$

where $P = 128 \times 10^{-4}\,\text{cm}^{-1}$, $\lambda = 135\,\text{cm}^{-1}$ and E_{d-d} is the energy of d-d transition

EPR spectrum of complex $[VO(BB)]_2$ (1) is recorded in polycrystalline state at 298 K and in DMF solution at 77 K (Fig. 3.9). In polycrystalline state the compound is axial with $g_{\parallel} = 1.991$ and $g_{\perp} = 1.997$. At half the field of the allowed $\Delta M_s = \pm 1$ transition, there occurs a signal corresponding to a forbidden $\Delta M_s = \pm 2$ transition with $g_{iso} = 3.823$ which indicates the possibility for a dimeric species and the signal splits into 15 lines $[2nI + 1;\ n = 2;\ I = 7/2]$. So it is evident that the spin-spin interaction in this compound is significant in the solid state. In the presence of magnetic field, the electronic ground state ($S = \frac{1}{2}$) is split into two ($m_s = +\frac{1}{2}$ and $-\frac{1}{2}$) and additional splitting occurs through the different magnetic orientations of the nuclear spin (m_I).

B (mT) →
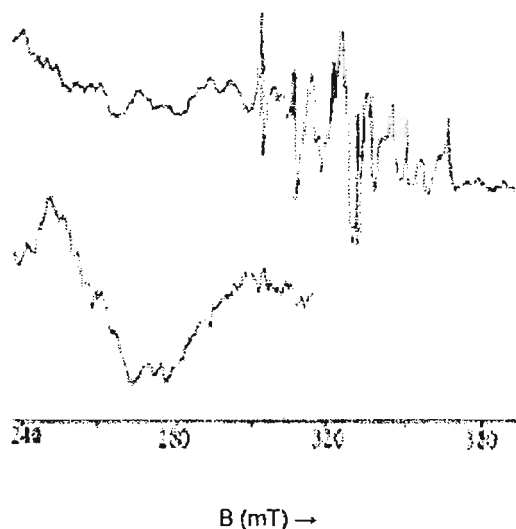
Fig. 3.9. EPR spectrum of $[VO(BB)]_2$ (1) in polycrystalline state at 298 K.

parent hydrazones disappear in the IR spectra of complexes **1-6**. This indicates the transformation of carbonyl moiety to enolic moiety, deprotonation of the phenolic group and subsequent coordination to the metal ion through enolate and phenolate oxygens [46] in addition to azomethine nitrogen. The $\nu(C=O)$ mode of the carbonyl group observed at $ca.$1670 cm^{-1} in the hydrazone H$_2$BN is shifted to lower wave numbers and appears at 1570–1600 cm^{-1} in the compound **7**. This suggests the bonding of the carbonyl oxygen to vanadium in this complex. In the case of compound **8**, hydrazone HFN is coordinated through enolate oxygen and azomethine nitrogen. This is quite evident from the disappearance of bands due to $\nu(N–H)$ and $\nu(C=O)$ modes at $ca.$ 3440 cm^{-1} and 1678 cm^{-1} from the absorption spectrum of the complex. This reveals the bidenticity of the ligand HFN with NO donor sites to coordinate to the metal center.

Table 3.9 Selected IR bands (cm^{-1}) with tentative assignments of vanadium (IV and V) complexes

Compound	$\nu(C=N)$	$\nu(C=N)^a$	$\nu(V=O)$	$\nu(C-O)$	$\nu(V-O)$	$\nu(V-N)$
[VO(BB)]$_2$ (1)	1604	1521	951	1245	489	428
[VO(BB)(bipy)]·H$_2$O (2)	1609	1526	966	1269	512	414
[VO(BB)(phen)]·H$_2$O (3)	1603	1515	949	1241	485	423
[VO(BB)(OCH$_3$)] (4)	1602	1534	979	1239	456	429
[VO(BN)]$_2$ (5)	1602	1532	951	1246	482	436
[VO(BN)(phen)] (6)	1605	1513	959	1241	461	425
[VO$_2$(HBN)] (7)	1608	·	949,890	-	475	421
[VO$_2$(FN)(H$_2$O)] (8)	1609	1520	959,883	1220	475	436

^{a} newly formed

IR spectra of complexes show a prominent band in the region 1505-1545 cm^{-1}, which is attributed to newly formed C=N due to enolization of the ligands during complexation. Bands occuring at the 1230-1285 cm^{-1} region in the metal complexes is assigned to the $\nu(C–O)$ (enolato) mode. The shifting of the band at $ca.$ 1620 cm^{-1} due to $\nu(C=N)$ (azomethine) mode of the free

hydrazones to wavenumbers lowered by 10-20 cm^{-1} in the metal complexes is an explicit evidence for the coordination of azomethine nitrogen to the metal. In complexes there is a symmetric shift in the position of the IR bands in the region 1600-1350 cm^{-1} due to C=C and C=N vibrational modes and their mixing patterns are different from that found in the spectra of free hydrazones [28].

In all the complexes of VO^{2+}, the V=O (oxidovanadium) stretching frequency occurs in the range 935-987 cm^{-1}. These values are observed in the usual range (960 ± 50 cm^{-1}) for monomeric VO^{2+} complexes [47]. The dioxidovanadium(V) complexes normally exhibit two sharp bands in the 891–980 cm^{-1} range due to sym $v(O=V=O)$ and asym $v(O=V=O)$ stretches, corresponding to the cis-$[V^VO_2]^+$ unit. In the present study monomeric neutral dioxido complexes 7 and 8 exhibit a second strong terminal V=O stretching frequency at $ca.$ 870-950 cm^{-1} [48] as given in the Table 3.9. The frequency range observed in complexes indicate that V=O bond is weakened by strong σ and π electron donation by enolate and phenoxy group to the antibonding orbital of the V=O [49]. A characteristic feature due to the V–O–V bridge vibrations in the form of a strong band at $ca.$ 833 cm^{-1} is also observed for the binuclear complexes 1 and 5 [43].

A band at 1130 cm^{-1} due to $v(N–N)$ stretch in the IR spectrum of the parent hydrazone undergoes a shift to lower wavenumbers due to small increase in the bond distance of N1–N2. In compound 4, for instance the bond distance increases from 1.3764(17) Å to 1.396(3) Å which is due to coordination through azomethine nitrogen and diminished repulsion between the lone pairs of adjacent nitrogen atoms on complexation [34]. The bands in the regions 475-515 cm^{-1} and 420-436 cm^{-1} can be assigned to the stretching modes of the metal to ligand bonds, $v(V–O)$ and $v(V–N)$, respectively [50]. In the IR spectra of complexes 2,

[2]   S.J. Lippard, J.M. Beng, Principles of Bioinorganic Chemistry, University Science Books, Mile Valley, California, (1994).

[3]   C. Djordjevic, P.C. Puryear, N. Vuletic, C.J. Allelt, S.J. Sheffield, Inorg. Chem. 27 (1998) 2926.

[4]   N.D. Chasteen, J.K. Grady, C.F. Holloway, Inorg. Chem. 25 (1986) 2754.

[5]   H. Sakurai, A. Katoh, Y. Yoshikawa, Bull. Chem. Soc. Jpn. 79 (2006) 1645.

[6]   A. Butler, Coord. Chem. Rev. 187 (1999) 17.

[7]   C.D. Garner, E.M. Armstrong, R.E. Berry, R.L. Beddoes, D. Collison, J.J.A. Cooney, S.N. Ertok, M. Helliwell, J. Inorg. Biochem. 80 (2000) 17.

[8]   W. Plass, Coord. Chem. Rev. 237 (2003) 205.

[9]   M.J. Clague , A. Butler, J. Am. Chem. Soc. 117 (1995) 3475.

[10]   M.R. Maurya, A.A. Khan, A. Azam, S. Ranjan, N. Mondal, A. Kumar, F. Avecilla, J.C. Pessoa, Dalton Trans. 39 (2010) 1345.

[11]   A. Butler, M.J. Clague, G.E. Meister, Chem. Rev. 94 (1994) 625.

[12]   C. Slebodnick, B.J. Hamstra, V.L. Pecoraro, Struct. Bond. (Berlin) 89 (1997) 51.

[13]   C. Djordjevic, G.L. Wampler, J. Inorg. Biochem. 25 (1995) 51.

[14]   J.H. McNeil, V.G. Yuen, H.R. Hoveyda, C. Orvig, J. Med. Chem. 35 (1992) 1489.

[15]   K.H. Thompson, J.H. McNeil, C. Orvig, Inorg. Chem. 38 (1999) 2288.

[16] M.R. Maurya, S. Khurana, C. Schulzke, D. Rehder, Eur. J. Inorg. Chem.2001 (2001) 779.

[17] K.H. Thompson, J.H. McNeill, C. Orvig, Chem. Rev. 99 (1999) 2561.

[18] K.H. Thompson, C. Orvig, Coord. Chem. Rev. 1033 (2001) 219.

[19] D. Rehder, Inorg. Chem. Commun. 6 (2003) 604.

[20] R.C. Maurya , S. Rajput, J. Mol. Struct. 833 (2007) 1331.

[21] A.M. Schmidt, L. Prade, R. Wever, Biol. Chem. 378 (1997) 309.

[22] S. Macedo-Ribeiro, W. Hemrika, R. Renirie, R. Wever, A. Messerschmidt, J. Biol. Inorg. Chem. 4 (1999) 209.

[23] K. Nakajima, M. Kojima, K. Toriumi, K. Saito, J. Fujita, Bull. Chem. Soc. Jpn. 62 (1989) 60.

[24] V. Vergopoulos, W. Priebsch, M. Fritzsche, D. Rehder, Inorg. Chem. 32 (1993) 1844.

[25] M.J. Clague, N.L. Kedar, A. Butler, Inorg. Chem. 32 (1993) 4754.

[26] M. Kuriakose, M.R.P. Kurup, E. Suresh, Polyhedron 26 (2007) 2713.

[27] P.B. Sreeja, M.R.P. Kurup, Spectrochim. Acta A 61 (2005) 331.

[28] P.K. Samal, A.K. Patra, M. Nethaji, A.R. Chakravarthy, Inorg. Chem. 46 (2007) 11112.

[29] C.A. Root, J.D. Hoeschele, C.R. Cornman, J.W. Kampf, V.L. Pecoraro, Inorg. Chem. 32 (1993) 3855.

[30] G. Asgedom, S. Sreedhara, J. Kivikoshi, E. Kolehmainen, C.P. Rao, J. Chem. Soc. Dalton Trans. (1996) 93.

[31]   M.R. Maurya, Coord. Chem. Rev. 237 (2003) 163.

[32]   M.R. Maurya, A. Kumar, A.R. Bhat, A. Azam, C. Bader, D. Rehder, Inorg. Chem. 45 (2006) 1260 .

[33]   M.R.P. Kurup, E.B. Seena, M. Kuriakose, Struct. Chem. 21 (2010) 599.

[34]   E.B. Seena, N. Mathew, M. Kuriakose, M.R.P. Kurup, Polyhedron 27 (2008) 1455.

[35]   A.W. Addison, T.N. Rao, R. Reedijk, J.V. Rigin, G.C. Verschoor, J. Chem. Soc., Dalton Trans. (1984) 1349.

[36]   D. Cremer & J.A. Pople, J.Amer.Chem.Soc., 97 (1975) 1354.

[37]   J.C.A. Boeyens, J.Cryst.Mol.Struct. 8 (1978) 317.

[38]   J. Echeverria, G. Aullo, D. Danovich, S. Shaik and S. Alvarez. Nature Chemistry (3) 2011 323.

[39]   H. Kon, E.Sharpless, J.Chem. Phys. 42 (1965) 906.

[40]   D. Kivelson, S.K. Lee, J.Chem. Phys. 41 (1964) 1896.

[41]   N.A. Mangalam, S. Sivakumar, S.R. Sheeja, M.R.P. Kurup, E.R.T. Tiekink, Inorg.Chim. Acta 362 (2009) 4191.

[42]   M.R. Maurya, S. Khurana, W. Zhang, D. Rehder, J. Chem. Soc. Dalton Trans. (2002) 3015.

[43]   N.A. Mangalam, M.R.P. Kurup, Spectrochim. Acta A 71 (2009) 2040.

[44]   D. Rehder, Bioinorganic Vanadium Chemistry, Wiely, Chichester, 2008.

[45]   S. Bhattacharya, T.Ghosh, Ind. J. of Chemistry, 38 A (1999) 601.

[46]   L.H. Huo, S. Gao, J.W. Liu, J. Li, S. W. Ng, Acta. Cryst. E60 (2004)   758.

[47]   R.K. Agarwal, I. Chakraborti, S.K. Sharma, Polish J. Chem. 68 (1994) 1085.

[48]   M.R. Maurya, A. Kumar, M. Abid, A. Azam, Inorg. Chim. Acta 359 (2006) 2439.

[49]   T. Ma, T. Kojima, Y. Matsuda, Polyhedron 19 (2000) 1167.

[50]   E.J. Baran, J. Coord. Chem. 54 (2001) 215.

[51]   G. Vighe and J. Selbin, J. Inorg. Nucl. Chem. 31 (1969) 3187.

[52]   B.J. McCormick, Inorg.Chem. 7 (1968) 1965

[53]   C.J. Ballhausen and H.B. Gray, Inorg. Chem. 1 (1962) 111.

[54]   J. Selbin, Chem. Rev. 65 (1965) 153.

[55]   H.J. Stoklosa, J.R. Wasson, B.J. McCormick, Inorg. Chem. 13 (1972) 592.

[56]   X.F. Chen, P. Cheng, X. Liu, B. Zhao, D.Z. Liao, P.P. Yan, Z.H. Jiang, Inorg. Chem. 40 (2001) 2652.

SYNTHESES AND SPECTRAL CHARACTERIZATION OF Mn(II/IV) COMPLEXES OF SOME AROYLHYDRAZONES

4.1 Introduction

Manganese shows versatile coordination chemistry with diverse Mn(II/III/IV/V) oxidation states. Among these different oxidation states, +2 is the most stable and dominant oxidation state. Mn(II) complexes are primarily high spin complexes because of the extra stability exhibited by the exactly half filled d^5 system. The most common geometry associated with Mn(II/IV) is octahedral, although there are reports on four, five and seven coordination. Manganese is an essential element in biological systems and it acts as an effective enzyme activator. It is also an active site in metalloproteins, where manganese exists in different oxidation states.

Manganese complexes are significant in various fields ranging from bioinorganic chemistry to solid-state physics. Mn(II) complexes display superoxide dismutase activity [1] and Mn(II/III/IV) ions act as water oxidation center of photosystem-II [2,3]. Manganese complexes play an important role in industrial catalysis. Processes of fractionalization of hydrocarbons involving high valent intermediates are effectively catalyzed by manganese porphyrins [4,5]. Complexes of manganese with non-heme ligands are found to be effective catalysts in olefin

epoxidation and alkane hydroxylation [6,7]. Chattopadhyay and his group have shown how the supramolecular architecture of Mn(II) aroylhydrazone complexes can be controlled by slight modification of the substituents attached to the ligand framework [8]. Metal ions can read the information coded in the organic ligands according to their coordination algorithm [9].

Wen *et al.* synthesized one dimensional chiral coordination polymers of Mn(II) using azide and a Schiff base (obtained from pyridine-2-carbaldehyde and 1-phenylethyl amine) as the auxiliary ligand [10]. An important goal in the field of modern inorganic chemistry is to find out new rational routes leading to materials with expected magnetic properties. Clusters of nanometer-size with high spin ground states are studied as single molecule magnets [11,12]. The magnetic properties of the cluster, $[Cu_4MnL_4][ClO_4]_2$ have been investigated in the temperature range 1.9-300 K by Tuna *et al.* [13]. The use of hydrazones in conjugation with heterocyclic bases and groups *viz.* perchlorate, azide etc. can give interesting results. In this chapter we report the syntheses and spectral characteristics of seven Mn(II) complexes of aroylhydrazones containing heterocyclic bases and perchlorate anions.

4.2 Experimental

4.2.1 Materials

All chemicals and reagents are of reagent grade quality. 2-Hydroxy-4-methoxybenzophenone (Aldrich), furan-2-carboxaldehyde (Aldrich), nicotinic hydrazide (Aldrich), benzhydrazide (Aldrich), manganese(II) acetate tetrahydrate (E-Merck), 2,2'-bipyridine (Qualigens), 1,10-phenanthroline (Ranchem) and DMF (S.D. Fine) were used without further purification. Methanol and ethanol were used as solvents.

4.2.2 Syntheses of the aroylhydrazones

The syntheses of aroylhydrazones were done as described in Chapter 2.

4.2.3 Syntheses of manganese(II) complexes

[Mn(BB)$_2$] (**9**): Methanolic solutions of H$_2$BB (0.692 g, 2 mmol), and Mn(CH$_3$COO)$_2$·4H$_2$O (0.245 g, 1 mmol) were mixed and refluxed for 5 h in presence of one or two drops of triethylamine. The dark brown colored product obtained was filtered, washed with methanol, followed by ether and dried over P$_4$O$_{10}$ *in vacuo*. Elemental Anal. Found (Calcd.) (%): C: 67.39 (67.83), H: 4.41 (4.34), N: 7.52 (7.53).

[Mn(BB)(phen)(CH$_3$OH)]·2CH$_3$OH (**10**): To a hot methanolic solution of H$_2$BB (0.346 g, 1 mmol), containing 1,10-phenanthroline (0.198 g, 1 mmol), Mn(CH$_3$COO)$_2$·4H$_2$O (0.245 g, 1 mmol) in methanol was added and the resulting brown colored solution was refluxed for 5 h. after adding one drop of triethylamine. The dark brown colored product obtained was filtered, washed with methanol, followed by ether and dried over P$_4$O$_{10}$ *in vacuo*. Elemental Anal. Found (Calcd.) (%): C: 64.58 (64.00), H: 5.52 (5.37), N: 8.07 (8.29).

[Mn(BB)(bipy)(CH$_3$OH)] (**11**): To a methanolic solution of Mn(CH$_3$COO)$_2$·4H$_2$O (0.245 g, 1 mmol) methanolic solutions of 2,2'-bipyridine (0.156 g, 1 mmol) and H$_2$BB (0.346 g, 1 mmol) were added. The resulting dark brown solution was refluxed for 4 h. after adding a drop of triethylamine and then kept at room temperature for cooling. Brown crystalline precipitate was separated, filtered, washed with methanol, followed by ether and dried over P$_4$O$_{10}$ *in vacuo*. Elemental Anal. Found (Calcd.) (%): C: 65.01 (65.42), H: 4.62 (4.80), N: 9.45 (9.54).

[Mn(BN)$_2$] (**12**): To methanolic solution of H$_2$BN (0.694 g, 2 mmol), methanolic solution of Mn(CH$_3$COO)$_2$·4H$_2$O (0.245 g, 1 mmol).was added. The resulting dark brown solution was refluxed for 4-5 h in presence of triethylamine. On cooling, brown crystalline precipitate was separated, filtered, washed with methanol, followed by ether and dried over P$_4$O$_{10}$ *in vacuo*. Elemental Anal. Found (Calcd.) (%): C: 63.89 (64.09), H: 4.43 (4.57), N: 10.78 (11.21).

[Mn(BN)(phen)]·H$_2$O (**13**) : To a hot methanolic solutions of H$_2$BN (0.347 g, 1 mmol), and 1,10-phenanthroline (0.198 g, 1 mmol), Mn(CH$_3$COO)$_2$·4H$_2$O (0.245 g, 1 mmol) in methanol was added and the resulting brown colored solution was refluxed for 5 h. after adding one drop of triethylamine. The dark brown colored product obtained was filtered, washed with methanol, followed by ether and dried over P$_4$O$_{10}$ *in vacuo*. Elemental Anal. Found (Calcd.) (%): C: 63.94 (64.22), H: 4.20 (4.21), N: 11.56 (11.7).

[Mn(BN)(H$_2$O)] (**14**): Methanolic solutions of the H$_2$BN (0.347 g, 1 mmol) and Mn(CH$_3$COO)$_2$·4H$_2$O (0.245 g, 1 mmol) were mixed in the ratio 1:1 and the resulting dark brown solution was refluxed for 4-5 h in presence of triethylamine. On cooling brown crystalline precipitate was separated, filtered, washed with methanol, followed by ether and dried over P$_4$O$_{10}$ *in vacuo*. Elemental Anal. Found (Calcd.) (%): C: 57.72 (57.43), H: 4.31 (4.10), N: 9.85 (10.05).

[Mn(FN)(phen)(ClO$_4$)$_2$]ClO$_4$ (**15**): To hot ethanolic solution of the HFN (0.215 g, 1 mmol) and 1,10-phenanthroline (0.198 g, 1 mmol), Mn(ClO$_4$)$_2$·6H$_2$O (0.362 g, 1 mmol) in ethanol was added and the resulting brown colored solution was stirred for 5-6 h. after adding one drop of triethylamine. The dark brown colored product obtained was filtered, washed with methanol, followed by ether

and dried over P_4O_{10} *in vacuo*. Elemental Anal. Found (Calcd.) (%): C: 36.52 (36.95), H: 2.31 (2.16), N: 9.12 (9.37).

4.3 Results and discussion

Seven manganese(II/IV) complexes were synthesized using different aroylhydrazones out of which four are mixed ligand complexes containing heterocyclic bases like 1,10-phenanthroline and 2,2-bipyridine as auxiliary ligands and perchlorate anion is incorporated in one of the compounds. They are found to be stable, brown in color and soluble in organic solvents like methanol, acetonitrile, DMF and DMSO. Based on the elemental analyses, conductivity and magnetic susceptibility measurements and spectral investigations, the complexes were formulated. The molar conductivities of the complexes in DMF (10^{-3} M) solution were measured at 298 K with a Systronic model 303 direct-reading conductivity bridge. The molar conductance values lie in the range 4-12 $ohm^{-1} cm^2 mol^{-1}$ for complexes **9-14** which shows their non-conducting nature [14]. The compound $[Mn(FN)(phen)(ClO_4)_2]ClO_4$ **(15)** is found to be a 1:1 electrolyte as seen from its conductance value of λ_m (DMF)(10^{-3} M) = 85 $ohm^{-1} cm^2 mol^{-1}$

The analytical data indicate that the observed C, H, N values of the complexes were in close agreement with that of the formula suggested and matched with the stoichiometry containing one molecule of lattice water in compound $[Mn(BN)(phen)]\cdot H_2O$ **(13)**, and one molecule of coordinated water in $[Mn(BN)(H_2O)]$ **(14)**, which is further supported by thermal analysis. Magnetic susceptibility measurements of the compounds are in agreement with the spin only value [15], thereby suggesting the paramagnetic nature of the Mn(II) complexes with a d^5 [16] and Mn(IV) complexes with a d^3 high spin configuration. The data obtained from magnetic susceptibility measurements

and partial elemental analyses are consistent with Mn(IV) oxidation state in compounds **9**, **12** and **15** and Mn(II) in **10**, **11**, **13** and **14**. Table 4.1 summarizes the molar conductivities and magnetic susceptibilities of the complexes.

Table 4.1 Molar conductivities and magnetic susceptibilities of Mn(II/IV)

Compound	$\lambda_m{}^\#$	μ_{eff} (B.M.)
[Mn(BB)₂] **(9)**	11	3.91
[Mn(BB)(phen)(CH₃OH)]·2CH₃OH **(10)**	14	5.86
[Mn(BB)(bipy)(CH₃OH)] **(11)**	13	5.58
[Mn(BN)₂] **(12)**	8	3.94
[Mn(BN)(phen)(H₂O)] **(13)**	12	5.87
[Mn(BN)(H₂O)] **(14)**	9	5.85
[Mn(FN)(phen)(ClO₄)₂]ClO₄ **(15)**	85	4.11

$^\#$molar conductivity (in ohm⁻¹ cm² mol⁻¹) taken in 10⁻³ M DMF solution.

4.3.1 EPR spectral studies

Electron paramagnetic resonance (EPR) of manganese has much significance as a spectroscopic probe of manganese centers in manganese proteins and it is one of the few techniques that can selectively sense and characterize Mn(II) ions. The Mn(II) state possesses Kramers doublets and exhibits characteristic transitions in the normal X-band regime. The spin Hamiltonian used to represent the EPR spectra of Mn(II) [17] is given by the equation

$$\hat{H} = g\beta BS + D[S_z^2 - S(S+1)/3] + E(S_x^2 - S_y^2)$$

Where B is the magnetic field vector, g is the spectroscopic splitting factor, β is the Bohr magneton, D is the axial zero field splitting parameter, E is the rhombic zero field splitting parameter and S is the electron spin vector [18]. The first two terms represent the electronic Zeeman and the electron nuclear hyperfine interactions respectively, whereas the last two terms define the zero field splitting interaction with D and E gauging the axial and the rhombic parts.

Low intensity lines are observed in between two major hyperfine splittings in the frozen solution spectra of compounds **10** and **13**. These forbidden lines corresponds to $\Delta M_I = \pm 1$ transitions, due to the mixing of the nuclear hyperfine levels by the zero field splitting factor D of the Hamiltonian [27]. The forbidden peaks are not visible in complex **11** due to broadening of the main hyperfine lines in the spectrum. In the scan range 200-400 mT, compound $[Mn(BN)(phen)]H_2O$ (**13**) shows a broad low field signal with g value of ~5.61, which indicates tetragonal distortion, in addition to the occurrence of a single sextet with g value 1.994.

4.3.2 Infrared spectra

The mode of coordination of the hydrazones to Mn(II/IV) center has been suggested by a careful comparison of the characteristic vibrational bands of the complexes with that of the free ligand. The main stretching frequencies of the IR spectra of the complexes and together with their tentative assignments are tabulated in Table 4.2.

Table 4.2 Infrared spectral assignments (cm^{-1}) of Mn(II) complexes

	$\nu(C=N)$	$\nu(C=N)^*$	$\nu(C-O)$	$\nu(Mn-O)$	$\nu(Mn-N)$
$[Mn(BB)_2]$ (**9**)	1602	1526	1239	512	429
$[Mn(BB)(phen)(CH_3OH)]\cdot 2CH_3OH$ (**10**)	1594	1519	1239	505	432
$[Mn(BB)(bipy)(CH_3OH)]$ (**11**)	1598	1518	1246	505	429
$[Mn(BN)_2]$ (**12**)	1601	1514	1238	509	422
$[Mn(BN)(phen)(H_2O)]$ (**13**)	1602	1510	1239	512	422
$[Mn(BN)(H_2O)]$ (**14**)	1602	1510	1240	513	436
$[Mn(FN)(phen)(ClO_4)_2]ClO_4$ (**15**)	1598	1510	1223	505	414

In the infrared spectra of all the seven complexes, we have not found any bands due to $\nu(C=O)$, $\nu(N-H)$ and $\nu(O-H)$ modes at 1640-1690, 3025-3200 and

4.3.5. Cyclic voltammetric studies

Cyclic voltammograms of Mn(II/IV) complexes were recorded in DMF/DMSO (10^{-3} M) and tetrabutylammonium phosphate as the supporting electrolyte at a scan speed of 100 mV s^{-1}. A three-electrode system design is incorporated in the experiment. In simple cases, the surface is started at a particular voltage with respect to a reference half-cell such as calomel or Ag/AgCl, with platinum wires as working and counter electrodes. The solution in contact with an electrode surface is electrolyzed (oxidized or reduced), and then making that surface sufficiently positive or negative in voltage to force electron transfer. The spectral and structural changes accompanying electron transfer in metal complexes with O, N, O- donor hydrazone ligands can be scrutinized using cyclic voltammetric studies [36].

The cyclic voltammograms of Mn (II/IV) complexes **9**, **14** and **15** consist of two or more reversible oxidation peaks and reduction peaks. The relevant electrochemical data of the hydrazone complexes of Mn (II/IV) are given in Table 4.4.

Table 4.4. Cyclic voltammetric data for Mn(II/IV) complexes

Compound	E_{pc} (V)	E_{pa} (V)	I_{pc} (μA)	I_{pa} (μA)
[Mn(BB)$_2$] (9)	0.2, -1.2	0.56,-0.51	20, 7.9	-6.1, -4.6
[Mn(FN)(phen)(ClO$_4$)$_2$]ClO$_4$ (15)	0.01, -0.48	-0.44, 0.49	3.88, 3.46	-2.15,-1.7
[Mn(BN)(H$_2$O)] (14)	0.17,-0.3	0.92, -1.5	4.7, 5.6	-7.1, 7.3

The cyclic voltammogram for the behavior of the Mn(IV) compounds **9** and **15** show reduction peaks at 0.2, -1.2 and 0.01, -0.48 V which are attributed to reduction steps involved in the conversion of Mn(IV) to Mn(0). On the reverse scan the corresponding anodic peak potentials occur at -0.51, 0.56 and -0.44, 0.49 V which can be attributed to the reverse series of oxidation of Mn(0)

[3] G. Christou, J.B. Vincent, Inorg. Chim. Acta 136 (1987) L41.

[4] B. Meunier, in Metalloporphyrin Catalysed Oxidations, ed. F. Montanari and L. Casella, Kluwer Academic Publishers, Dordrecht, (1994) 1

[5] J. Bendix, H.B. Gray, G. Golubkov, Z. Gross, Chem. Commun. (2000) 1957.

[6] K. Nehru, S.J. Kim, I.Y. Kim, M.S. Seo, Y. Kim, S.-J. Kim, J. Kim, W. Nam, Chem. Commun. (2007) 4623

[7] K.F. Sibbons, K. Shastri, M. Watkinson, Dalton Trans. (2006) 645.

[8] S. Naskar, M. Corbella, A.J. Blake, S.K. Chattopadhyay, Dalton Trans. (2007) 1150.

[9] J.M. Lehn, Supramolecular Chemistry, Concepts and Perspectives, VCH, New York, (1995).

[10] H.R. Wen, C.-F. Wang, Y. Song, J.-L. Zuo, X.-Z. You, Inorg. Chem. 44 (2005) 9039.

[11] M.W. Wemple, L.H. -Tsai, W.E. Streib, D.N. Hendrickson, G. Christou, J. Chem. Soc. Chem. Commun. (1994) 1031.

[12] K. Fegy, D. Luneau, E. Belorizky, M. Novac, J.-L. Tholence, C. Paulsen, T. Ohm, P. Rey, Inorg. Chem. 37 (1998) 4524.

[13] F. Tuna, L. Patron, M. Andruh, Inorg. Chem. Commun. 6 (2003) 30.

[14] W.J. Geary, Coord. Chem. Rev. 7 (1971) 81.

[15] N.A. Mangalam, S.R. Sheeja, M.R.P. Kurup, Polyhedron 29 (2010) 3318.

[16] A.A.A. Abu-Hussen, A.A.A. Emara, J. Coord. Chem. 57 (2004) 973.

[17] R.D. Dowsing, J.B. Gibbson, J. Chem. Phy. 50 (1969) 294.

[18] D.J.E. Ingram, Spectroscopy at Radio and Microwave Frequencies, 2nd ed., Butterworth, London, (1967).

[19] B.S. Garg, M.R.P. Kurup, S.K. Jain, Y.K. Bhoon, Transition Met. Chem. 13 (1988) 92.

[20] C. Mantel, C. Baffert, I. Romero, A. Deronzier, J. Pe´caut, M.N. Collomb, C. Duboc, Inorg. Chem. 43 (2004) 6455.

[21] H. Levanon, Z. Luz, J. Chem. Phys. 49 (1968) 2031.

[22] S.I. Chan, B.M. Fung, H. Lutje, J. Chem. Phys. 47 (1967) 2121.

[23] W.E. Buschmann, C. Vasquez, M.D. Ward, N.C. Jones, J.S. Miller, Chem. Comm, (1997) 409.

[24] S. Sreesha, M. Sithambaresan, M.R.P. Kurup, H.-K. Fun, Polyhedron 29 (2010) 2643.

[25] R. Kumar, S. Chandra, Spectrochim. Acta. Part A 67 (2007) 188.

[26] P.F. Rapheal, E. Manoj, M.R.P. Kurup, Polyhedron 26 (2007) 5088.

[27] B. Bleany, R.S. Rubins, Proc. Phys. Soc. London 77 (1961) 103. [28] E.B. Seena, N. Mathew, M Kuriakose, M.R.P. Kurup, Polyhedron 27 (2008) 1455.

[28] M. Morshedi, M. Amirnasr, A.M.Z. Slawin. J.D. Woollins, A.D. Khalaji, Polyhedron 28 (2009) 167.

[29] S.N. Rao, D.D. Mishra, R.C. Maurya, N.N. Rao, Polyhedron 16 (1997) 1825.

[30] M.R.P. Kurup, E.B. Seena, M. Kuriakose, Struct. Chem. 21 (2010) 599.

[31] M.S. Abdel-Moez, S.L. Stefan, M.M. El-Behairy, B.A. El-Shetary, Can. J. Chem. 68 (1990) 774.

[32] A.B.P. Lever, Inorganic Electronic Spectroscopy, 2nd Edition, Elsevier, Amsterdam (1984).

[33] M.S. Refat, S. Chandra, M. Tyagi, J. Therm. Anal. Calorim. 100 (2009) 261.

[34] H. Cesur, T.K. Yazicilar, B. Bati, V.T. Yilmaz, Synth. React. Inorg. Met. -Org. Chem. 31 (2001) 1271.

[35] A.M. Bond, R.L. Martin, Coord. Chem. Rev 54 (1984) 23.

SYNTHESES, CRYSTAL STRUCTURE AND SPECTRAL CHARACTERIZATION OF Co(II/III) COMPLEXES OF SOME AROYLHYDRAZONES

5.1. Introduction

In view of the growing importance of aroylhydrazone and as their metal complexes mimic the functional properties of some enzymes, the chemical, structural and electrochemical properties have been studied in detail by many researchers [1,2]. A number of cobalt complexes of substituted polypyridine ligands were synthesized and investigated as possible alternatives to the volatile and corrosive iodide/triiodide redox couple commonly used as an electron-transfer mediator in dye-sensitized solar cells (DSSCs). Sapp *et al.* have recently discovered that the best mediator, based on tris(4,4'-di-tert-butyl-2,2'-dipyridyl)-cobalt(II/III) perchlorate, resulted in DSSCs exhibiting efficiencies within 80% of that of a comparable iodide/triiodide-mediated DSSC [3].

The interaction of transition metal polypyridyl complexes with DNA has received considerable attention in recent years [4]. Small molecules can interact with double-stranded DNA in a number of ways [5,6] and in most cases it is non-covalent, which involves intercalation of planar aromatic molecules between the base pairs of DNA helix. Barton has reported that chiral

phenanthroline–cobalt(III) complexes recognize different local structures of DNA [7]. Therefore, mixed ligand complexes of cobalt(III) having phenanthroline/bipyridine/picoline and aroylhydrazones were prepared and studied their properties through spectral and electrochemical methods [8].

Cobalt(III) complexes synthesized from symmetrical and unsymmetrical Schiff bases are quite relevant as biologically active compounds [9]. The central metal ion of cobalt (II/III) complexes shows reactivity in the transmethylation reaction and reversible absorption of molecular oxygen [10]. Studies on mixed ligand complexes of cobalt(III) have been reported [11]. Cobalt(III) complexes containing bidentate bases like 2,2'-bipyridine (bipy) or 1,10-phenanthroline (phen) as auxiliary ligands for coordination with cobalt metal have also been studied [12]. This was the first structural report of a Co(III) $^1\eta$ -azido complex of N(4)-substituted thiosemicarbazones and heterocyclic bases.

Vitamin B_{12}, which is involved in the production of red blood cells is a cobalt(III) complex with a substituted corrin macrocycle. Cobalt(III) complexes have shown specific hypoxic radiosensitization and thermosensitization as well as antitumor activity $in\ vivo$ [13]. As cobalt is a first row transition metal, dissociation and exchange of ligands may occur rapidly in the case of Co(II). It is difficult to oxidise divalent cobalt compounds with d^7 configuration and are very stable. However, in basic solutions, oxidation of Co^{2+} to Co^{3+} takes place relatively easily. When we consider complex formation, Co(II) complexes are readily oxidized to Co(III) since the overall formation constant is greater for the higher oxidation state. Also the crystal field stabilization energy of Co(III) with a d^6 configuration is higher than that for Co(II) with a d^7 configuration. Low spin six coordinate complexes are widely reported for Co(III) and are found to be diamagnetic [12,14]. Reports on high/low spin five coordinate and four

coordinate complexes of Co(II) are common and are paramagnetic in nature [15]. It is observed that Co(II) complexes exhibit tetrahedral geometry than any other transition metal ion, except Zn(II), as d^7 configuration, supports a tetrahedral geometry than an octahedral alignment [16]. The two geometries of Co(II) are of comparable stability so that there exists an equilibrium between the two structures [17]. Tridentate ligands are expected to improve significantly the stability of the cobalt complex compared with bidentate ligands.

Azide is a versatile ligand since it exhibits a variety of coordination modes such as monodentate, end-on bridging mode (μ-1, 1), end-to-end bridging mode (μ-1, 3) etc. among many others [18]. Azide acts as an inhibitor for several enzymes like ATPases [19]. Hence the study of metal-azido complexes is very useful for the understanding of biological processes. Cobalt(II) complex of azide anion and bis(pyrazol-1-yl)methane has been reported [20]. Cobalt(III) complexes with azide anion has been previously reported with 1,10-phenanthroline [21]. In this chapter, we report cobalt(II/III) complexes of aroylhydrazones, with azide, thiocyanate and heterocyclic bases as coligands.

5.2. Experimental

5.2.1. Materials

All the chemicals and solvents used for the syntheses were of analytical grade. 2-Hydroxy-4-methoxybenzophenone (Aldrich), furan-2-carboxaldehyde (Aldrich), nicotinic hydrazide (Aldrich), benzhydrazide (Aldrich), cobalt(II) acetate tetrahydrate (BDH), potassium thiocyanate (Merck), sodium azide (Reidel-De Haen), 4-picoline, 2,2'-bipyridine (Qualigens), 1,10-phenanthroline (Ranchem) and DMF (S.D. Fine) were used without further purification. Methanol and ethanol were used as solvents.

5.2.2. Syntheses of the aroylhydrazones

The aroylhydrazones, 2-hydroxy-4-methoxybenzophenone benzoylhydrazone (H_2BB), 2-hydroxy-4-methoxybenzophenone nicotinoylhydrazone (H_2BN) and furan-2-carboxaldehyde nicotinoylhydrazone (HFN) were synthesized as described in Chapter 2.

5.2.3. Syntheses of cobalt(II/III) complexes

[Co(BB)]₂ (16) : To a hot methanolic solution of the H_2BB (0.346 g, 1 mmol), cobalt(II) acetate tetrahydrate (0.249 g, 1 mmol) in methanol (20 mL) was added and refluxed the solution for 4 hours. Then the solution is cooled in room temperature. The dark brown crystalline precipitate of **16** obtained was washed with methanol followed by ether and then dried over P_4O_{10} *in vacuo*. Yield: 78.9%. λ_m (DMF): 7 ohm⁻¹ cm² mol⁻¹. μ (*B.M.*): 4.84. Elemental Anal. Found (Calcd.) (%): C: 62.32 (62.54), H: 3.78 (4.00), N: 6.9.

[Co(BB)(bipy)N₃]·H₂O (17): Cobalt(II) acetate tetrahydrate (0.249 g, 1 mmol) in methanol (20 mL) was added to a hot methanolic solution of the aroylhydrazone H_2BB (0.346 g, 1 mmol) and 2,2'-bipyridine (0.156 g, 1 mmol). To this solution, NaN_3 (0.065 g, 1 mmol) in methanol (10 mL) was added and stirred the solution for 4 hours. The dark brown precipitate of **17** obtained was washed with methanol followed by ether and then dried over P_4O_{10} *in vacuo*. Yield: 74.5%. λ_m (DMF): 9 ohm⁻¹ cm² mol⁻¹. μ (*B.M.*): 4.89. Elemental Anal. Found (Calcd.) (%): C: 59.56 (59.81), H: 4.59 (4.70), N: 16.22 (15.75).

[Co(BB)(phen)N₃] (18): Methanolic solutions of H_2BB (0.346 g, 1 mmol), and 1,10-phenanthroline (0.198 g, 1 mmol) were mixed and cobalt(II) acetate tetrahydrate (0.249 g, 1 mmol) dissolved in hot methanol was added. To this solution, NaN_3 (0.065 g, 1 mmol) in methanol (10 mL) was added and stirred the solution for 4 hours. The brown precipitate of **18** obtained was washed with

methanol followed by ether and then dried over P_4O_{10} *in vacuo*. Yield: 34.9%. λ_m (DMF): 13 ohm^{-1} cm^2 mol^{-1}. μ (*B.M.*): 4.92. Elemental Anal. Found (Calcd.) (%): C: 63.27 (63.36), H: 3.76 (3.87), N: 15.45 (15.67).

[Co(BB)(4,4'bipy)N₃] (19): To a solution of H_2BB (0.346 g, 1 mmol) and 4,4'-dimethyl-2,2'-bipyridine (0.156 g, 1 mmol) in methanol, cobalt(II) acetate tetrahydrate (0.249 g, 1 mmol) dissolved in hot methanol was added. NaN_3 (0.065 g, 1 mmol) in methanol (10 mL) was added and stirred the solution for 4 hours. The brown precipitate of **19** obtained was washed with methanol, followed by ether and dried over P_4O_{10} *in vacuo*. Elemental Anal. Found (Calcd.) (%): C: 62.29 (62.86), H: 4.43 (4.64), N: 15.29 (15.55).

[Co(BB)(pi)₃] (20): A solution of H_2BB (0.346 g, 1 mmol) and 4-picoline (2-3 mL) in methanol were mixed with cobalt(II) acetate tetrahydrate (0.249 g, 1 mmol) dissolved in hot methanol and DMF (10:1 ratio v/v) and refluxed for about 5 hours. The brown colored crystalline product was filtered, washed with methanol, followed by ether and dried over P_4O_{10} *in vacuo*. Dark brown plate like crystals suitable for single crystal X-ray diffraction studies were obtained by slow evaporation of its solution in ethanol and DMF (10:1 ratio v/v). Yield: 68.2%. Elemental Anal. Found (Calcd.) (%): C: 68.35 (68.61), H: 4.94 (5.46), N: 9.79 (10.26).

[Co(BN)(OCH₃)(H₂O)] (21): This complex was prepared by refluxing cobalt(II) acetate tetrahydrate (0.249 g, 1 mmol), H_2BN (0.347 g, 1 mmol) and 4-picoline (2-3 mL) in methanol and DMF (10:1 ratio v/v) for about 5 hours. The brown precipitate of **21** was washed with methanol followed by ether and then dried over P_4O_{10} *in vacuo*. Yield: 58.4%. λ_m (DMF): 13 ohm^{-1} cm^2 mol^{-1}. μ (*B.M.*): 4.85 Elemental Anal. Found (Calcd.) (%): C: 55.39 (55.64), H: 4.08 (4.45), N: 9.10 (9.27).

[Co$_2$(BN)$_2$N$_3$(OCH$_3$)]·2H$_2$O (22): This complex was prepared by mixing cobalt(II) acetate tetrahydrate (0.249 g, 1 mmol), H$_2$BN (0.347 g, 1 mmol) and NaN$_3$ (0.065 g, 1 mmol) in methanol (10 mL) and stirred the solution for about 5 hours. The brown precipitate of **22** was washed with methanol followed by ether and then dried over P$_4$O$_{10}$ *in vacuo*. Yield: 58.4%. λ$_m$ (DMF): 13 ohm^{-1} cm^2 mol^{-1}. μ (*B.M.*): 4.85 Elemental Anal. Found (Calcd.) (%): C: 53.27 (53.49), H: 4.84 (4.38), N: 13.22 (13.69).

[Co(BN)(phen) N$_3$] (23): Methanolic solutions of H$_2$BN (0.347 g, 1 mmol), and 1,10-phenanthroline (0.198 g, 1 mmol) were mixed and cobalt(II) acetate tetrahydrate (0.249 g, 1 mmol) dissolved in hot methanol was added. To this NaN$_3$ (0.065 g, 1 mmol) in methanol (10 mL) was added and stirred the solution for 4 hours. The brown precipitate of **23** obtained was washed with methanol followed by ether and then dried over P$_4$O$_{10}$ *in vacuo*. Elemental Anal. Found (Calcd.) (%): C: 61.27 (61.35), H: 3.56 (3.70), N: 17.45 (17.89).

[Co(BN)(4,4'bipy)N$_3$] (24): To a mixture of solutions of H$_2$BN (0.347 g, 1 mmol) and 4,4'-dimethyl-2,2'-bipyridine (0.156 g, 1 mmol) in methanol cobalt(II) acetate tetrahydrate (0.249 g, 1 mmol) dissolved in hot methanol was added. To this NaN$_3$ (0.065 g, 1 mmol) in methanol (10 mL) was then added and stirred for 4 hours. The brown precipitate of **24** obtained was washed with methanol, followed by ether and dried over P$_4$O$_{10}$ *in vacuo*. Elemental Anal. Found (Calcd.) (%): C: 60.39 (60.95), H: 4.10 (4.32), N: 17.46 (17.77).

[Co(BN)(bipy)(NCS)]·H$_2$O (25): Cobalt(II) acetate tetrahydrate (0.249 g, 1 mmol) in methanol (20 mL) was added to a mixture of hot methanolic solutions of H$_2$BN (0.347 g, 1 mmol) and 2,2'-bipyridine (0.156 g, 1 mmol). To this solution, KSCN (0.097 g, 1 mmol) in methanol (10 mL) was added and refluxed the solution for 4 hours. The dark brown precipitate of **25** obtained was washed

with methanol followed by ether and then dried over P_4O_{10} *in vacuo*. Elemental Anal. Found (Calcd.) (%): C: 58.08 (58.49), H: 3.94 (3.96), N: 12.64 (13.20).

[Co(FN)$_2$] (26): Methanolic solutions of the HFN (0.430 g, 2 mmol), cobalt(II) acetate tetrahydrate (0.249 g, 1 mmol) were mixed and refluxed for about 5 hours. The solution was kept overnight. The dark brown product obtained was filtered, washed with methanol followed by ether and dried over P_4O_{10} *in vacuo*. Elemental Anal. Found (Calcd.) (%): C: 53.83 (54.22), H: 3.74 (4.00), N: 16.91 (17.24).

Caution: Azido complexes of metal ions with organic ligands are potentially explosive. Only a small amount of the material should be prepared, and it should be handled with care.

5.3. Results and discussion

Eleven cobalt(II/III) complexes of aroylhydrazones were prepared out of which seven contain heterocyclic bases as auxiliary ligands. Five among them **17, 18, 19, 23** and **24** are azido and one **25**, thiocyanato complexes. They are formed by the reaction of the aroylhydrazone and heterocyclic base with cobaltous acetate followed by metathetical displacement of the acetate anion by azide or thiocyanate anions and cobalt(II) is oxidized to cobalt(III) in these complexes. They are found to be stable, brown in color and soluble in organic solvents like methanol, acetonitrile and DMF. Based on the elemental analyses, conductivity and magnetic susceptibility measurements and spectral investigations, the complexes were formulated. The molar conductivities of the complexes in DMF (10^{-3} M) solution were measured at 298 K with a Systronic model 303 direct-reading conductivity bridge. The values are shown in Table 5.1. The molar conductance values lie in the range 4-12 ohm^{-1} cm^2 mol^{-1} which shows that all the complexes are non-conducting in nature [22].

The elemental analysis data of compounds **17, 18, 19, 23** and **24** suggests a formulation of [MLBN$_3$]. This along with the conductance, magnetic susceptibility and IR data indicate that the azide ion is coordinated to the metal in all these complexes. In compound **25** thiocyanate ion, in **21** methoxy group and in **22** both azide ion and methoxy group are bound to the central metal ion. Magnetic susceptibility measurements at room temperature reveals that all these complexes are diamagnetic which confirms the +3 oxidation state of cobalt and its d^6 electronic arrangement, in strong field showing that it has no unpaired electrons, with a spin paired octahedral configuration. The data obtained from elemental analysis match with the stoichiometry containing one molecule of lattice water in compounds **17** and **25**, two molecules of lattice water in **22** and one molecule of coordinated water in **21**, which is further supported by thermal analysis.

The magnetic moment measurement and partial elemental analyses data are consistent with formulation of compound **16** as [CoL]$_2$, **20** as [Co(BB)(pi)$_3$] (supported by crystal data) and **26** as [Co(FN)$_2$]. The magnetic moment values observed for cobalt(II) complexes are generally investigative of the coordination geometry about the metal ion (as shown in Table 5.1). The magnetic moment of tetrahedral cobalt(II) complex **26**, is 4.5 *B.M.* with an orbitally non-degenerate ground term, which is higher than the spin only value as there is contribution from higher orbitally degenerate terms. The contribution due to ^4T_g ground term is still larger in octahedral cobalt(II) complexes and exhibit μ_{eff} in the range 4.8–5.6 *B.M.* [23].

For the compound **20** the observed effective magnetic moment $\mu = 5.1$ *B.M.* which shows that it has three unpaired electrons and is typical for a high spin cobalt(II) system [16] with octahedral geometry. This value is larger than

the spin only value of high-spin cobalt(II) (3.87 $B.M$; $\mu_{SO} = [4S(S+1)]^{1/2}$; $S = 3/2$) but close to the value obtained [$\mu_{LS} = [L(L+1) /4S(S+1)]^{1/2}$; $L = 3, S = 3/2$] when spin and orbital angular momenta exist independently.

Compound **16** exhibit subnormal magnetic moment ($\mu_{eff} = 1.5$ $B.M.$ at room temperature) due to strong antiferromagnetic exchange proposing a dimeric nature to the compound. X-ray quality single crystal of one of the compound, [Co(BB)(pi)$_3$] (**20**) were obtained from reaction mixture. The compound crystallizes into a monoclinic space group $P 1 2_1/c 1$.

Table 5.1 Molar conductivities and magnetic susceptibilities of Co(II/III)

Compound	λ_m#	μ_{eff} (B.M.)
[Co(BB)]$_2$ (**16**)	9	1.5
[Co(BB)(bipy)N$_3$]·H$_2$O (**17**)	12	diamagnetic
[Co(BB)(phen)N$_3$] (**18**)	8	diamagnetic
[Co(BB)(4,4'-bipy)N$_3$]. (**19**)	10	diamagnetic
[Co(BB)(pi)$_3$] (**20**)	11	5.1
[Co(BN)(OCH$_3$)(H$_2$O)](**21**)	9	diamagnetic
[Co$_2$(BN)$_2$N$_3$(OCH$_3$)] 2H$_2$O (**22**)	13	diamagnetic
[Co(BN)(phen)N$_3$] (**23**)	7	diamagnetic
[Co(BN)(4,4'-bipy)N$_3$].(**24**)	10	diamagnetic
[Co(BN)(bipy)(NCS)]·H$_2$O (**25**)	9	diamagnetic
[Co(FN)$_2$] (**26**)	8	4.5

5.3.1. Crystal structure of [Co(BB)(pi)$_3$] (**20**) .

The Single crystal X-ray diffraction data of [Co(BB)(pi)$_3$] (**20**) were collected on an Oxford Xcalibur Eos (Mova) Diffractometer at 100 K using Mo Kα radiation (λ=0.7107 Å) with X-ray generator operating at 50 kV and 1 mA. The structures were solved and refined using SHELX97 module in the program suite WinGX. The molecular diagrams were generated using ORTEP-3 and the packing diagrams were generated using Mercury 2.3. The geometric

square plane are occupied by N1, O3, N3, and O4 atoms and the axial positions by N4 and N7 atoms. The equatorial bond lengths are shorter than the axial Co–N4 and Co–N7 bond lengths. There is slight deviation for the equatorial bond angles from the expected value of 90.0° which indicates a distortion of the basal plane from a square geometry. The apical Co–N4 bond is not exactly perpendicular to the basal square plane and N4–Co–N7 is not exactly linear, as seen from the bond angles of N4–Co–N3 and N4–Co–N7, 89.49° and 178.91° which indicates distortion from regular octahedral geometry and is confirmed by the fact that the two trans O atoms are at an angle of 179.65°. The two trans N atoms are also not exactly linear as N1–Co–N3, bond angle being 174.27°.

5.3.2. Infrared spectra

The IR spectra of the hydrazones and their Co(II) complexes were recorded in the solid state as KBr discs. The characteristic bands in the IR spectra of the free hydrazones differ from those of their complexes. The bands of diagnostic importance are listed in Table 5.3. IR spectral analyses provide significant indications regarding the bonding sites of the ligands.

Table 5.3 IR spectral data (cm^{-1}) of cobalt(II/III) complexes

Compounds	$v(C=N)$	$v(C=N)^a$	$v(C-O)$	$v(Co-O)$	$v(Co-N)$	$v_a(N_3)$
[Co(BB)]$_2$ (16)	1608	1514	1239	576	442	....
[Co(BB)(bipy)N$_3$]·H$_2$O (17)	1602	1510	1246	565	444	2025
[Co(BB)(phen)N$_3$] (18)	1609	1512	1276	588	422	2018
[Co(BB)(4,4'-bipy)N$_3$] (19)	1609	1510	1269	573	451	2018
[Co(BB)(pi)$_3$] (20)	1602	1510	1240	573	442	....
[Co(BN)(OCH$_3$)·H$_2$O] (21)	1603	1541	1269	565	436	....
[Co$_2$(BN)$_2$N$_3$(OCH$_3$)]·2H$_2$O (22)	1608	1521	1245	573	451	2023
[Co(BN)(phen)N$_3$] (23)	1609	1510	1239	582	448	2025
[Co(BN)(4,4'-bipy)N$_3$] (24)	1607	1516	1242	573	444	2027
[Co(BN)(bipy)(NCS)]·H$_2$O (25)	1602	1518	1246	573	422	2070
[Co(FN)$_2$] (26)	1602	1526	1239	565	423	....

^{a}newly formed

transitions of the azomethine and amide function are masked by strong bands due to π-π^* transitions. The intraligand bands of the free hydrazones are slightly shifted upon complexation. The intense broad band observed for the complexes in the region 24110-25280 cm^{-1} corresponds to the intramolecular ligand to metal charge transfer (LMCT) transitions involving the whole molecule [31].

The electronic spectra of spin paired trivalent octahedral cobalt complexes of d^6 configuration have the following assignments of d-d bands. ν_1: $^1T_{1g} \leftarrow {}^1A_{1g}$, ν_2: $^1T_{2g} \leftarrow {}^1A_{1g}$, ν_3: $^3T_{1g} \leftarrow {}^1A_{1g}$, ν_4: $^3T_{2g} \leftarrow {}^1A_{1g}$ [32]. The ν_1 bands are assigned values ~ 20600 cm^{-1} and ν_2 ~ 25000 cm^{-1}. Very weak bands at ~ 17300 18100 cm^{-1} corresponds to spin forbidden $^3T_{2g} \leftarrow {}^1A_{1g}$ transitions. Assignment of the two high-energy bands is complicated by overlap of interligand and charge transfer transitions. $^3T_{2g} \leftarrow {}^1A_{1g}$ is also difficult to assign because this weak spin forbidden band is always at the onset of other high-energy intense bands. For octahedral Co(III) complexes with a low spin d^6 configuration only one weak d-d transition is observed at around 18000 cm^{-1} as given in the Table.5.4.

Table 5.4. Electronic spectral data (cm^{-1}) of Co (II/ III) complexes in acetonitrile

Compound	Intraligand transitions	LMCT	d-d
[Co(BB)]$_2$ (**16**)	28750, 37048, 41980	24651	15116,16704,17499
[Co(BB)(bipy)N$_3$]·H$_2$O (**17**)	28961, 33582, 40303	24328	18100
[Co(BB)(phen)N$_3$] (**18**)	29905, 37148, 43769	24229	
[Co(BB)(4,4'-bipy)N$_3$] (**19**)	29061, 37570,41980	24862	
[Co(BB)(pi)$_3$] (**20**)	29261, 36018, 40878	24774	17820
[Co(BN)(OCH$_3$)H$_2$O] (**21**)	30948,38374,44548	24844	17882
[Co$_2$(BN)$_2$N$_3$(OCH$_3$)]·2H$_2$O (**22**)	32200,38522,44035	23740	
[Co(BN)(phen)N$_3$] (**23**)	30878, 37418, 44113	24548	18030
[Co(BN)(4,4'-bipy)N$_3$] (**24**)	30287,39331,44749	24479	
[Co(BN)(bipy)(NCS)]·H$_2$O (**25**)	30380, 37515, 43969	248765	17900
[Co(FN)$_2$] (**26**)	28783, 36536, 40970	24324	15206

For tetrahedral Co^{2-} complexes three bands corresponding to the spin allowed transitions $^4T_2(F) \leftarrow {}^4A_2$, $^4T_1(F) \leftarrow {}^4A_2$ and $^4T_1(P) \leftarrow {}^4A_2$ are expected. The electronic spectra of compounds **16** and **26** showed two-three bands in the range 15100-17500 cm^{-1} which may be due to $^4T_1(F) \leftarrow {}^4A_2$ and $^4T_1(P) \leftarrow {}^4A_2$ transitions [35,36] (Fig. 5.12). The transition $^4T_2(F) \leftarrow {}^4A_2$ occurs in the near IR region and is not observed.

5.3.5. Cyclic voltammetric studies

Cyclic voltammograms of the hydrazones and their Co(II) complexes were recorded on a CHI 608D electrochemical analyzer. The electrochemical studies of selected complexes were performed using DMF as the solvent and TBAP (tetrabutylammonium phosphate) as the supporting electrolyte at a scan speed of 100 mV s^{-1}. A three-electrode system design is an essential feature of all cyclic voltammetry systems, and this was incorporated in the present experiment. In simple cases, the surface is started at a particular voltage with respect to a reference half-cell such as calomel or Ag/AgCl, with platinum wires as working and counter electrodes.

Co(II/III) complexes of hydrazones are electrochemically reactive and there are often quite interesting differences in redox reversibility, stability of reduced and oxidized forms, and pH effects. In typical cyclic voltammetry, a solution component is electrolyzed (oxidized or reduced) by placing the solution in contact with an electrode surface, and then making that surface sufficiently positive or negative in voltage to force electron transfer. The electrochemical behavior of metal complexes with O, N, O - donor ligands have been studied so as to scrutinize spectral and structural changes accompanying electron transfer [3,37].

A comparative study of the cyclic voltammetric behavior of the hydrazones with their metal complexes gives the information that redox reactions of the metal

The electrochemical data of the hydrazone complexes of Co(II/III) are given in Table 5.5 and selected cyclic voltammograms for complexes are shown in Fig 5.13. For compound [Co(BB)(pi)$_3$] (20), the reduction peak at -0.47 V is attributed to Co(II)/Co(I) reduction. On the reverse scan the corresponding oxidation peak occurs at 0.79 V can be attributed to the Co(I)/Co(II) oxidation. On the other hand, Co(III) complex [Co(BB)(phen)N$_3$] (18) shows two anodic and two cathodic peak potentials in the forward and reverse scans as given in the Table 5.5.

Table 5.5. Cyclic voltammetric data for Co(II/III) complexes

Compound	E_{pc} (V)	E_{pa} (V)	I_{pc} (μA)	I_{pa} (μA)
[Co(BB)(pi)$_3$] (20)	-0.47	0.78	2.87	-5.45
[Co(BB)(phen)N$_3$] (18)	1.11, -0.07	1.12, -0.11	1.93	-5.09, -1.15

As seen from Fig. 5.13, the cyclic voltammogram of complex [Co(BB)(phen)N$_3$] (18) shows two redox processes in which one of them corresponds to the formation of Co(III)/Co(II) couple at Epc = 1.11 V and Epa = 1.12 V which is found to be reversible. The other one corresponds to the formation of Co(II)/Co(I) couple at Epc = -0.07 V and the associated anodic peak at Epa = -0.11 V.

References

[1] M.S. Rao, K.H. Reddy, Indian J. Chem. A 38 (1999) 262.

[2] M.R. Reddy, K.H. Reddy, K.M. Raju, Polyhedron 17 (1998) 1355.

[3] S.A. Sapp, C.M. Elliott, C. Contado, S. Caramori, C.A. Bignozzi, J. Am. Chem. Soc. 124 (2002) 11215.

[4] S. Chan, W.T. Wong, Coord. Chem. Rev. 138 (1995) 219.

[5]   C.V. Kumar, W.B. Tan, P.W. Betts, J. Inorg. Biochem. 68 (1997) 177.

[6]   C.A. Hastings, J.K. Barton, Biochemistry 38 (1999) 10042.

[7]   J.K. Barton, Science (Washington, DC) 233 (1986) 727.

[8]   S. Srinivasan, J. Annaraj, P.R. Athappan, J. Inorg. Biochem. 99 (2005) 876.

[9]   R.K. Parashar, R.C. Sharma, A. Kumar, G. Mohan, Inorg. Chim. Acta 151 (1988) 201.

[10] H. Chen, D. Han, H. Yan, W. Tang, Y. Yang, H. Wang, Polyhedron 12 (1993) 1097.

[11] N. Mondal, D.K. Dey, S. Mitra, K.M.A. Malik, Polyhedron 19 (2000) 2707.

[12] R.P. John, A. Sreekanth, M.R.P. Kurup, S. M. Mobin, Polyhedron 21 (2002) 2515.

[13] I.J. Stratford, Int. J. Rad. Oncol. Biol. Phys. 22 (1992) 529.

[14] P.F. Raphael, E. Manoj, M.R.P. Kurup, E. Suresh, Polyhedron 26 (2007) 607.

[15] P. Bindu, M.R.P. Kurup, Indian J. Chem. Sect. A 38 (1999) 388.

[16] M.J. Hossain, H. Sakiyama, Inorg. Chim. Acta 338 (2002) 255.

[17] J. S. Wood, Inorg. Chem. 7 (1968) 852.

[18] J. Ribas, A. Escuer, M. Monfort, R. Vicente, R. Cortes, L. Lezama, T. Rojo, Coord. Chem. Rev. 1027 (1999) 193.

[19] A.F. Knowles, A.K. Nagy, Eur. J. Biochem. 262 (1999) 349.

[20] L.-F. Tang, H.-Q. Shi, Z.-H. Wang, L. Zhang, J. Chem. Cryst. 30 (2000) 159.

[21] Q. Zhao, X. Wang, R. Fang, E.R.T. Tiekink, Acta Cryst. E59 (2003) m690.

[22] W.J. Geary, Coord. Chem. Rev. 7 (1971) 81.

[23] S. Yamada, Coord. Chem. Rev. 1 (1966) 415.

[24] C. Place, J.-C. Zimmermann, E. Mulliez, G. Guillot, C. Bois, J.-C. Chottard, Inorg. Chem. 37 (1998) 4030.

[25] N. Mathew, M. Sithambaresan, M.R.P. Kurup, Spectrochim. Acta Part A 79 (2011) 1154.

[26] K. Nakamoto, Infrared and Raman Spectra of Inorganic and Coordination Compounds, 5th ed., Wiley, New York (1997).

[27] A.L. Balch, L.A. Fosset, R.R. Guimerans, M.M. Olmstead, P.E. Reed, F.E. Wood, Inorg.Chem. 25 (1986) 1248.

[28] K. Nakamoto, Infrared and Raman Spectra of Inorganic and Coordination Compounds, 5th ed., Wiley, New York (1978) 124.

[29] M. Joseph, V. Suni, M.R.P. Kurup, M. Nethaji, A. Kishore, S.G. Bhat, Polyhedron 23 (2004) 3069.

[30] M. Joseph, V. Suni, M.R.P. Kurup, M. Nethaji, A. Kishore, S.G. Bhat, Polyhedron 25 (2006) 61.

[31] A.B.P. Lever, Inorganic Electronic Spectroscopy, First ed., Elsevier, Amsterdam (1968).

[32] R. Osterberg, Coord. Chem. Rev. 12 (1974) 309.

[33] S. Chandra, Sangeetika, V.P. Tyagi, S. Raizada, Synth. React. Inorg. Met Org. Chem. 33 (2003) 147.

[34] A.B.P. Lever, J. Lewis, J. Chem. Soc. (1963) 2552.

[35] S. AbouEl-Enein, F.A. El-Saied, S.M. Emam, M.A. Ell-Salamony, Spectrochim. Acta Part A 71 (2008) 421.

[36] A.B.P. Lever, Inorganic Electronic Spectroscopy, 2nd edition, Elsevier, Amsterdam (1984).

[37] A.M. Bond, R.L. Martin, Coord. Chem. Rev. 54 (1984) 23.

SYNTHESES, CRYSTAL STRUCTURES AND SPECTRAL CHARACTERIZATION OF COPPER(II) COMPLEXES OF SOME AROYLHYDRAZONES

6.1 Introduction

Coordination chemistry of copper(II) complexes are of great interest not only due to their versatile applications in various fields such as biological [1,2] catalytical [3,4], magnetochemistry [5], NLO [6], pharmacological [7] etc. but also because of their intriguing variety of architectures and new topologies. The diversity in the structures and topology of the coordination polymers can be attributed to the selection of metal centers and organic building blocks as well as reaction pathways. So far, a large number of coordination complexes of copper(II) composed of chains, sheets and 3D networks based on mixed ligands have been reported [8,9].

Among the metal ions used to build molecule-based magnetic materials, copper(II) has played a prominent role both from experimental and theoretical point of view [10]. However, looking at the structural aspects, the plasticity of the coordination sphere of the copper(II) ion, which accounts for the richness and

variety of its coordination chemistry, is at the origin of the diversity of the topologies and connectivities occurring in the extended assemblies containing this metal ion.

The d^9 configuration of the Cu(II) cation favors either a square planar (4-coordinate) or a square pyramidal (5-coordinate) geometry [11] in coordination complexes under present investigation. It can also offer tetrahedral, trigonal bipyramidal and distorted octahedral geometries with coordination numbers 4, 5 and 6 respectively. Nonspherical symmetry of the Cu(II) ion with d^9 configuration leads to distortion from the basic stereochemistries predicted by the classical molecular mechanics approach. Jahn Teller active ground state supports this deviation to lower symmetry. Square planar or square pyramidal geometries of some of the mixed ligand complex molecules in the present study are confirmed by single crystal X-ray crystallographic analyses.

We can expect non-linear response for copper(II) complexes of hydrazones which are non centrosymmetric or posses inversion centers in the crystalline form. Proper choice of the metal and its oxidation state and of the ligands allows the fragment to behave as an electron donor or acceptor group [12]. Coe *et al.* showed that NLO materials, having the property of limiting the transmitted light (OLs) intensity to a maximum value, i.e. are transparent to weak signals and opaque to strong signals have received considerable attention with increasing application of optical techniques and interdisciplinary fields of the THz-technologies such as spectroscopic imaging, environmental detection and inspection etc [13]. The ability of copper(II) ion to form chelates and its positive redox potential help to involve in biological transport reactions. In redox reactions of copper containing enzymes interconversion of Cu(I) and Cu(II) oxidation states occur which is an essential factor for most of the properties of these enzymes [14,15]. Thus Cu(II) becomes the active centers in

several metalloenzymes and proteins and show variety of biological roles in electron transport, dioxygen transport, oxygenation, disproportionation and redox reaction [16]. '

Copper(II) complex is more potent than the metal free chelate suggesting that metal complex is the biologically active species. For instance copper is required for the activity of monoxigenases: a particulate form of methane monoxigenase (pMMO) and ammonia monoxigenase [17,18]. There is a correlation between copper concentration in the growth medium and in *vitro* and in *vivo* pMMO activity.

Spectral and crystallographic investigations continue to play a key role in proposing the structural features suitable for an activity. Copper enzymes exhibit unique spectroscopic features reflecting novel electronic structures that can make major contributions to reactivity. It has also allowed the identification and detailed description of oxygen intermediates in the copper cluster enzymes [19].

Tamasi *et al.* synthesized copper(II)-benzoylpyridine-2-quinolinylhydrazone complex and analysed its crystal structure by X-ray diffraction analysis and also showed that it is potentially anticancerous and anti-inflammatory [20]. Manoj *et al.* made magnetic and EPR spectral studies of copper(II) complexes of an anticancer drug analogue. EPR spectral simulation of most of the compounds is in agreement with the presence of two uncoupled copper(II) species in solution [21].

Mixed ligand copper(II) complexes of aroylhydrazones, as principal ligands, derived from acetophenone, benzaldehyde, salicylaldehyde and their derivatives were reported [22,23]. We have synthesized copper(II) complexes of aroylhydrazones focused on carbonyl compounds such as 2-hydroxy-4-methoxybenzophenone, furan-2-carboxaldehyde and 5-bromo-3-methoxysalicylaldehyde. Among the heterocyclic

bases, 4-picoline, 1,10-phenanthroline and 2,2'-bipyridine have been used [24]. In the case of monoanionic bidentate hydrazone we incorporate different anions and pseudohalogens into copper precursor complexes. The formation of pseudohalide bridged complexes is interesting because of the structural diversity, magnetic and spectral properties [25]. Single crystals of five of the copper complexes, suitable for X-ray diffraction studies were obtained and crystal structures were solved by direct method of SHELXS-97 [26].

6.2 Experimental

6.2.1 Materials

All chemicals and reagents are of reagent grade quality. 2-Hydroxy-4-methoxybenzophenone (Aldrich), furan-2-carboxaldehyde (Aldrich), 5-bromo-3-methoxysalicylaldehyde (Aldrich), nicotinic acid hydrazide (Aldrich), benzhydrazide (Aldrich), N'-4-nitrobenzoylhydrazide(Aldrich), copper(II) acetate monohydrate (Qualigens), copper(II) chloride dihydrate (E-Merck), sodium azide (Reidel-De Haen), potassium thiocyanate (E-Merck), 4-picoline, (Aldrich), 2,2'-bipyridine (Qualigens), 1,10-phenanthroline (Ranchem) and DMF (S.D.Fine) were used without further purification. Methanol and ethanol were used as solvents.

6.2.2 Syntheses of the aroylhydrazones

The method of synthesis of aroylhydrazones, 2-hydroxy-4-methoxybenzophenone benzoylhydrazone (H_2BB), 2-hydroxy-4-methoxybenzophenone nicotinoylhydrazone (H_2BN), N-2-hydroxy-4-methoxybenzophenone-N'-4-nitrobenzoylhydrazone (H_2BF), furan-2-carboxaldehyde nicotinoylhydrazone (HFN) and 5-Bromo-3-methoxysalicylaldehyde benzoylhydrazone [H_2SB] is described in Chapter 2.

6.2.3 Syntheses of copper(II) complexes

[Cu₂(BB)₂](27): To a hot methanolic solution of the aroylhydrazone H_2BB (0.346 g, 1 mmol), $Cu(OAc)_2 \cdot H_2O$ (0.199 g, 1 mmol) dissolved in hot methanol was added. On refluxing, pale green amorphous product was separated at once. This was filtered, washed with ether and dried over P_4O_{10} *in vacuo*. Elemental Anal. Found (Calcd.) (%): C, 61.44 (61.83); H, 4.09 (3.95); N, 6.84 (11.98).

[Cu(BB)phen] **(28)**: Methanolic solutions of H_2BB (0.346 g, 1 mmol), and 1,10-phenanthroline (0.198 g, 1 mmol) were mixed and refluxed for about half an hour. $Cu(OAc)_2 \cdot H_2O$ (0.199 g, 1 mmol) dissolved in hot methanol and DMF (10:1 ratio v/v) was added and refluxed for 4-5 h. On slow evaporation green plate like crystals suitable for single crystal X-ray diffraction studies were obtained and 2-3 crystals were separated. The remaining product was filtered, washed with methanol, followed by ether and dried over P_4O_{10} *in vacuo*. Elemental Anal. Found (Calcd.) (%): C: 66.88 (67.28), H: 4.03 (4.28), N: 9.72(9.51).

[Cu(BB)bipy]·C₂H₅OH (29): To a refluxing solution of H_2BB (0.346 g, 1 mmol) and 2,2'-bipyridine (0.156 g, 1 mmol) in ethanol, $Cu(OAc)_2 \cdot H_2O$ (0.199 g, 1 mmol) dissolved in hot ethanol and DMF (10:1 ratio v/v) were added and refluxed for about 5h. On slow evaporation dark green block shaped crystals suitable for single crystal X-ray diffraction studies were obtained and a few crystals were collected. The remaining green colored crystalline product was filtered, washed with ethanol, followed by ether and dried over P_4O_{10} *in vacuo*. Elemental Anal. Found (Calcd.) (%):C: 65.51 (65.89), H: 4.23 (4.46), N: 9.49 (9.91).

[Cu(BB)pi] **(30)**: A solution of H_2BB (0.346 g, 1 mmol) and 4-picoline (2-3 mL) in methanol were mixed with $Cu(OAc)_2 \cdot H_2O$ (0.199 g, 1 mmol) dissolved in hot methanol and DMF (10:1 ratio v/v) and refluxed for about 5 hours. The brown colored crystalline product was filtered, washed with methanol, followed by ether and dried over P_4O_{10} *in vacuo*. Dark brown plate like crystals suitable for single crystal X-ray diffraction studies were obtained by slow evaporation of its solution in ethanol and DMF (10:1 ratio v/v). Elemental Anal. Found (Calcd.) (%): C: 64.38 (64.72), H: 4.32 (4.63), N: 9.26 (9.58).

[Cu$_2$(BN)$_2$] **(31)**: To a hot methanolic solution of $Cu(OAc)_2 \cdot H_2O$ (0.199 g, 1 mmol), methanolic solution of the hydrazone H_2BN (0.347 g, 1 mmol) was added with stirring. Pale green amorphous product separated was filtered, washed with ether and dried over P_4O_{10} *in vacuo*. Elemental Anal. Found (Calcd.) (%): C: 58.23 (58.75), H: 3.08 (3.70), N: 10.14 (10.28).

[Cu(BN)phen]·H$_2$O **(32)**: This complex was prepared by refluxing 1:1:1 ratio of $Cu(OAc)_2 \cdot H_2O$ (0.199 g, 1 mmol), 1,10-phenanthroline (0.198 g, 1 mmol) and H_2BN (0.347 g, 1 mmol) in methanol and DMF (10:1 ratio v/v) for about 6 h. Dark green product obtained was filtered, washed with methanol followed by ether and dried over P_4O_{10} *in vacuo*. Dark green elongated blocks of crystals suitable for single crystal X-ray diffraction studies were obtained by slow evaporation of its solution in methanol and DMF (10:1 ratio v/v). Elemental Anal. Found (Calcd.) (%): C: 62.91 (63.31),   H: 3.95 (4.15), N: 11.27 (11.54).

[Cu$_2$(BF)$_2$] **(33)**: A hot methanolic solution of the hydrazone H_2BF (0.391 g, 1 mmol), was added to a hot methanolic solution of $Cu(OAc)_2 \cdot H_2O$ (0.199 g, 1 mmol), with stirring. Pale yellow amorphous product separated was filtered, washed with ether and dried over P_4O_{10} *in vacuo*. Elemental Anal. Found (Calcd.) (%): C: 55.86 (55.69), H: 3.01 (3.34), N: 9.20 (9.28).

[Cu(FN)₂] **(34)**: Methanolic solutions of the ligand, HFN (0.430 g, 2 mmol), Cu(OAc)$_2$·H$_2$O (0.199 g, 1 mmol) and 2,2'-bipyridine (0.156 g, 1 mmol) were mixed and refluxed for about 6-7 h. The solution was kept overnight. The dark brown product obtained was filtered, washed with methanol followed by ether and dried over P$_4$O$_{10}$ *in vacuo*. Elemental Anal. Found (Calcd.) (%):C: 53.64 (53.71), H: 3.36 (3.28), N: 16.94 (17.08).

[Cu(FN)Cl(H₂O)]·2H₂O **(35)**: Hot ethanolic solutions of the aroylhydrazone, HFN (0.215 g, 1 mmol) and CuCl$_2$·2H$_2$O (0.170 g, 1 mmol) were mixed and refluxed for about 2 h. The dark green crystalline product obtained was filtered, washed with ethanol followed by ether and dried over P$_4$O$_{10}$ *in vacuo*. Elemental Anal. Found (Calcd.) (%):C: 36.42 (35.98), H: 3.50 (3.84), N: 11.34 (11.44).

[Cu₂(FN)₂(μ-NCS)₂] **(36)**: Ethanolic solutions of the aroylhydrazone, HFN (0.215 g, 1 mmol), KSCN (0.097 g, 1 mmol) and Cu(OAc)$_2$·H$_2$O (0.199 g, 1 mmol) were mixed and refluxed for about 2 h. The dark green crystalline product obtained was filtered, washed with ethanol followed by ether and dried over P$_4$O$_{10}$ *in vacuo*. Elemental Anal. Found (Calcd.) (%): C: 42.35 (42.92), H: 2.16 (2.40), N: 16.47 (16.68).

[Cu₂(FN)₂(μ-N₃)₂] **(37)**: To an ethanolic solution of the aroylhydrazone, HFN (0.215 g, 1 mmol), ethanolic solution of NaN$_3$ (0.065 g, 1 mmol) was added dropwise while the mixture was stirred for half an hour. To this solution, ethanolic solution of Cu(OAc)$_2$·H$_2$O (0.199 g, 1 mmol) was added. The dark green amorphous product obtained was filtered, washed with ethanol followed by ether and dried over P$_4$O$_{10}$ *in vacuo*. Elemental Anal. Found (Calcd.) (%):C: 40.15 (40.97), H: 2.66 (3.44), N: 24.17 (23.89).

[Cu₂(SB)₂](38): To a hot methanolic solution of the ligand H_2SB (0.231 g, 1 mmol), $Cu(OAc)_2 \cdot H_2O$ (0.199 g, 1 mmol) dissolved in hot methanol was added. Dark green amorphous product was formed on refluxing. This was filtered, washed with ether and dried over P_4O_{10} *in vacuo*. Elemental Anal. Found (Calcd.) (%):C: 40.31 (40.84), H: 2.38 (2.45), N: 10.14 (10.21).

[Cu(SB)(pi)]·H₂O (39): A solution of H_2SB (0.231 g, 1 mmol) and 4-picoline (2-3 mL) in ethanol were mixed with $Cu(OAc)_2 \cdot H_2O$ (0.199 g, 1 mmol) dissolved in hot ethanol and DMF (10:1 ratio v/v) and refluxed for about 5. The brown colored crystalline product was filtered, washed with methanol, followed by ether and dried over P_4O_{10} *in vacuo*. Dark brown plate like crystals suitable for single crystal X-ray diffraction studies were obtained by slow evaporation of its solution in ethanol and DMF (10:1 ratio v/v). Elemental Anal. Found (Calcd.) (%):C: 47.11 (47.58), H: 3.29 (3.39), N: 11.02 (11.10).

6.3 Results and discussion

The newly synthesized copper complexes are quite stable in air and their melting points are found to be greater than 250 °C. The observed elemental analyses data are in good agreement with the calculated value of the proposed formulae of the complexes. They are soluble in organic solvents like acetonitrile and DMF. The molar conductance measurements of all the Cu(II) complexes are in the range 3-12 ohm^{-1} cm^2 mol^{-1} that confirm the non-electrolytic nature of the complexes. Magnetic moments of the complexes are calculated by magnetic susceptibility measurements at 298 K. Diamagnetic corrections are also considered. The magnetic moment values for the complexes **27, 31, 33, 36, 37** and **38** showed substantial decrease and lie in the range of 1.05 -1.35 B. M. which is much less than the spin only value. Such a low value of magnetic moment indicates antiferromagnetic interaction between two metal

centres having unpaired electrons suggesting dimeric nature to these complexes [27-28]. The observed magnetic susceptibility values of the complexes **29, 34, 35** and **39** are in close agreement with the spin only value for a d^9 copper system and that for the compounds **28, 30** and **32** show small decrease from the spin only value. So there may be some interaction between the magnetic centers in the solid state owing to the noncovalent interactions in close packing [29]. The experimental values of magnetic moments are in good agreement with EPR results. The magnetic susceptibility and molar conductivity values of the complexes are presented in Table 6.1. X-ray quality single crystals of five Cu(II) compounds, **28, 29, 30, 32** and **39** were obtained by slow evaporation of the solution of corresponding compounds in CH_3OH or C_2H_5OH and DMF.

Table 6.1 Molar conductivities and magnetic moments of copper(II) complexes

Compound	$\lambda_m^{\#}$	μ_{eff} (B. M.)
$[Cu_2(BB)_2]$ **(27)**	9	1.10
[Cu(BB)phen] **(28)**	6	1.34
$[Cu(BB)bipy]\cdot C_2H_5OH$ **(29)**	8	1.90
[Cu(BB)pi] **(30)**	4	1.36
$[Cu_2(BN)_2]$ **(31)**	6	1.02
$[Cu(BN)phen]\cdot H_2O$ **(32)**	7	1.29
$[Cu_2(BF)_2]$ **(33)**	5	1.07
$[Cu(FN)_2]$ **(34)**	10	1.87
$[Cu(FN)Cl.H_2O]\cdot 2H_2O$ **(35)**	11	1.82
$[Cu_2(FN)_2 (\mu\text{-}CNS)_2]$ **(36)**	10	1.21
$[Cu_2(FN)_2 (\mu\text{-}N_3)_2]$ **(37)**	12	1.23
$[Cu_2(SB)_2]$ **(38)**	7	1.30
$[Cu(SB)(pi)]\cdot H_2O$ **(39)**	9	1.91

$^{\#}$molar conductivity (in mho cm^2 mol^{-1}) taken in 10^{-3} M DMF.

6.3.1 Single Crystal XRD studies

The Single crystal X-ray diffraction analyses of [Cu(BB)phen] **(28)** and [Cu(BB)bipy]·C_2H_5OH **(29)** were performed with a Bruker SMART APEX CCD

X–ray diffractometer at the University of Hyderabad, using graphite monochromated Mo Kα radiation (λ=0.71073 Å, φ and ω scans. The structure was solved using SHELXS–97 and full matrix least squares refinement against F^2 was carried out using SHELXL–97 in anisotropic approximation for non-hydrogen atoms.   All hydrogen atoms were assigned on the basis of geometrical considerations and were allowed to ride upon the respective carbon atoms.

The Single crystal X-ray diffraction data of [Cu(BB)pi] (**30**) were collected on an Oxford Xcalibur Eos (Mova) Diffractometer at 100 K using Mo Kα radiation (λ=0.7107 Å) with X-ray generator operating at 50 kV and 1 mA. The structures were solved and refined using SHELX97 module in the program suite WinGX. . The geometric calculations were carried out by PARST95 and PLATON and all the hydrogen atoms were fixed in calculated positions.

The single crystal X-ray diffraction data of [Cu(BN)phen]·H_2O(**32**) and [Cu(SB)(pi)]·H_2O (**39**), were collected using Bruker SMART APEX diffractometer, equipped with graphite –crystal, incident-beam monochromator, and a fine focus sealed tube with Mo Kα (λ = 0.71073 Å) as the X-ray source The structure was solved by direct methods and refined by full-matrix least-squares calculations with the SHELXL-97 software package and all hydrogen atoms on carbon were placed in calculated positions, guided by difference maps and refined isotropically.

In all the cases the molecular diagrams were generated using ORTEP-3 and the packing diagrams were generated using Mercury 2.3. and DIAMOND version 4.2g.

Table 6.2. Crystal data and structure refinement for [Cu(BB)(phen)].

Empirical formula	$C_{33} H_{24} Cu N_4 O_3$
Formula weight	588.11
Temperature	298(2) K
Wavelength	0.71073 Å
Crystal system, space group	Monoclinic, $P2_1/c$
Unit cell dimensions	a = 18.0207(11) Å α = 90°.
	b = 10.3748(6) Å β = 101.9450(10)°.
	c = 14.7870(9) Å γ = 90°
Volume	2704.7(3) Å ^{3}
Z, Calculated density	4, 1.444 Mg/m^3
Absorption coefficient	0.850 mm^{-1}
F(000)	1212.0
Crystal size	0.36 x 0.22 x 0.03 mm
Theta range for data collection	1.15 to 26.06°
Limiting indices	$-22 \leq h \leq 22$, $-12 \leq k \leq 12$, $-18 \leq l \leq 18$
Reflections collected / unique	26876 / 5360 [R(int) = 0.0705]
Completeness to theta	= 26.06° 99.6%
Absorption correction	Semi-empirical from equivalents
Max. and min. transmission	0.821 and 0.191
Refinement method	Full-matrix least-squares on F^2
Data / restraints / parameters	5339 / 0 / 371
Goodness-of-fit on F^2	1.028
Final R indices [I > 2sigma(I)]	R_1 = 0.0574, wR_2 = 0.1284
R indices (all data)	R_1 = 0.0981, wR_2 = 0.1471
Largest diff. peak and hole	0.650 and -0.243 e.A^{-3}

$R_1 = \Sigma||F_o| - |F_c|| / \Sigma|F_o|$ $wR_2 = [\Sigma w(F_o^2-F_c^2)^2 / \Sigma w(F_o^2)^2]^{1/2}$

The bond length of C14–O2, 1.305(5) Å agrees with the coordinating pattern of hydrazone *via* enolate form. The heterocyclic base phenanthroline which acts as the co-ligand binds asymmetrically to Cu(II) as there is a longer Cu -N3 bond (axial) when compared with strongly bound Cu–N4 bond (equatorial) and forms a five membered chelate ring. The Cu–N1, O1 and O2 bond lengths are less than 2 Å and that of Cu–N4 is 2.031 Å indicating a strong coordination of phenanthroline and the ligand [30] to the metal centre. The bond distances are in the range of those reported in the Cambridge Structural Database for amide and carbonyl compounds [31] and other similar compounds [12, 22, 28, 29].

Table 6.3 Selected bond lengths and bond angles for [Cu(BB)(phen)]

Bond length (Å)		Bond angles (°)	
Cu–N4	2.031(3)	N3–Cu–O1	98.05(11)
Cu–N3	2.344(3)	N3–Cu–O2	97.73(11)
Cu–O1	1.908(3)	N3–Cu–N1	116.18(12)
Cu–O2	1.939(3)	N3–Cu–N4	75.84(12)
Cu–N1	1.939(3)	O1–Cu–N1	92.29(12)
Cu–N2	2.817(3)	N1–Cu–O2	82.74(12)
C14–O2	1.305(5)	O2–Cu–N4	92.13(12)
C1–O1	1.290(5)	N4–Cu–O1	89.56(12)
C7–N1	1.293(5)	O1–Cu–O2	164.06(12)
N1–N2	1.411(4)	N1–Cu–N4	167.39(13)
N2–C14	1.339(5)		
C14–C15	1.463(6)		

The five coordinated complex adopts a square pyramidal structure [32] but deviates from a regular square pyramidal geometry, as evidenced from the following observations. The apical and the basal coordination positions of the square pyramid are occupied by N3, O2, N1, O1 and N4 atoms. The apical Cu–N3 bond is not exactly perpendicular to the basal square plane as seen from the bond angles, N3–Cu–N1 (116.18°), N3–Cu–O1 (98.05°) etc. The equatorial bond angles deviate slightly from the expected value of 90.0° as given in the Table 6.3. When these bond angles are summed it comes below 360.0° which illustrates that the basal portion has a little distortion from planarity and copper atom slightly shifted from the square plane. Also the two trans O atoms are at an angle of 164.06° and the two trans N atoms are not completely linear N1 Cu–N4, bond angle being (167.39°).

The angular structural parameter τ = 0.0555, {τ = (β – α)/60}, shows that there is only a small distortion from square pyramidal towards trigonal

H18···π(edge) interactions with interaction geometries 2.866 Å, 172.17° as shown in Fig. 6.2. Strong classical hydrogen bonds are absent in the crystal structure. C–H···π molecular dimers are interlinked by C–H···π (edge) interactions, 2.758 Å, 147.07° and C29–H29···O1 interactions, 2.541(3) Å, 168.2(2)° in a bifurcated manner as seen in Fig. 6.3. phenanthroline rings Cg[9] and Cg[4] are involved in π–π stacking with a distance of 3.554(2) Å, β=14.09° stacks up the supramolecular chains as given in Fig. 6.4 which is assisted by weak C24–H24···O2 interactions 2.711(2) Å, 131.94(28)°.

Table 6.4 H-bonding and π-π interaction parameters of the compound [Cu(BB)(phen)]

H-bonding				
D–H···A	D–H (Å)	H···A (Å)	D···A (Å)	D–H···A (°)
C(22)–H(22)···O(3)	0.93	2.58	3.469 (6)	161
C(29)–H(29)···O(1)	0.93	2.541 (3)	3.457 (5)	168.23 (26)
C(24)–H(24)···O(2)	0.93	2.711 (2)	3.658 (6)	131.94 (28)
π-π interaction				
Cg(I) ··· Cg(J)	Cg··· Cg (Å)	α (°)	β (°)	
Cg(9) ··· Cg(4)[a]	3.554 (2)	1.07 (18)	14.09	
Cg(4) ··· Cg(5)[b]	3.746 (2)	19.49 (19)	9.42	
Equivalent position codes				
a = 1-x,-y,1-z		b = 1-x,-1/2+y,1/2-z		
Cg (4) = N(3), C(22) - C(25), C(33)		Cg (5) = N(4), C(28) - C(32)		
Cg (9) = C(25)- C(28), C(32), C(33)				

D, donor; A, acceptor; Cg, centroid; α (°), dihedral angle between planes I and J; β (°), angle between Cg(I)·Cg(J) vector and normal to plane I;

The interchain stacking interaction between the phenanthroline rings in the compound is remarkably strong and it may be due to larger π system in phenanthroline ligand [22]. The crystal packing is supported by more Cg(π)-Cg(π), C–H···π and weak hydrogen bonding interactions. The interaction

Table 6.5. Crystal data and structure refinement for
[Cu(BB) (bipy)]·C_2H_5OH

Empirical formula	$C_{33} H_{30} Cu N_4 O_4$
Formula weight	610.16
Temperature	153(2) K
Wavelength	1.54184 Å
Crystal system, space group	Monoclinic, $P2_1/n$
Unit cell dimensions	a = 14.0974(9) Å α = 90 °.
	b = 12.1021(9) Å β = 100.190(7) °
	c = 17.3687(14) Å γ = 90 °.
Volume	2916.5(4) Å³
Z, Calculated density	4, 1.390 Mg/m³
Absorption coefficient	1.421 mm⁻¹
F(000)	1268.0
Crystal size	0.40 x 0.32 x 0.28 mm
Theta range for data collection	3.73 to 72.98 °.
Limiting indices	-17≤h≤17, -15≤k≤15, -16≤l≤21
Reflections collected / unique	10999 / 5821 [R(int) = 0.0295]
Completeness to theta = 72.98	91.2 %
Absorption correction	Semi-empirical from equivalents
Max. and min. transmission	1.00000 and 0.88107
Refinement method	Full-matrix least-squares on F^2
Data / restraints / parameters	5309 / 0 / 383
Goodness-of-fit on F^2	0.956
Final R indices [I > 2sigma(I)]	R_1 = 0.0501, wR_2 = 0.1230
R indices (all data)	R_1 = 0.0832, wR_2 = 0.1349
Extinction coefficient	0.00005(9)
Largest diff. peak and hole	0.313 and -0.475 e.A⁻³

The coordination environment around the Cu(II) centre is square pyramidal in this complex but deviates from a regular square pyramidal geometry, as evidenced from the following observations. The relevant bond angles and bond lengths and are presented in Table 6.6. The five and six membered chelate rings Cg(1){Cu, N1, N2, C14, O2} and Cg(3) {Cu, N1, C7, C6, C1,O1} occupying the basal plane are fused along a common axis Cu–N1 making a dihedral angle of 9.81(12)° between them which indicates deviation

from planarity. The other five membered chelate ring Cg(2) {Cu, N3, C26, C27, N4} making dihedral angles of 87.86(14)° and 84.92(13)° with the above said five and six membered chelate rings respectively shows the axial disposition of the bipyridyl system with the basal plane.

Table 6.6. Selected bond lengths and bond angles for [Cu(BB)(bipy)]·C_2H_5OH

Bond length (Å)		Bond angle (°)	
Cu–N4	2.225(3)	N3–Cu–O1	91.27(10)
Cu–N3	2.026(3)	N3–Cu–O2	94.81(10)
Cu–O1	1.918(2)	N3–Cu–N1	176.51(11)
Cu–O2	1.947(2)	N3–Cu–N4	77.37(12)
Cu–N1	1.934(3)	O1–Cu–N1	92.22(10)
Cu–N2	2.808(3)	N1–Cu–O2	81.84(10)
C14–O2	1.291(4)	O2–Cu–N4	94.09(11)
C1–O1	1.325(4)	N4–Cu–O1	103.64(11)
C7–N1	1.302(4)	O1–Cu–O2	162.13(10)
N1–N2	1.397(4)	N1–Cu–N4	101.83(11)
N2–C14	1.319(4)		
C14–C15	1.492(5)		

The coordination positions of the basal square plane are occupied by N3, O2, N1, and O1 atoms and the apex by N4 atom. The equatorial bond lengths are shorter than the axial Cu–N4 bond lengths. This is a consequence of the Jahn Teller effect observed in d^9 electronic ground state of the five coordinate complex which elongates one coordinate bond while shortening the remaining four. The apical Cu–N4 bond is not exactly perpendicular to the basal square plane as seen from the bond angles of N4–Cu–N1, 101.83°(11)°, N4–Cu–O1, 103.64(11)° etc. There is slight deviation for the equatorial bond angles from the expected value of 90.0° which indicates a distortion of the basal plane from a square geometry and is confirmed by the fact that the two trans O atoms are at

via enolate form. 4-picoline, the heterocyclic base which acts as the co-ligand is strongly bound to Cu(II) as seen from the bond length of Cu–N7, 1.9912 Å.

Table 6.8. Crystal data and structure refinement for [Cu(BB)(pi)] (30)

Empirical formula	$C_{27}H_{23}N_3O_3Cu$
Formula weight	501.03
Temperature (T) K	293(2)
Crystal system	triclinic
Space group	P-1
a (Å), b (Å), c (Å)	9.757(5), 10.908(6), 12.930(7)
α/°, β/°, γ/°	114.388(8), 90.814(9), 110.151(9)
Volume (Å^3)	1156.8(11)
Z	2
ρ_{calc} (mg mm^{-3})	1.438
μ (mm^{-1})	0.979
F(000)	518
Crystal size (mm^3)	0.20 × 0.20 × 0.20
2Θ range for data collection	3.52 to 52°
Index ranges	-12 ≤ h ≤ 12, -13 ≤ k ≤ 13, -15 ≤ l ≤ 15
Reflections collected	11927
Independent reflections	4503[R(int) = 0.0235]
Data/restraints/parameters	4503/0/309
Goodness-of-fit on F^2	0.988
Final R indexes [I > 2σ (I)]	R_1 = 0.0358, wR_2 = 0.0914
Final R indexes [all data]	R_1 = 0.0494, wR_2 = 0.0944
Largest diff. peak/hole e (Å^{-3})	0.366/-0.198

$R_1 = \Sigma||F_o| - |F_c|| / \Sigma|F_o| \quad wR_2 = [\Sigma w(F_o^2 - F_c^2)^2 / \Sigma w(F_o^2)^2]^{1/2}$

The Cu–N5, O2 and O3 bond lengths are also less than 2 Å indicating a strong coordination of 4-picoline and the principal ligand [30] to the metal

centre. The bond distances are in the range of those reported in the Cambridge Structural Database for amide and carbonyl compounds [31].

Table 6.9. Selected bond lengths and bond angles for [Cu(BB)(pi)]

Bond length (Å)		Bond angle (°)	
Cu–O3	1.9208	N7–Cu–O3	90.36
Cu–O2	1.8703	O3–Cu–N5	82.08
Cu–N5	1.9229	N5–Cu–O2	94.91
Cu–N7	1.9912	O2–Cu–N7	92.80
Cu–N6	2.801	N5–Cu–N7	170.95
C10–O3	1.296(3)	O3–Cu–O2	176.46
C10–N6	1.315(3)	C14–C10–N6	117.9(2)
N6–N5	1.398(3)	N5–C12–C9	119.5(2)
N5–C12	1.308(3)	C12–C11–C13	124.4(2)
C12–C11	1..443(3)	C13–C11–C8	116.7(2)
C11–C13	1.437(3)	O3–C10–C14	117.2(2)
C13–O2	1.326(3)		
C15-O4	1.362(3)		

The four coordinate complex adopts a square planar structure but deviates from its regular geometry, as evidenced from the following observations. The four equatorial coordination positions of the square plane are occupied by N5, O2, N7 and O3 atoms around Cu(II) centre. Relevant values of bond angles and bond lengths are summarized in Table 6.9. They are comparable to the corresponding values in similar compounds [12]. The equatorial bond angles deviate slightly from the expected value of 90.0°, the maximum deviation being 7.92°. The O3–Cu–N5 chelating angle is more acute than the remaining bite angles subtending at the metal centre, which is due to the steric binding constrains imposed by the small bite angles of the ligand. When these bond angles are summed it comes to 360.15° which illustrates that the basal portion has a little distortion from planarity and copper atom slightly shifted from the square plane. Also the two trans O atoms and the two trans N

also supported by intermolecular $Cu\cdots\pi$ interactions of different interaction distances (3.54 Å and 3.84 Å, see Table 6.10) on either sides of the central Cu atom in this square planar complex (Fig. 6.11b). The molecular conformation is found to be significantly deviating from planarity in order to accommodate various modes of intermolecular interactions. The $Cg(\pi)$ - $Cg(\pi)$ stacking interactions between rings with Cg-Cg distances of 3.6548 Å and 3.7022 Å can support the packing stability in the absence of strong classical hydrogen bonds.

Table 6.10. Ring-metal and π-π interaction parameters of the compound [Cu(BB)(pi)]

Ring-Metal Interactions			
$Cg(I)\cdots Me(J)$	$Cg(I)\cdots Me(J)$ (Å)	β (°)	
$Cg(4)^a \cdots Cu$	3.541	13.33	
$Cg(6)^b \cdots Cu$	3.843	32.74	
π-π interaction			
$Cg(I)\cdots Cg(J)$	$Cg\cdots Cg$ (Å)	α (°)	β (°)
$Cg(2)\cdots Cg(4)^a$	3.6548	1.92(10)	19.59
$Cg(1)\cdots Cg(4)^a$	3.7022	2.80(11)	21.33
$Cg(2)\cdots Cg(6)^b$	4.2227	25.90(12)	25.45
Equivalent position codes			
a = 1-x,1-y,1-z b = 1-x,-y,-z			
Cg (1) = Cu, O(3), N(5), N(6), C(10) Cg (4) = C(8), C(11), C(13), C(15), C(16)			
Cg (2) = Cu, O(2), N(5), C(11) · C(13) Cg (6) = C(14), C(18), C(23), C(28), C(29),C(32)			

D, donor; A. acceptor; Cg, centroid; α (°), dihedral angle between planes I and J; β (°), angle between Cg(I)-Cg(J) vector and normal to plane I;

6.3.1.4. Crystal structure description of [Cu(BN)(phen)]·H$_2$O (32)

The compound crystallizes in space group $C2/c$ with Z = 4. The molecular structure along with atom labeling scheme is shown in Fig. 6.13. A summary of the crystal data and structure refinement parameters is given in Table 6.11. Selected bond lengths and angles for **32** are listed in Table 6.12. Single crystals of [Cu(BN)(phen)] ·H$_2$O (**32**) suitable for X-ray diffraction

Table 6.11. Crystal data and structure refinement for [Cu(BN)(phen)] $\cdot H_2O$ (**32**)

Empirical formula	$C_{64} H_{49} Cu_2 N_{10} O_7$
Formula weight	1197.23
Temperature	296(2) K
Wavelength	0.71073 A
Crystal system, space group	Monoclinic, $C2/c$
Unit cell dimensions	a = 14.5423(13)Å α = 90°
	b = 18.6908(16)Å β= 98.233(3)°
	c = 19.8681(16)Å γ= 90°
Volume	5344.6(8) Å³
Z, Calculated density	4, 1.488 Mg/m³
Absorption coefficient	0.864 mm^{-1}
F(000)	2468.0
Crystal size	0.40 x 0.20 x 0.20 mm
Theta range for data collection	1.79 to 25.00°
Limiting indices	$-17 \leq h \leq 17$, $-18 \leq k \leq 22$, $-23 \leq l \leq 23$
Reflections collected / unique	19327 / 4714 [R(int) = 0.0613]
Completeness to theta =	25.00 99.9%
Absorption correction	Semi-empirical from equivalents
Max. and min. transmission	0.841 and 0.813
Refinement method	Full-matrix least-squares on F^2
Data / restraints / parameters	4711 / 3 / 382
Goodness-of-fit on F^2	1.121
Final R indices [I > 2sigma(I)]	R_1 = 0.0422, wR_2 = 0.1216
R indices (all data)	R_1 = 0.0522, wR_2 = 0.1393
Largest diff. peak and hole	0.621 and -0.786 e.Å^{-3}

$R_1 = \Sigma ||F_o| - |F_c|| / \Sigma |F_o|$ $wR_2 = [\Sigma w(F_o^2 - F_c^2)^2 / \Sigma w(F_o^2)^2]^{1/2}$

The five coordinate complex exhibits a square pyramidal structure but deviates from a regular square pyramidal geometry, as evidenced from the following observations. The index of trigonality, τ = 0.1852 for **32**, describing the continuum between square–pyramidal (τ = 0) and trigonal–bipyramidal (τ = 1), defined by Addison *et al.* [33], which indicates that the geometry of the complex is distorted from a regular square–pyramid. The geometric requirements of the ligand means that the geometry around the Cu(II) centre is

not regular. The angle subtended at Cu(II) in **32** by the two oxygen atoms, O(1)–Cu(1)–O(2), 164.34(9)° is significantly compressed, and the bite angles of N(1)–Cu(1)–O(1), 93.11(9)° and O(2)–Cu(1)–N(1), 82.02(9)° are distorted from 90°. Most of the angles involving the central copper atom are widely different from 90° and 180° as given in the Table 6.12 indicating significant distortion from square pyramidal geometry.

Table 6.12. Selected bond lengths and bond angles of [Cu(BN)(phen)] · H_2O (**32**)

Bond length (Å)		Bond angle (°)	
Cu–N4	2.013(2)	N4–Cu–O1	90.78(9)
Cu–N5	2.306(3)	N4–Cu–O2	94.82(8)
Cu–O1	1.889(2)	N4–Cu–N1	175.45(10)
Cu–O2	1.962(2)	N5–Cu–N1	100.18(9)
Cu–N1	1.922(1)	O1–Cu–N1	93.11(9)
Cu–N2	2.811(1)	N1–Cu–O2	82.02(9)
C14–O2	1.278(3)	N5–Cu–N4	76.97(9)
C1–O1	1.292(4)	N5–Cu–O1	97.21(9)
C7–N1	1.280(4)	O1–Cu–O2	164.34(9)
N1–N2	1.423(3)	N5–Cu–O2	98.29(9)
N2–C14	1.312(4)		
C14–C15	1.488(4)		

These distortions arise from the rigidity of the chelate rings [36], compounded by the Cu(II) covalent radius. The bite angles are comparable to those reported for other Cu(II) complexes containing both five- and six membered chelate rings with oxygen and nitrogen donor atoms [37]. The five-membered chelate rings, Cg(1) Cu, O(2), N(1), N(2),C(14) and Cg(2) Cu, N(4), N(5), C(31), C(32) are practically planar (largest deviation 0.025(2) Å for N1 and -0.028(2) Å for N5), and the rings are not puckered. But atoms O1 and N(4) occupying the basal coordination positions deviate significantly by 0.437(2) Å and -0.179(2) Å from the plane of Cg(1). The six-membered chelate ring Cg(3)-

length of C7–O2, 1.302(7) Å corresponds to the coordinating mode of hydrazone *via* enolate form. 4-Picoline, the heterocyclic base which acts as the co-ligand is strongly bound to Cu(II) as seen from the bond length of Cu–N1, 1.989(4) Å. The bond lengths of other equatorial bonds Cu–N2, O1 and O2 are also less than 2 Å indicating a strong coordination of 4-picoline and the principal ligand [30] to the metal centre. The bond distances are in the range of those reported in the Cambridge Structural Database [31] for amide and carbonyl compounds [22].

Table 6.14. Crystal data and structure refinement for [Cu(SB)(pi)]·H$_2$O (**39**)

Empirical formula	C$_{21}$ H$_{18}$ Br Cu N$_3$ O$_3$
Formula weight	503.83
Temperature	296(2) K
Wavelength	0.71073 Å
Crystal system, space group	Monoclinic, C2/c
Unit cell dimensions	a = 25.6019(13) Å α = 90°
	b = 13.1562(6) Å β = 121.279(3)°
	c = 14.3488(7) Å γ = 90°.
Volume	4130.5(4) Å^3
Z, Calculated density	8, 1.620 Mg/m^3
Absorption coefficient	3.019 mm^{-1}
F(000)	2024.0
Crystal size	0.25 x 0.25 x 0.20 mm
Theta range for data collection	1.81 to 25.99 °
Limiting indices	-31≤h≤31, -16≤k≤16, -17≤l≤17
Reflections collected / unique	31398 / 4055 [R(int) = 0.0575]
Completeness to theta	= 25.99 100.0 %
Absorption correction	Semi-empirical from equivalents
Max. and min. transmission	0.652 and 0.592
Refinement method	Full-matrix least-squares on F^2
Data / restraints / parameters	4058 / 0 / 264
Goodness-of-fit on F^2	1.084
Final R indices [I > 2sigma(I)]	R$_1$ = 0.0548, wR$_2$ = 0.1596
R indices (all data)	R$_1$ = 0.0782, wR$_2$ = 0.1868
Largest diff. peak and hole	2.699 and -1.005 e.A^{-3}

R$_1$ = $\Sigma||F_o| - |F_c|| / \Sigma|F_o|$; wR$_2$ = $\{\Sigma w(F_o^2-F_c^2)^2 / \Sigma w(F_o^2)^2\}^{1/2}$

We can assign a square planar structure to this four coordinate complex but slightly deviates from its regular geometry, as evidenced from the following observations. The entire molecule is nearly planar as seen from the mean plane deviation calculation of the plane containing all the non hydrogen atoms. It shows a maximum mean plane deviation of -0.294(8) Å for C6. The Cu(II) atom is shared by two fused five and six membered chelate rings Cg(1){Cu, N3, N2, C7, O2} and Cg(2) {Cu, N2, C14, C19, C21,O1} with a dihedral angle of only 1.9(2)° between them. The phenyl ring of hydrazide part is slightly shifted from the rest of the molecule as it makes dihedral angles of 12.5(3)°,10.5(3)° and 11.8(3)° with the aromatic ring of picoline, five and six membered chelate rings respectively. The four equatorial coordination positions of the square plane are occupied by N1, O2, N2 and O1 atoms around Cu(II) centre and the plane A4 containing these atoms shows a maximum mean plane deviation of 0.042(5) Å for N2 which assigns much planarity to the square plane. From ring puckering analysis [34] it is clear that rings present in the complex are not puckered.

Table 6.15. Selected bond angles and bond lengths of [Cu(SB)(pi)]·H_2O (39)

Bond length (Å)		Bond angle (°)	
Cu1–N1	1.989(4)	N1–Cu1–O1	91.55(16)
Cu1–O1	1.886(3)	O1–Cu1–N2	93.55(17)
Cu1–O2	1.925(4)	N2–Cu1–O2	81.18(17)
Cu1–N2	1.918(4)	O2–Cu1–N1	93.79(17)
C1–C7	1.496(8)	O2–Cu1–O1	174.52(16)
C7–N3	1.296(7)	N1–Cu1–N2	173.97(19)
N3–N2	1.390(6)	O1–C14–C19	125.81(5)
N2–C21	1.278(7)	C14–C19–C21	121.93(5)
C21–C19	1.415(8)	C19–C21–N2	126.2(5)
C14–O1	1.298(7)	N2–N3–C7	108.84(4)
C7–O2	1.302(7)	N3–C7–O2	124.8(5)
C17–Br1	1.898(5)		
C20-O3	1.405(9)		

6.3.2. Electron paramagnetic resonance spectroscopy

EPR spectroscopy is an effective tool that can be used for the study of structures of paramagnetic copper(II) complexes. The effective spin of copper(II) ion, with a d^9 configuration, $S = \frac{1}{2}$ and is associated with a spin angular momentum, $M_s = \pm\frac{1}{2}$, leading to a doubly degenerate spin state in the absence of a magnetic field. When a magnetic field is applied, the degeneracy is removed and the energy difference between them is given by $\Delta E - h\nu = g\beta B$

where h is Planck's constant, ν is the microwave frequency for transition between the two levels, g is the Lande splitting factor (equal to 2.0023 for a free electron), β is the Bohr magneton and B is the magnetic field. In the case of a $3d^9$ copper(II) ion, the appropriate spin Hamiltonian assuming a B_{1g} ground state is given by

$$\hat{H} = \beta[g\ H_a S + g_-(H_x S_x + H_y S_y)] + A_\parallel I_z S_z + A_\perp\ (I_x S_x + I_y S_y)$$

where all the symbols have their usual meaning. The nuclear spin of ^{63}Cu ($I = \frac{3}{2}$) interacts with the unpaired electron of copper(II) ion (d^9) with an effective spin of $S = \frac{1}{2}$ which give rise to four hyperfine lines ($2nI+1 - 4$).

EPR spectra of the copper(II) complexes were recorded in polycrystalline state at 298 K and in DMF as a frozen sample at liquid nitrogen temperature (77 K) in the X-band, using 100 kHz modulation, modulation amplitude 2G and 9.1 GHz microwave frequency; g factors were quoted relative to the standard marker TCNE ($g = 2.00277$), at SAIF, IIT, Bombay, India. The spectra typically indicate a $d_{x^2-y^2}$ ground state ($g_\parallel > g_\perp > 2.0023$). Some of the EPR spectra were simulated and the experimental (red) and simulated (blue) best fits are presented.

The EPR spectrum of the complex $[Cu_2(BB)_2]$ (27) in the polycrystalline state at 298 K exhibits weak signals due to strong antiferromagnetic interaction between the Cu(II) centers. The nature of the EPR spectra is consistent with strong coupling interactions between Cu(II) electrons through their connecting moiety which suggests a dimeric structure.

However in frozen DMF at 77 K the EPR spectra exhibit signals characteristic of uncoupled Cu(II) species at ~ 330 mT. They do not show half field signals and hyperfine features typical for coupled binuclear complexes are absent. The spectral features in frozen DMF are in contradiction with that in solid state, which is attributed to the possible fragmentation in DMF at low concentrations. The binuclear complex is connected with the antiferromagnetic coupling of two Cu(II) ions, leading to a singlet ground state and an excited spin triplet state. For a coupled system of two Cu(II) species equally distributed seven hyperfine features [$2nI+1$; $n=2$ and $I=3/2$] are expected.

The spectrum shows a well-resolved axial spectrum with four hyperfine lines with weak superhyperfine splittings in the parallel region due to coupling of the electron spin with nuclear spin (^{63}Cu, $I = 3/2$) with $g_{\parallel} > g_{\perp} > 2.0023$ relationship consistent with a $d_{x^2-y^2}$ ground state in a square planar geometry [38]. Kivelson and Nieman have reported that $g_{\parallel}$ values less than 2.3 indicate considerable covalent character to M–L bonds, while a value greater than 2.3 indicate ionic character. In the present system $g_{\parallel} < 2.3$ showing significant covalent character to M–L bond. The perpendicular region exhibits superhyperfine splittings in addition to hyperfine signals with an average spacing 66×10^{-4} which arise from the coupling of the electron spin with nuclear spin of the coordinating nitrogen atom which is an indication of the participation of azomethine nitrogen in bonding.

site away from planarity [42]. The value of $A_{\parallel}$ less than 0.0140 cm^{-1} rules out the possibility of square planar nature for such copper(II) centers as such values are not reported for any complexes even with four sulfur ligands. The square planar complexes undergo tetragonal distortion and that depends on the nature of the coordinated atoms [43]. The value may vary from 105 to 135 for small to extreme distortion in square planar complexes. The estimated value of f for the complex $[Cu_2(BB)_2]$ is 100 indicating negligible distortion from planarity [44].

The spectral parameter α^2 is a covalency factor which describes the in-plane sigma bonding arises from the dipole–dipole interaction between magnetic moments associated with the spin motion of the electron and the nucleus and its value decreases with increasing covalency [45]. The expected value of α^2 is equal to 1 for 100% ionic character of the bonds and less than 1 for covalent character and becomes smaller with increasing covalent bonding. The value of in plane sigma bonding parameter α^2 is estimated using the expression given below.

$$\alpha^2 = -\frac{A_{\parallel}}{0.036} + (g_{\parallel} - 2.0023) + \frac{3(g_{\perp} - 2.0023)}{7} + 0.04$$

The EPR parameters $g_{\parallel}$, $g_{\perp}$, $A_{\parallel}$ and the energies of d-d transitions are used to evaluate the bonding parameters α^2, β^2 and γ^2 which may be regarded as measures of covalency in the in-plane σ-bonds, in-plane π-bonds and out-of-plane π-bonds respectively. The orbital reduction factors $K_{\parallel}$ and $K_{\perp}$ calculated using the following expressions [46].

$$K_{\parallel}^2 = (g_{\parallel} - 2.0023)\frac{\Delta E(d_{xy} \to d_{x^2-y^2})}{8\lambda_0}$$

$$K_\perp^2 = (g_\perp - 2.0023) \frac{\Delta E(d_{xz,} d_{yz} \to d_{x^2-y^2})}{2\lambda_0}$$

$$K_\parallel = \alpha^2 \beta^2$$

$$K_\perp = \alpha^2 \gamma^2$$

where λ_0 is the spin-orbit coupling constant and has a value –828 cm^{-1} for Cu(II) d^9 system.

Hathaway suggested that [47], for pure σ-bonding $K_\parallel \approx K_\perp \approx 0.77$ and for in-plane π-bonding $K_\parallel < K_\perp$, while for out-of-plane π-bonding $K_\perp < K_\parallel$. Herein the compound [Cu$_2$(BB)$_2$] (27), $K_\perp < K_\parallel$ indicates the presence of out-of-plane π-bonding. The value of bonding parameters α^2, β^2 and $\gamma^2 <1$ confirms the covalent nature of the complex. EPR spectral data and the bonding parameters are summarized in Table 5.5.

The EPR spectra of the complexes [Cu$_2$(BN)$_2$] (31) and [Cu$_2$(BF)$_2$] (33) in the polycrystalline state at 298 K suggest a dimeric structure as they are EPR silent and exhibit no characteristic signal due to strong antiferromagnetic interaction between the Cu(II) centers.

However in frozen DMF at 77 K the EPR spectrum of [Cu$_2$(BN)$_2$] (31) is axial even though the hyperfine splittings are not very clear. The spectra typically indicate a $d_{x^2-y^2}$ ground state in a square planar geometry ($g_\parallel > g_\perp > 2.0023$). The f value calculated for the complex [Cu$_2$(BN)$_2$] (31) is 101 indicating negligible distortion from planarity. They do not show half field signals and hyperfine features typical for coupled binuclear complexes are absent which may be due to the possible fragmentation in DMF at low concentrations or due to slight loss of magnetic coupling

The EPR spectrum of [Cu(BB)(phen)] (**28**) in DMF at 77 K, (Fig. 6.27) is axial with four well-resolved hyperfine lines [^{63,65}Cu, $I = 3/2$] corresponding to -3/2, -1/2, 1/2 and 3/2 transitions in the parallel region with the hyperfine splitting constant $A_. = 180 \times 10^{-4}$ cm^{-1}. The spectrum shows five nitrogen superhyperfine lines in the perpendicular region which arise from the coupling of the electron spin with the nuclear spin of the coordinating nitrogen atoms (equatorial) with the superhyperfine splitting constant $A_{\perp} = 17 \times 10^{-4}$ cm^{-1}. The spectra typically indicate a $d_{x^2-y^2}$ ground state ($g_. > g_- > 2.0023$). The $g_. > g_-$ values suggest a distorted square pyramidal structure and rules out the possibility of a trigonal bipyramidal structure for which $g_. > g_.$ is expected. Half field signals are absent in the spectra which shows that there is no significant amount of copper- copper interaction and suggests monomeric structure. $G > 4.4$ also support the absence of extensive metal - metal interaction. Thus the coordination polyhedron comprises of one phenanthroline nitrogen, an azomethine nitrogen, an enolate oxygen and a phenolate oxygen of the hydrazone which form the base of the pyramid and the remaining phenanthroline nitrogen occupies the axial position, as the results obtained from the single crystal XRD results.

The EPR spectrum of the complex [Cu(BB)(Bipy)]·C$_2$H$_5$OH (**29**) in the polycrystalline state at 298 K is isotropic in nature, consisting of a broad signal, at $g_{iso} -2.0913$. The peak to peak line width ΔB_{pp} is 6 mT. Such isotropic broad spectra consisting of only one signal arise from extensive exchange coupling through misalignment of the local molecular axes between different molecules (dipolar broadening) and enhanced spin lattice relaxation. These types of spectra unfortunately give no information on the electronic ground state of the metal ion present in the complexes.

of copper - copper interaction and suggests monomeric structure. The geometric parameter, $G = 4.4$ also support the absence of extensive metal - metal interaction. Thus the complex has a distorted square pyramidal structure similar to compound **28** with its axial position occupied by bipyridyl nitrogen, and is confirmed by the results obtained from the single crystal XRD data.

The EPR spectrum of the complex [Cu(BB)(pi)] (**30**) in the polycrystalline state at 298 K is axial with weak hyperfine lines though the splittings are not clear. The spectra typically indicate a $d_{x^2-y^2}$ ground state $(g_{\parallel} > g_{\perp} > 2.0023)$. Additional transitions occurs associated with $\Delta M_s = \pm 2$ values in the X-band spectra which generate an absorption at the half field value of *ca.* 150 mT. The presence half field signal with g value 4.030 is a useful criterion for dipolar interaction arises from the coupling of the two Cu(II) centers which suggest a dimeric structure. Here G value = 3.25, which also indicates Cu-Cu interaction. But from X-ray structural analysis it is found that the compound has a monomeric structure. It has been known that if the separation between the two metal centers is less than 3.5 Å an interaction is expected. From the single crystal XRD results of crystal packing the distance between two copper ions is less than 5 Å. Here the seven line hyperfine splitting is not observed. In addition the dihedral angle between the two copper atoms and the connecting ligand atoms also play an important role in deciding the extent of interaction. The observation $g_{\parallel} > g_{\perp}$ values accounts to the distorted square planar structure and rules out the possibility of a trigonal pyramidal structure. The estimated value of f is less than 100 which also shows planarity of the molecule. These observations are confirmed by single crystal XRD studies .

Table 6.17. EPR spectral assignments and bonding parameters of copper(II) complexes in polycrystalline state at 298 K, in DMF solution at 298 K and in DMF solution at 77 K.

a	27	28	29	30	31	32	33	39
Polycrystalline (298 K)								
$g_\parallel$		2.166		2.209		2.160		2..221
$g_\perp$		2.057		2.066		2.060		2.071
g_{sol}/g_{av}		2.093		2.113		2.093		2.121
G		2.993		3.245		2.733		3.183
DMF (77 K)								
$g_\parallel$	2.187	2.235	2.240	2.181	2.158	2.240	2.179	2.201
$g_\perp$	2.027	2.055	2.057	2.037	2.046	2.055	2.022	2.043
g_{av}	2.080	2.115	2.118	2.085	2.083	2.116	2.074	2.068
$A_\parallel$ [a]	218.3	180.0	180.0	233.3	210.0	178.0	214.2	215.0
f	100.1	124.1	124.4	93.48	102.7	125.0	101.7	102.3
α^2	0.8538	0.8164	0.8234	0.8928	0.8015	0.8167	0.8298	0.8692
β^2		0.8889	---	0.7289	0.7616	0.922		0.7761
γ^2		0.846		0.6425	0.8069	0.8683		0.7025
$K_\parallel$		0.7257		0.6508	0.6104	0.753		0.6746
$K_\perp$	...	0.6907		0.5736	0.6427	0.7091	...	0.6106

[a] Expressed in units of cm^{-1} multiplied by a factor of 10^{-4}.

6.3.3. Infrared spectra

Vibrational spectra of newly synthesized complexes have been recorded in the region 4000-400 cm^{-1} and a comparison of selected vibrational bands with that of their respective free hydrazones gives an idea about the coordination pattern of the ligands in the complexes. The selected IR bands of the hydrazones and complexes and their tentative assignments are presented in Table 6.18 and selected spectra in Figs. 6.38-6.42.

A careful analysis of the IR spectra of the hydrazone compounds H_2BB, H_2BN, H_2BF, H_2SB and the metal complexes showed that upon complexation significant variations have occurred in the characteristic frequencies.

Table 6.18 IR data of the hydrazones and their copper(II) complexes with tentative assignments.

Compound	ν(C=O)	ν(C=N)	ν(C=N)ᵃ	ν(Cu-N)	ν(N-N)	Heterocyclic breathing	ν(C-O)
H₂BB	1680	1626	----	----	1128	----	1365
[Cu₂(BB)₂] (27)		1601	1526	419	1130	----	1360
[Cu(BB)phen] (28)		1602	1507	410	1135	1420, 725	1362
[Cu(BB)bipy]·C₂H₅OH (29)		1604	1503	409	1155	1435, 735	1364
[Cu(BB)pi] (30)		1609	1518	407	1145	1450, 758	1357
H₂BN	1687	1628			1125		1342
[Cu₂(BN)₂] (31)		1607	1518	414	1162		1335
[Cu(BN)phen]·H₂O(32)	----	1609	1516	412	1145	1425, 720	1340
H₂BF	1690	1625			1122		1345
[Cu₂(BF)₂] (33)		1606	1538	407	1138		1342
HFN	1678	1622	----		1126		1334
[Cu(FN)₂] (34)		1617	1533	420	1143		1330
[Cu(FN)Cl(H₂O)]·2H₂O(35)		1609	1526	418	1135		1328
[Cu₂(FN)₂(μ-NCS)₂] (36)		1618	1535	422	1124		1326
[Cu₂(FN)₂ (μ-N₃)₂] (37)	----	1609	1522	413	1130		1320
H₂SB	1650	1627			1118		1348
[Cu₂(SB)₂] (38)		1606	1530	408	1123	----	1332
[Cu(SB)(pi)]·H₂O (39)	----	1608	1528	422	1132	1452, 736	1341

The medium bands due to ν(O–H) observed at 3370, 3365, 3375, 3574 and ν(N–H) at 3050, 3049, 3054, 3059 cm⁻¹ and a sharp band due to ν(C=O) seen around 1680 cm⁻¹, 1687 cm⁻¹, 1690 cm⁻¹, 1650 cm⁻¹ respectively in the infrared spectra of the free hydrazones are absent or much shifted in all these copper complexes. This is a clear evidence for the coordination through deprotonated phenolate and enolate oxygens of the ligand and supports the fact that iminol form predominates amido form during tautomerization of the ligand and coordinates to the metal centre.

6.3.4 Electronic spectra

Electronic spectra of Cu(II) complexes comprise bands due to intraligand, charge transfer and d-d transitions. The significant electronic absorption spectral data of the complexes in DMF or acetonitrile with their possible assignments are summarized in Table 6.19 and the spectra in (Figs. 6.43-6.46).

Table.6.19. Electronic spectral assignments (cm^{-1}) of Cu(II) complexes

Compound	Intraligand transitions	LMCT	d-d
[Cu₂(BB)₂] (27)	29899, 36149	25662	....
[Cu(BB)phen] (28)	30639, 31847, 37087	24515	14990
[Cu(BB)bipy]·C₂H₅OH (29)	30525, 31311, 37032	24573	....
[Cu(BB)pi] (30)	30234, 31577, 36213	24878	15700
[Cu₂(BN)₂](31)	30162, 35213	25210	15850
[Cu(BN)phen]·H₂O(32)	30112, 31582, 36773	25436	15800
[Cu₂(BF)₂] (33)	30217, 31659, 36687	25476	....
[Cu(FN)₂] (34)	29901, 39525	26525	14430
[Cu(FN)Cl(H₂O)]·2H₂O (35)	31055, 38314	24691	14531
[Cu₂(FN)₂(µ-NCS)₂] (36)	31354, 39031	25545	
[Cu₂(FN)₂ (µ-N₃)₂] (37)	32467, 38022	25763	
[Cu₂(SB)₂] (38)			
[Cu(SB)(pi)]·H₂O (39)	30534, 32045, 39363	26023	15172

It is rather difficult to interpret electronic spectra of Cu(II) complexes as they possess flexible stereochemistry. The outer electronic configuration for copper(II) ion is $3d^9$ with ^2D as ground state term which will be split by an octahedral field in to two levels $^2T_{2g}$ and ^2E_g. So the expected excitation in an octahedral d^9 system is from ^2E_g to $^2T_{2g}$ results in a single absorption band. However the geometry around copper(II) ion lacks cubic symmetry and the tetragonal distortion yields other distorted forms of basic stereochemistries. Jahn-Teller distortions cause further splitting of the $^2T_{2g}$ and ^2E_g. So the possible

Table 6.20. Electrochemical data of Cu(II) complexes in DMF

Compound	$E_{pc}/V(I_{pc}/A \times 10^6)$	$E_{pa}/V(I_{pa}/A \times 10^6)$
[Cu₂(BB)₂] (27)	-0.13 (2.52), 0.24 (2.02)	0.89 (-4.17), -5.55 (-1.61)
[Cu(BB)phen] (28)	0.44 (2.39), -0.23 (3.86)	1.04 (-7.18), 0.31 (-3.26)
[Cu₂(BN)₂](31)	-0.27 (26.01), -0.93 (23.52)	-0.04 (-6.86), -0.67 (-2.45)
[Cu₂(BF)₂] (33)	0.158 (2.51), -0.23 (2.90)	0.70 (-4.37), -0.19 (-1.94)
[Cu(FN)Cl(H₂O)]·2H₂O (35)	-0.13 (8.78), -0.43 (8.67)	-0.56 (-0.79), 0.45 (-4.65)
[Cu₂(FN)₂ (μ-N₃)₂] (37)	0.20 (5.71), -1.17 (1.54)	0.63 (-6.37), -0.27 (-3.36)

A comparative study of the cyclic voltammetric behavior of the hydrazones with their metal complexes gives the information that redox reactions of the metal complexes are metal centered and the potentials of the metal centered oxidation and reduction reflect the influence of the electronic nature of the ligand. The cyclic voltammograms of six Cu(II) complexes were studied and all of them consist of two reduction peaks and two oxidation peaks corresponding to redox processes involved in the formation of Cu(II)/Cu(I) and Cu(I)/Cu couple [1,58]. The electrochemical data of the hydrazone complexes of Cu(II) are given in Table 6.20 and the cyclic voltammograms for the behaviors of the complexes 27, 28, 31, 33, 35 and 37 are shown in Figs. 6.49-6.51. The cyclic voltammograms for the complexes show reversible reduction waves in the range -1.17 to 0.44 V and reversible oxidation peaks in the range -0.67 to 1.04 V and additional peaks observed are assigned to the ligand or coligand based redox processes. For some complexes certain peaks are not well resolved or even absent which may result from kinetic complications during electron transfer, uncompensated solution resistance, etc.

References

[1]   P. Bindu, M.R.P. Kurup, T.R. Satyakeerty, Polyhedron 18 (1999) 321.

[2]   D.X. West, A.E. Liberta, K.G. Rajendran, I.H. Hall, Anticancer Drugs 4 (1993) 241.

[3]   F.G. Mutti, R. Pievo, M. Sgobba, M. Gullotti, L. Santagostini, Bioinorg. Chem. Appl. 2008 (2008), Article ID 762029, 9 pages.

[4]   D.K. Seth, S. Bhattacharya, Polyhedron 30 (2011) 2438.

[5]   Y. Song, S. Ohkoshi, Y. Arimoto, H. Seino, Y. Mizobe, K. Hashimoto, Inorg. Chem. 42 (2003) 1848.

[6]   M.F. Iskander, T.E. Khalil, R. Werner, W. Haase, I. Svoboda, H. Fuess, Polyhedron 19 (2000) 1181.

[7]   Raman, H.K. Singh, H.K. Salman, S.S.Parmar, J. Pharm. Sci. 82 (1993) 167.

[8]   E. Coropceanu, L. Croitor, M. Gdaniec, B. Wicher, M. Fonari, Inorg. Chim. Acta 362 (2009) 2151.

[9]   E.B. Coropceanu, L.M. Croitor, Yu.M. Chumakov, M.S. Fonari, Crystallogr. Rep.54 (2009) 883.

[10]   O. Kahn, Acc. Chem. Res. 33 (2000) 647.

[11]   E. Coropceanu, L. Croitor, M. Botoshansky, A. Siminel, M. Fonari, Polyhedron 30 (2011) 2592–2598.

[12]   B.N. Bessy Raj, M.R.P. Kurup, E. Suresh, Spectrochim Acta A, 71 (2008) 1253.

[13]   B. Coe, in: J. McCleverty, T. Meyer (Eds.), Comprehensive Coordination Chemistry II, Elsevier-Pergamon, Oxford, 9 (2004) 621.

[14]   E.L. Ulrich, J.L. Markey, Coord. Chem. Rev. 27 (1978) 109.

[15]   K. Pierloot, J.O.A. De Kerpel, U. Ryde, M.H.M. Olsson, B.O. Roos, J. Am. Chem. Soc. 120 (1998) 13156.

[16] I. Solomon, L.B. La Croix, D.W. Randall, Pure Appl. Chem. 70 (1998) 799.

[17] K.J. Burows, A. Cornish, D Scott, I.J. Higgins, J. Gen. Microbiol. 130 (1984) 3327.

[18] R. M. Berka, F. Xu, S. A. Thompson. International Patent Application PCT/US95/06816, 1995.

[19] A. Messerschmidt, H. Luecke, R. Huber, J. Mol. Biol. (1993) 997.

[20] G. Tamasi, L. Chiasserini, L. Savini, A. Sega, R. Cini, J. Inorg. Biochem. (2005) 1347

[21] E. Manoj, M.R.P. Kurup, A Punnoose, Spectrochim. Acta Part A 72 (2009) 474.

[22] N. Mathew, M. Sithambaresan, M.R.P. Kurup, Spectrochim. Acta Part A 79 (2011) 1154.

[23] P.B. Sreeja, M.R.P. Kurup, A. Kishore, C. Jasmin, Polyhedron 23 (2004) 575.

[24] B. Rather, M.J. Zaworotko, Chem. Commun. (2003) 830.

[25] P. Mukherjee, M.G.B. Drew, C.J.G. Garcia, A. Ghos, Inorg. Chem. 48 (2009) 5848

[26] G.M. Sheldrick, SHELXS-97, Programs for X-ray Crystal Structure Solution, University of Göttingen, Göttingen, 1997.

[27] N. Filipovic, H. Borrmann, T. Todorovic, M. Borna, V. Spasojevic, D. Sladic, I. Novakovic, K. Andjelkovic, Inorg. Chim. Acta 362 (2009) 2000.

[28] N.A. Mangalam, S. Sivakumar, M.R.P. Kurup, E. Suresh, Spectrochim. Acta Part A 75 (2010) 686.

[29] N.A. Mangalam, M.R.P. Kurup, Spectrochim. Acta Part A 78 (2011) 926.

[30] C. Place, J.-C. Zimmermann, E. Mulliez, G. Guillot, C. Bois, J.-C. Chottard, Inorg. Chem. 37 (1998) 4030.

[31] Cambridge Structural Database (CSD) version 5.30 update 4 (Sept. 2009).

[32] F.H. Urena, A.L.P. Chamorro, M.N.M. Carretero, J.M. Amigo, V. Esteve, T. Debaerdemaeker, Polyhedron 18 (1999) 2205.

[33] A.W. Addison, T.N. Rao, R. Reedijk, J.V. Rigin, G.C. Verschoor, J. Chem. Soc., Dalton Trans. (1984) 1349.

[34] D. Cremer, J.A. Pople, J. Am. Chem. Soc. 97 (1975) 1354.

[35] G.G. Evans, J.A. Boeyens, Acta Cryst. B45 (1989) 581.

[36] M.F. Iskander, T.E. Khalil, R.Werner,W. Haase, I. Svoboda, H. Fuess, Polyhedron 19 (2000) 1181.

[37] S. Das, G.P. Muthukumaragopal, S. Pal, S. Pal, New J. Chem. 27 (2003) 1102.

[38] M.J. Bew, B.J. Hathaway, R.R. Faraday, J. Chem. Soc., Dalton Trans. (1972) 1229.

[39] B. Viossat, F.T. Greenaway, G. Morgant, J.C. Daran, N.-H. Dung, J.R.J. Sorenson, J. Inorg. Biochem. 99 (2005) 355.

[40] B.J. Hathaway, D.E. Billing, Coord. Chem. Rev. 5 (1970) 143.

[41] A. Sreekanth, M.R.P. Kurup Polyhedron 22 (2003) 3321.

[42] P. Peisach, W.E. Blumberg, Arch. Biochem. Biophys. 165 (1974) 691.

[43] R. Pogni, M.C. Bartto, A. Diaz, R. Basosi, J. Inorg. Biochem. 79 (2000) 333.

[44] S.I. Findone, K.W.H. Stevens, Proc. Phys. Soc. 73 (1959) 116.

[45] A. Rockenbauer, J. Magn. Reson. 35 (1979) 429.

[46] B.N. Figgis, Introduction to Ligand Fields, Interscience, New York (1996) 295.

[47] B.J. Hathaway, J. Chem. Soc., Dalton Trans. (1972) 1196.

[48] St. Stoll, Spectral Simulations in Solid-state EPR, PhD thesis, ETH, Zurich, 2003.

[49] R.S. Baligar, V.K. Revankar, J. Serb. Chem. Soc. 71 (2006) 1301.

[50] N.A. Mangalam, M.R.P. Kurup, Spectrochim. Acta Part A 71 (2009) 2040.

[51] J. Chakraborty, S. Thakurta, G. Pilet, D. Luneau, S. Mitra, Polyhedron 28 (2009) 819.

[52] R.C. Maurya, S. Rajput, J. Mol. Struct. 833 (2007) 133.

[53] M.X. Li, H. Wang, S.W. Liang, M. Shao, X. He, Z.X. Wang, S.R. Zhu, Crystal Growth and Design 9 (2009) 11.

[54] K. Nakamoto, Infrared and Raman spectra of Inorganic and Coordination compounds, 5th ed., Wiley, New York, 1997.

[55] S. Patai, The Chemistry of Carbon-Nitrogen Double Bond, Interscience publishers, John Wiley and Sons, London (1970).

[56] H.Y. Bai, J. F. Ma, Y. Y. Liu, J. Yang, Inorg. Chim. Acta 376 (2011) 332.

[57] A.M. Bond, R.L. Martin, Coord. Chem. Rev. 54(1984) 23.

[58] R. Bakshi, M. Rossi, F. Caruso, P. Mathur, Inorg. Chim. Acta 376 (2011) 175.

SYNTHESES AND SPECTRAL CHARACTERIZATION OF Zn/Cd(II) COMPLEXES OF SOME AROYLHYDRAZONES

7.1 Introduction

Zinc plays either a structural or analytical role in several proteins. Zinc(II) ion provides a number of coordination compounds because of its affinity towards different types of ligands and flexible coordination number ranging from two to eight. It has been accepted as an important cofactor in biological molecules either as a structural template in protein folding or as a Lewis acid catalyst that can readily adopt 4-, 5-, or 6- coordination [1]. Zinc is able to play a catalytic role in the activation of thiols as nucleophiles at physiological pH. Mononuclear zinc complexes may serve as model compounds for zinc enzymes such as phospholipase C, bovine lens leucine aminopeptidase, ATPases, carbonic anhydrases and peptide deformylase. Binuclear cores are versatile active sites of many metalloenzymes and play essential role in biological systems. Dowling and Perkin investigated Zn(II) complexes with N, O and S coordination to understand the reactivity of the pseudotetrahedral zinc center in proteins [2]. Parrilha *et al.* reported an evaluation of the analgesic and anti-nociceptive activities of salicylaldehyde 2-chlorobenzoylhydrazone, its regioisomer salicylaldehyde 4-chlorobenzoylhydrazone, salicylaldehyde

semicarbazone and their zinc(II) complexes [3]. Zn(II) complexes of furan-2-aldehyde thiosemicarbazone (HL) have been synthesized and characterized [4]. Epstein *et al.* reported chloroform-soluble Schiff-base Zn(II) or Cd(II) complexes from a dynamic combinatorial library [5].

Cadmium is an extremely toxic element that is naturally present in the environment and it is also formed as a result of human activities. This metal competes with Zn and blocks active sites of metal-enzymes and as a relatively soft acid it can dislodge Zn(II) in cysteine-coordinated zinc compounds or Ca(II) ions in bone cells [6]. The development of chelating agents is essential for the treatment of cadmium intoxication. *In vivo* cadmium mobilization and an assessment of cadmium chelating drugs have drawn the interest of many biochemists [7]. Cadmium is well known to form complexes with acetates and carboxy-ligands to yield both charged and neutral compounds [8]. The possibility of forming structures with higher coordination numbers has resulted in the observation of unusual coordination geometries about the metal atom and formation of polymeric species [9].

Sen *et al.* have reported the synthesis, spectral characterization and crystal structures of two new octahedral cadmium complexes which are synthesized using a tridentate hydrazone ligand and they are characterized by elemental analysis, IR spectra, NMR spectra, thermal studies and finally the structures have been determined by single crystal X-ray diffraction [10]. Reena *et al.* reported synthesis, spectral and structural studies of cadmium(II) complexes derived from di-2-pyridyl ketone and N4-phenylsemicarbazide. Some of them have dimeric structure and the coordination geometry around cadmium(II) is distorted octahedral, as obtained by X-ray diffraction studies [11].

There are several reports of the transition metal complexes including some cadmium complexes containing different types of hydrazone ligands in the literature [12,13]. Though cadmium has been known as a toxic metal and is often associated with mercury and lead as one of the biologically harmful metal ions, the cadmium(II) ion has recently been found to serve as the catalytic center in a newly discovered carbonic anhydrase [10,14].

The filled d shell does not offer crystal field stabilization for Zn^{2+} and Cd^{2+} ions and therefore coordination number and stereochemistry are determined by the size of the Zn(II) and Cd(II) cation and the steric requirements of the ligands. In zinc and cadmium complexes, commonly found geometries are tetrahedral and octahedral. Six coordinate complexes may be octahedral or trigonal prismatic.

Complexes of group 12 metals, mainly zinc and cadmium can provide an interesting range of stoichiometries depending on the preparative salt. Here we report the synthesis and characterization of three each of Zn(II) and Cd(II) complexes of aroylhydrazones.

7.2 Experimental

7.2.1 Materials

All chemicals and reagents are of reagent grade quality. 2-Hydroxy-4-methoxybenzophenone (Aldrich), furan-2-carboxaldehyde (Aldrich), nicotinic hydrazide (Aldrich), benzhydrazide (Aldrich), zinc(II) acetate dihydrate (S.D. Fine) and cadmium(II) acetate dihydrate (E-Merck) were used without further purification. Methanol, ethanol and DMF were used as solvents.

7.2.2 Syntheses of aroylhydrazones

The syntheses of aroylhydrazones were done as described in Chapter 2.

7.2.3 Syntheses of Zn(II)/Cd(II) complexes

[Zn(BB)]$_2$ (**40**): To a solution of H$_2$BB (0.346 g, 1 mmol) in methanol, Zn(CH$_3$COO)$_2$·2H$_2$O (0.219 g, 1 mmol) in methanol was added. Yellow amorphous product formed immediately which was filtered, washed with methanol, followed by ether and dried over P$_4$O$_{10}$ *in vacuo*. Elemental Anal. Found (Calcd.) (%): C, 49.05 (48.93), H, 3.01 (3.52), N, 12.50 (12.23).

[Zn(BN)]$_2$ (**41**): Zn(CH$_3$COO)$_2$·2H$_2$O (0.219 g, 1 mmol) in methanol was added to the H$_2$BN solution in methanol (0.347 g, 1 mmol) and stirred for about one hour. The yellow product formed was filtered, washed with methanol, followed by ether and dried over P$_4$O$_{10}$ *in vacuo*. Elemental Anal. Found (Calcd.) (%): C, 50.90 (50.37), H, 3.58 (3.94), N, 11.75 (11.75).

[Zn(FN)$_2$(H$_2$O)$_2$] (**42**): To a hot ethanolic solution of HFN (0.215 g, 1 mmol), Zn(CH$_3$COO)$_2$·2H$_2$O (0.219 g, 1 mmol) in ethanol was added and refluxed for 4-5 h. The clear solution was kept at room temperature overnight. Pale yellow crystalline product was filtered off and washed with ethanol, followed by ether and dried over P$_4$O$_{10}$ *in vacuo*. Elemental Anal. Found (Calcd.) (%): C, 52.04 (51.86), H, 3.83 (4.10), N, 7.18 (7.11).

[Cd(BB)]$_2$ (**43**): The complex **43** was obtained by refluxing methanolic solutions of H$_2$BB (0.346 g, 1 mmol) and Cd(CH$_3$COO)$_2$·2H$_2$O (0.266 g, 1 mmol) containing 2-3 mL of DMF for about 4 hours. The pale yellow colored crystalline product separated was filtered, washed with methanol, followed by ether and dried over P$_4$O$_{10}$ *in vacuo*. Elemental Anal. Found (Calcd.) (%): C, 54.89 (55.27), H, 3.59 (4.06), N, 7.99 (8.06).

[Cd(BN)]₂ (**44**): Methanolic solutions of H_2BN (0.347 g, 1 mmol) and $Cd(CH_3COO)_2 \cdot 2H_2O$ (0.266 g, 1 mmol) containing 2-3 mL of DMF was refluxed for about half an hour. The bright yellow colored amorphous product separated was filtered, washed with methanol, followed by ether and dried over P_4O_{10} *in vacuo*. Elemental Anal. Found (Calcd.) (%): C, 54.89 (55.27), H, 3.59 (4.06), N, 7.99 (8.06).

[Cd(FN)₂] (**45**): The aroylhydrazone, HFN (0.215 g, 1 mmol) was dissolved in ethanol and DMF (10:1, v/v) and ethanolic solution of $Cd(CH_3COO)_2 \cdot 2H_2O$ (0.266 g, 1 mmol) was added to it and refluxed for 3-4 hours. Pale yellow product separated was filtered, washed with ethanol, followed by ether and dried over P_4O_{10} *in vacuo*. Elemental Anal. Found (Calcd.) (%): C, 54.89 (55.27), H, 3.59 (4.06), N, 7.99 (8.06).

7.3 Results and discussion

Three each of Zn(II) and Cd(II) complexes were synthesized using different aroylhydrazones. They are quiet stable, yellow in color and soluble in organic solvents like methanol, acetonitrile, DMF and DMSO. Based on the elemental analyses, conductivity, magnetic susceptibility measurements and spectral investigations, the complexes were formulated. Experimental and calculated C, H, N values of the complexes are in close agreement in the case of all the six complexes. The analytical data match with the stoichiometry containing two molecules of coordinated water in compound $[Zn(FN)_2(H_2O)_2]$ (**42**), which is further supported by thermal analysis. The molar conductivities of the complexes in DMF (10^{-3} M) solution were measured at 298 K with a Systronic model 303 direct-reading conductivity bridge. The molar conductivity values lie in the range 4-12 ohm^{-1} cm^2 mol^{-1} for complexes **40-45** which is much less than the value of 65-90 ohm^{-1} cm^2 mol^{-1} obtained for a 1:1 electrolyte in the

same solvent [15] and so they are non-conducting in nature [16]. The conductivity values are tabulated in Table 7.1.

Magnetic susceptibility studies indicate diamagnetic nature for all the complexes which can be attributed to d^{10} outer electronic configuration of Zn(II)/Cd(II).

Table 7.1 Molar conductivity measurements

Compound	λ_m #
[Zn(BB)]₂ (40)	11
[Zn(BN)]₂ (41)	10
[Zn(FN)₂(H₂O)₂] (42)	12
[Cd(BB)]₂ (43)	9
[Cd(BN)]₂ (44)	11
[Cd(FN)₂] (45)	10

molar conductivity (in ohm⁻¹ cm² mol⁻¹) taken in 10⁻³ M DMF.

7.3.1 Infrared spectra

Vibrational spectra of newly synthesized complexes have been recorded in the region 4000-400 cm⁻¹ and significant IR spectral bands of the complexes are listed in Table 7.2. The significant bands in the IR spectra of the complexes can be compared with those of the free ligands. They display certain changes, from which we can derive some information about the nature of coordination and their structure. Free hydrazones H₂BB, H₂BN and HFN showed strong absorptions in the 1678-1690 cm⁻¹ region which are assigned to carbonyl group. The bands due to azomethine group are resolved around 1625 cm⁻¹ and medium bands due to ν(N–H) are seen in the range 3050-3440 cm⁻¹. These bands are found to be absent or much shifted in the corresponding Zn(II)/Cd(II)

complexes. Prominent bands occur at *ca.* 3370 and 3365 cm^{-1} in the IR spectra of the hydrazones H$_2$BB and H$_2$BN respectively due to ν(O–H), which are absent in their complexes.

Table 7.2 Selected IR bands (cm^{-1}) with tentative assignments of Zn(II) complexes

Compound	ν(C=N)	ν(C=N)^a	ν(C–O)	ν(Zn–O)	ν(Zn–N)
[Zn(BB)]$_2$ (**40**)	1602	1534	1239	519	467
[Zn(BN)]$_2$ (**41**)	1602	1518	1239	512	451
[Zn(FN)$_2$(H$_2$O)$_2$] (**42**)	1602	1518	1239	535	451
[Cd(BB)]$_2$ (**43**)	1602	1518	1239	512	467
[Cd(BN)]$_2$ (**44**)	1602	1518	1246	512	467
[Cd(FN)$_2$] (**45**)	1602	1518	1259	505	444

^{a} newly formed

These are clear evidences for the coordination through deprotonated phenolate and enolate oxygens of the ligand. This supports the fact that iminol form predominates amido form during tautomerization of the ligand and coordinates to the metal centre. Coordination of hydrazones to the zinc and cadmium ion through the azomethine nitrogen atom is expected to reduce the electron density in the azomethine link and thus lower the ν(C=N) absorption frequency by 15-25 cm^{-1}. Here this band undergoes a shift to a lower wavenumber *ca* 1602 cm^{-1} [17,18]. In the compound [Zn(FN)$_2$(H$_2$O)$_2$] (**42**) a broad band is seen at about 3439 cm^{-1} due to coordinated water and is supported by the data obtained from TG analyses. The above observations explain the tridentate ligating nature of the hydrazone systems H$_2$BB and H$_2$BN with ONO donor sites in complexes **40, 41, 43** and **44** and the bidenticity of the ligand HFN with NO donor sites in complexes **42** and **45**.

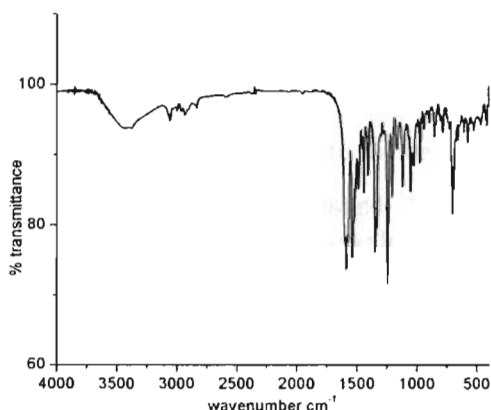**Fig.7.1.** IR spectrum of [Zn(BB)]₂ (**40**).

In all complexes the newly formed –C=N–N=C– moiety gave bands at 1518 and 1534 cm^{-1} suggesting the change of bond order and strong electron delocalization upon chelation [19,20]. A characteristic band of the free hydrazone due to v(N–N) at 1190 cm^{-1} undergoes a shift to lower wavenumbers in the range 1160-1170 cm^{-1} in complexes which indicates coordination through azomethine nitrogen.
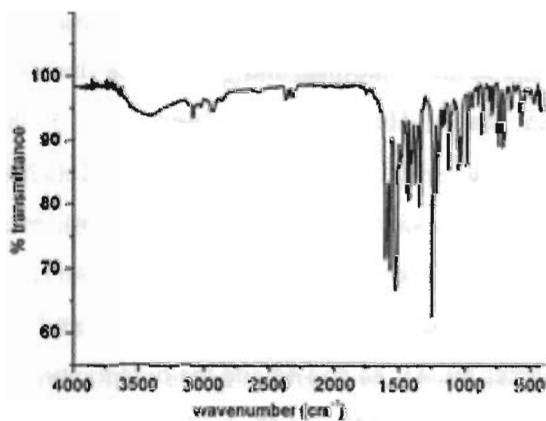

Fig. 7.2. IR spectrum of [Zn(BN)]₂ (**41**).

For all the complexes, phenolic C–O stretching occurs at lower wavenumber when compared to that of the ligands thereby indicating the deprotonation and coordination of phenolic OH. Appearance of new bands in the regions of 505-535 and 444-467 cm^{-1} are assignable to v(Zn/Cd–O) and v(Zn/Cd–N) respectively. The IR spectra of the complexes are shown in the Figs. 7.1-7.6.
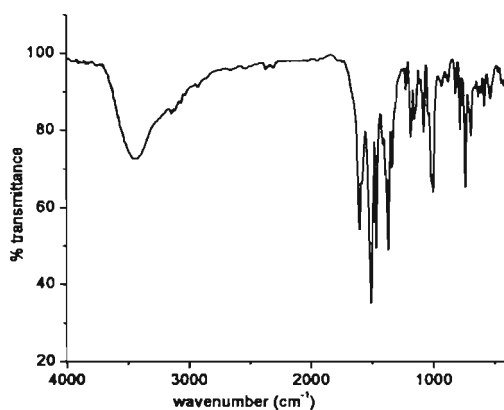

Fig. 7.3. IR spectrum of [Zn(FN)$_2$(H$_2$O)$_2$] (**42**).
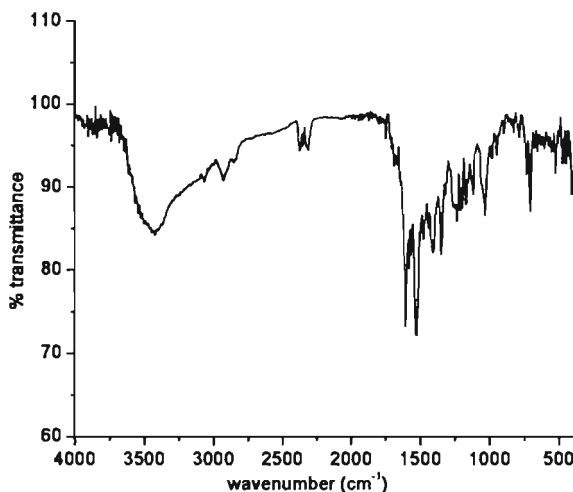
Fig. 7.4. IR spectrum of [Cd(BB)]$_2$ (**43**).
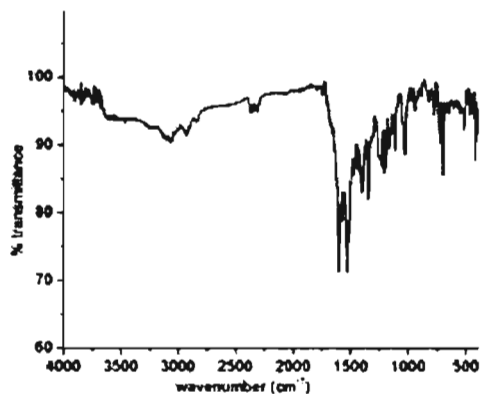
Fig. 7.5. IR spectrum of $[Cd(BN)]_2$ **(44)**.
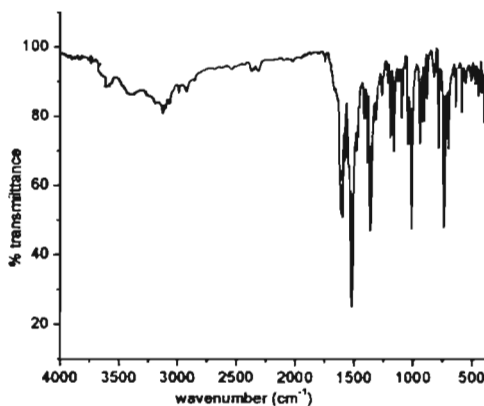
Fig. 7.6. IR spectrum of $[Cd(FN)_2]$ **(45)**.
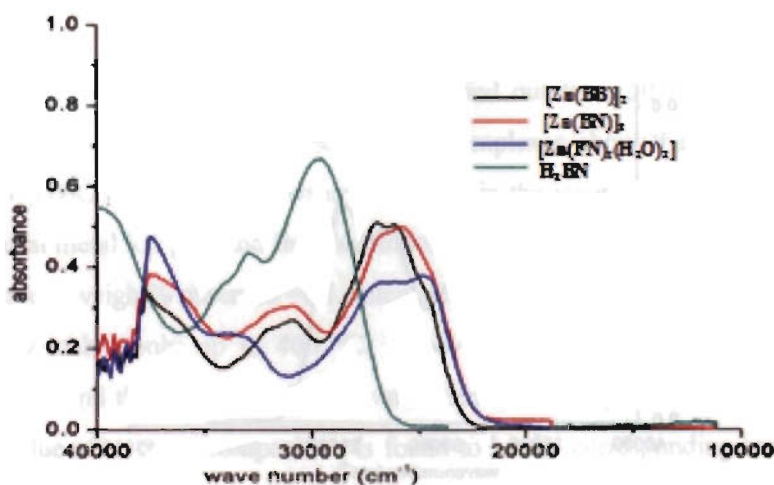
7.3.2 Electronic spectra

The electronic spectra of the ligands and complexes were recorded in DMF solutions on a UVD-3500, UV-vis Double Beam Spectrophotometer. The significant electronic absorption spectral data of the complexes in DMF or acetonitrile with their possible assignments are summarized in Table 7.3 and the spectra are shown in Figs. 7.7-7.9.

Table 7.3 Electronic spectral assignments (cm^{-1}) of Zn(II)/Cd(II) complexes

Compound	Intraligand transitions	Charge transfer transition
[Zn(BB)]₂ **(40)**	30915, 32115sh, 37727	26063, 27003
[Zn(BN)]₂ **(41)**	30855, 31735sh, 37533	24363sh, 25749, 26822
[Zn(FN)₂(H₂O)₂] **(42)**	33248, 37473	24616, 26822
[Cd(BB)]₂ **(43)**	31041, 32000sh,36087,37727	24550sh, 26256
[Cd(BN)]₂ **(44)**	30602, 32181, 37800	25689, 27009
[Cd(FN)₂] **(45)**	32501, 37680	24711, 26913

Zn(II) and Cd(II) ions have d^{10} configuration. Due to filled d orbitals, d-d transitions are not expected in the case of Zn(II)/Cd(II) complexes. Mainly these complexes are yellow colored and the colors of the complexes are attributed to metal to ligand charge transfer transitions. MLCT bands which are highly intense were observed in the range of 24360-27000 cm^{-1} [21] and the transitions occur between molecular orbitals which are essentially centered on different atoms. Free hydrazones show electronic absorption spectral bands in the region 29700-37100 cm^{-1} which are due to π-π^* transitions.

Fig. 7.7. Electronic spectra of Zn complexes **40-43**.

The azomethine chromophore which is in conjugation with olefinic or aryl groups change the spectrum significantly. Relatively weak bands due to n-π* transitions are submerged by strong absorptions associated with π-π* transitions [22]. These intraligand transitions are slightly shifted on complexation [23] as shown in the Table 7.3. It is observed that the spectra of the complexes are dominated by intense intraligand and charge transfer bands.
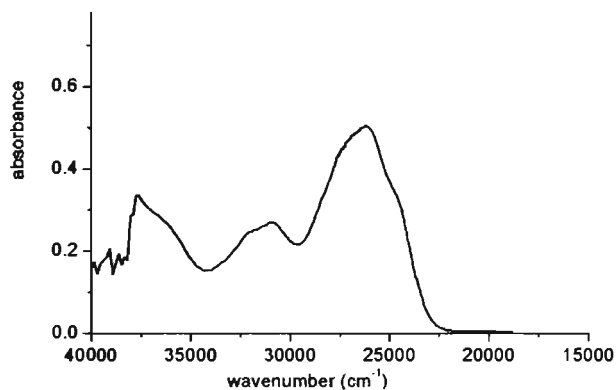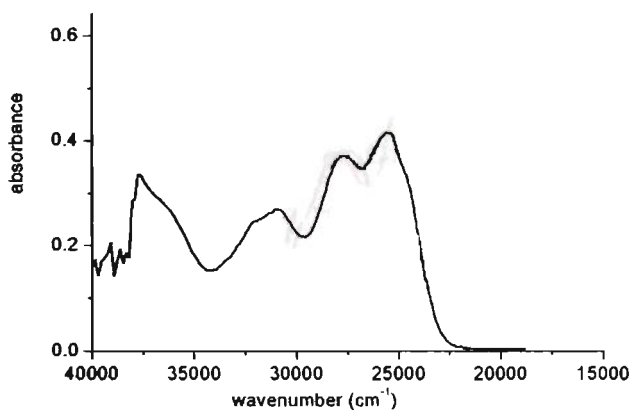

Fig. 7.8. Electronic spectrum of [Cd(BB)]₂ (**43**).

Fig. 7.9. Electronic spectrum of [Cd(BN)]₂ (**44**).

7.3.3 Thermal analyses

During the past few years, the thermal properties of metal complexes have been investigated extensively as one of the most interesting topics in the field of coordination chemistry [24-26]. We have studied the thermal decomposition of complexes to detect the presence of water and analyse its mode of coordination to the central metal ion.
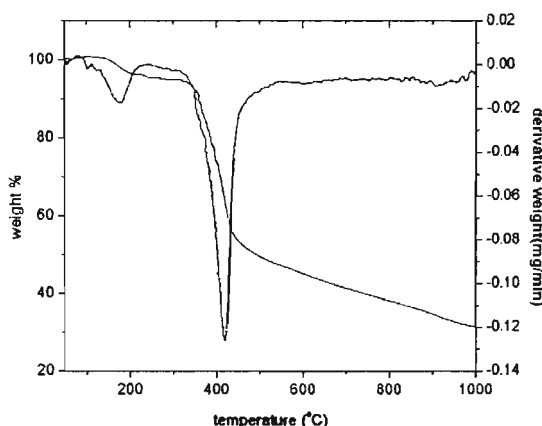

Fig. 7.10. TG-DTG plots of $[Zn(FN)_2(H_2O)_2]$ (**42**).

Thermogravimetric analyses were carried out from 50 to 1000 °C under nitrogen atmosphere. TG analyses of the complexes show that the compound $[Zn(FN)_2(H_2O)_2]$ (**42**) contain water molecules in the inner coordination sphere of the central metal ion [27] and first decomposition starts at 135 °C and a weight loss is observed (weight% observed =6.1, calculated = 6.8). The anhydrous compound is thermally stable only up to 400 °C. Above 400 °C the complexes begin to decompose and the decomposition was not seen to be completed even at 1000 °C. The residue after the decomposition is found to be the corresponding metal. The observed value for the mass loss of the complex during decomposition agrees with the theoretical value. TG-DTG plot of complex $[Zn(FN)_2(H_2O)_2]$ (**42**) is shown in Fig. 7.10.

References

[1]   K. Peariso, C.W. Goulding, S. Huang, R.G. Matthews, J.E. Penner-Hahn, J. Am. Chem. Soc. 120 (1998) 8410.

[2]   C. Dowling, G. Perkin, Polyhedron 15 (1996) 2463.

[3]   G.L. Parrilha, R.P. Vieira, A.P. Rebolledo, I.C. Mendes, L.M. Lima, E.J. Barreiro, O.E. Piro, E.E. Castellano, H. Beraldo, Polyhedron 30 (2011) 1891.

[4]   M.R.P. Kurup, M. Joseph, Synth. React. Inorg. Met. Org. Chem. 33 (2003) 1275.

[5]   D.M. Epstein, S. Choudhary, M.R. Churchill, K.M. Keil, A.V. Eliseev, J.R. Morrow, Inorg. Chem. 40 (2001) 1591.

[6]   W. Kaim, B. Schwederski, Bioinorganic Chemistry: Inorganic Elements in Chemistry of Life, Wiley: New York (1994).

[7]   R.H. Prince, G.R. Wilkinson, D. Gillard, J.A. McCleverty, Comprehensive Coordination Chemistry; Pergamon: Oxford 5 (1987).

[8]   M.L. Post, J. Trotter, J. Chem. Soc., Dalton Trans. (1974) 674.

[9]   P.A. Prasad, S. Neeraj, S. Natarajan, C.N.R. Rao, J. Chem. Soc., Chem. Commun. (2000) 1251.

[10] S. Sen, P. Talukder, G. Rosair, S. Mitra, Struct. Chem. 16 (2005) 605.

[11] T.A. Reena, E.B. Seena, M.R.P Kurup, Polyhedron 27 (2008) 1825.

[12] D.G. Paschalidis, I.A. Tossidis, M. Gdaniec, Polyhedron 19 (2000) 1629.

[13] N.R. Sangeetha, S. Pal, C.E. Anson, A.K. Powell, Inorg. Chem. Commun. 3 (2000) 415.

[14] T.W. Lane, F.M Morel, M. Proc. Natl. Acad. Sci. USA, 97 (2000) 4627.

[15] W. Zhang, J.L. Loebach, S.R. Wilson, E.N. Jacobsen, J. Am. Chem. Soc. 112 (1990) 2801.

[16] W.J. Geary, Coord. Chem. Rev 7 (1971) 81.

[17] M.S. Nair, R.S. Joseyphus, Spectrochim. Acta Part A 70 (2008) 749.

[18] L. Latheef, E. Manoj, M.R.P. Kurup, Polyhedron 26 (2007) 4107.

[19] N.A. Mangalam, M.R.P. Kurup, Spectrochim. Acta Part A 71 (2009) 2040.

[20] J. Chakraborty, S. Thakurta, G. Pilet, D. Luneau, S. Mitra, Polyhedron 28 (2009) 819.

[21] T.A. Reena, E.B. Seena, M.R.P. Kurup, Polyhedron 27 (2008) 3461.

[22] S. Patai, Chemistry of Carbon-Nitrogen Double Bond, Interscience publishers, John Wiley and Sons, London (1970).

[23] V. Philip, V. Suni, M.R.P. Kurup, M. Nethaji, Polyhedron 24 (2005) 1133.

[24] J.O. Hill, R.J. Magee, Rev. Inorg. Chem. 3 (1981) 141.

[25] S.K. Sengupta, S. Kumar, Thermochim. Acta 72 (1984) 349.

[26] M.R.P. Kurup, S.V. Chandra, K. Muraleedharan, J. Therm. Anal. Cal. 61 (2000) 909.

[27] A.A.A. Emara, B.A. El Sayed, E.A.E. Ahmed. Spectrochim. Acta Part A 69 (2008) 757.

Aroylhydrazones are known to be a class of versatile ligands, capable of generating varied molecular architectures and coordination polyhedra. Hydrazones are a class of azomethines having the group –C=N–NH–, are interesting ligands in coordination chemistry. They are synthezised by the condenzation reaction between a hydrazide and a carbonyl compound and are distinguished by other members of this family by the presence of two interlinking nitrogen atoms. When a –C=O group is incorporated in the hydrazide part increases the electron delocalization and denticity of the hydrazone and the resulting compound is known as an aroylhydrazone. Over the past few decades, aroylhydrazones having general formula R-CO-NH-N=CH-R' have been an important ligand construction unit in both the neutral and anionic forms. These organic molecules with potential donor atoms in their structural skeleton fascinate coordination chemists with their versatile chelating behavior. The ligands are readily prepared from inexpensive starting materials, and their electronic and steric properties can easily be modified and tuned by varying the substituents in the acylhydrazine and acylhydrazone units. The substituents have a clear effect on the catalytic activity as in the case of the copper-catalyzed Ullmann reaction. Metal complexes of hydrazones have been used as luminescent probes as well as molecular sensors. Amido-iminol tautomerism is shown by aroylhydrazones and when aroylhydrazones coordinate to the metal in the iminol form, the conjugation is improved thereby enhancing the nonlinearity.

Second-order nonlinear optical properties of copper and palladium complexes of N-salicylidene-N'-aroylhydrazines were studied by Cariati *et al.* and the results showed that the complexes have considerable nonlinearity.

The thesis contains seven chapters and deals with the crystal structures, spectroscopic and other physicochemical investigations of aroylhydrazones and their mixed ligand metal chelates. We have synthezised five aroylhydrazones and fortunately we could grow X-ray quality single crystals of all the five compounds and analyzed the crystal structures of all of them. Metal complexes, including mixed ligand metal chelates, of vanadium, manganese, cobalt, copper, zinc and cadmium were synthezised and characterized. Crystal structures of five copper, two vanadium and one cobalt complexes were resolved and analyzed.

Chapter 1 deals with an introduction to aroylhydrazones mentioning amido-iminol tautomerism, geometrical isomerism, their mode of coordination in complexes and applications in different areas. The objectives of the present work and the details of various physicochemical techniques carried out for the present investigation including X-ray crystallography are also presented in this chapter.

Chapter 2 deals with the syntheses of five different aroylhydrazones and their characterization by elemental analyses, FTIR, ^{1}H NMR and UV–Vis spectral studies. X-ray quality single crystals of all the five compounds were grown and their crystal structures were analyzed using single crystal X-ray diffraction studies. An interesting feature in the crystal packing of one of the ligands is the interlinking between the molecular stacks *via* C-H···H-C dipolar interaction.

The aroylhydrazones synthesized and their abbreviations follow

1. 2-Hydroxy-4-methoxybenzophenone benzoylhydrazone (H₂BB)
2. 2-Hydroxy-4-methoxybenzophenone nicotinoylhydrazone (H₂BN)
3. N-2-Hydroxy-4-methoxybenzophenone-N'-4-nitrobenzoylhydrazone (H₂BF)
4. Furan-2-carboxaldehyde nicotinoylhydrazone (HFN)
5. 5-Bromo-3-methoxysalicylaldehyde benzoylhydrazone (H₂S)

Chapter 3 describes the syntheses and characterization of eight vanadium complexes. X-ray quality single crystals of two compounds [one oxidovanadium (V) and a second one dioxido vanadium (V)] were grown and analyzed by single crystal XRD studies. The coordination geometry of the complexes is found to be distorted square pyramidal. Three compounds are vanadium(V) and are diamagnetic and the remaining five compounds are paramagnetic in nature with vanadium in +4 oxidation state as seen from the magnetic susceptibility measurements. All the complexes are characterized by various physicochemical techniques such as elemental analyses, FTIR, EPR, electronic spectral studies, thermogravimetric analyses, cyclic voltammetric studies, conductance and magnetic susceptibility measurements. The molar conductivity measurements in 10^{-3} M DMF solution reveal that all the complexes are non-electrolytic in nature. The hydrazones are found to coordinate in the amido form in one complex and in iminol form in all other complexes. EPR spectra of the compounds in DMF at 77 K displayed axial features with eight hyperfine splitting and in all complexes the $g_{\parallel} < g_{\perp}$ and $A_{\parallel} > A_{\perp}$ relationship, show an axially compressed d^1_{xy} configuration. For dimeric species EPR spectrum in polycrystalline state exhibits half field signal due to spin-spin interaction.

Chapter 4 deals with the syntheses and characterization of seven manganese(II/IV) complexes including mixed ligand complexes. The complexes were characterized by elemental analyses, IR, UV-Vis, EPR spectral studies, thermogravimetric analyses, cyclic voltammetric studies, conductance and magnetic susceptibility measurements. The molar conductivity measurements in DMF (10^{-3} M) solution indicate that all the complexes except one are non-electrolytes and the electrolyte is probably a 1:1 electrolyte. Magnetic susceptibility measurements suggest that all the compounds are paramagnetic with central metal atom having d^5/d^3 high spin configuration. The EPR spectrum of most of the complexes in the polycrystalline state were very broad and it is a characteristic feature of Mn(II) complexes in the polycrystalline state, which arises due to dipolar interactions and enhanced spin lattice relaxation. The spectra in DMF revealed six line hyperfine splittings for two complexes. In addition to the hyperfine pattern, a pair of low intensity lines is found in between each of the two main hyperfine lines. These are the forbidden lines corresponding to the mixing of the nuclear hyperfine levels with the zero field splitting factor. The g value is very close to the free electron spin value of 2.0023 which is consistent with the typical Mn(II).

Chapter 5 describes the syntheses and characterization of eleven Co(II/III) complexes. Heterocyclic bases and anions (azido and thiocyanato) are also incorporated. All the compounds were characterized by various spectrochemical studies as in the previous cases. Magnetic susceptibility measurements revealed that Co(III) complexes to be diamagnetic and octahedral and Co(II) complexes are paramagnetic. The molar conductivity measurements in DMF (10^{-3} M) solution indicate that all the complexes are non-electrolytes. The hydrazones are found to coordinate in anionic form in all the complexes as evidenced by the IR spectral data.

Chapter 6 deals with the syntheses and characterization of 13 Cu(II) complexes. Heterocyclic bases and anions (azido and thiocyanato) are also incorporated. Among the neutral ligands, 4-pycoline, 1,10-phenanthroline and 2,2'-bipyridine have been used. In the case of monoanionic bidentate hydrazone we incorporate different anions and pseudohalogens in to copper precursor complexes. We could isolate single crystals of five of the copper complexes, suitable for X-ray diffraction studies and crystal structures were solved by direct method of SHELXS-97. The coordination geometries of the complexes are found to be distorted square pyramidal and square planar. Packing in some of the compounds is stabilized by strong $\pi - \pi$ stacking interactions. In addition to the $\pi - \pi$ stacking interactions significant C–H⋯π interactions and hydrogen bonding are also present. A very interesting feature in the crystal packing of one of the compounds is C–H⋯H–C dihydrogen interaction which contributes to the stability of crystal packing.

The effective magnetic moment (μ_{eff}) values for the mononuclear copper(II) complexes (d^9 system) were found to be close to the spin only value, which corresponds to a single unpaired electron. The low magnetic moment values for some complexes may be due to some interaction between metal centers. IR spectroscopy could be used as a very valuable tool to get information regarding the coordination mode of the anionic coligands. In the electronic spectral studies, the broadness of the d-d transitions restricted the assignment of the three d-d transitions. EPR spectra of the complexes were taken in polycrystalline state at 298 K and in DMF at 77 K. The $g// > g\perp > 2.0023$ indicate that in most of the complexes the unpaired electron in Cu(II) resides in the ground state $d_{x^2-y^2}$ orbital. Half field signals due to the spin-spin

interaction of two copper centers are obtained for some of the complexes. This is a good evidence for the dinuclear species.

Chapter 7 describes the syntheses and characterization of three Zn(II) complexes and three Cd(II) complexes. The characterization techniques include elemental analyses, FTIR, electronic spectral studies, thermogravimetric analyses and conductance measurements. All the complexes are non-electrolytic in DMF.

T 582